0008-7114

Caryologia

International Journal of Cytology, Cytosystematics and Cytogenetics

2025
Vol. 78 - n. 1

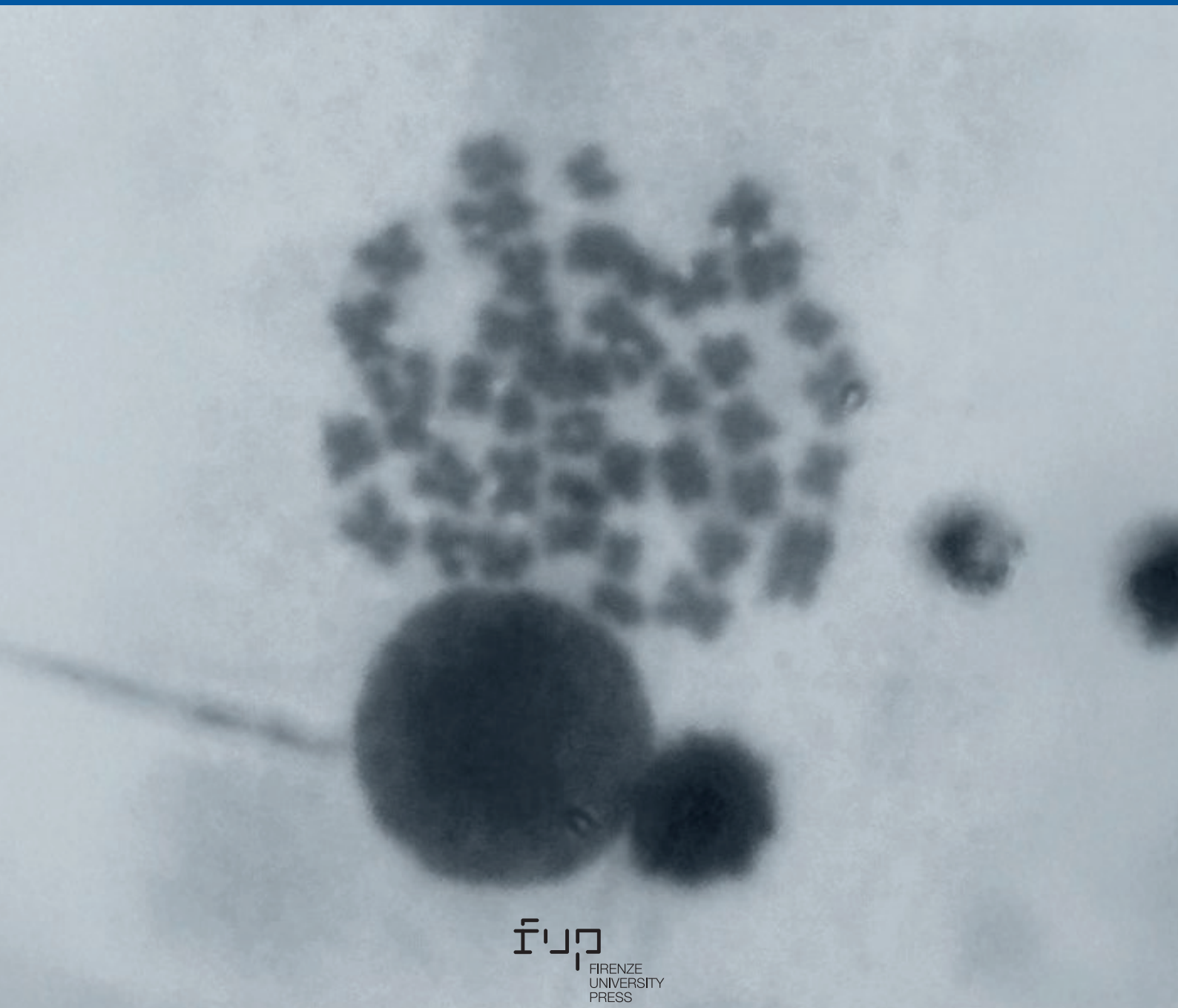

FIRENZE UNIVERSITY PRESS

Caryologia. International Journal of Cytology, Cytosystematics and Cytogenetics
Caryologia is devoted to the publication of original papers, and occasionally of reviews, about plant, animal and human karyological, cytological, cytogenetic, embryological and ultrastructural studies. Articles about the structure, the organization and the biological events relating to DNA and chromatin organization in eukaryotic cells are considered. *Caryologia* has a strong tradition in plant and animal cytosystematics and in cytotoxicology. Bioinformatics articles may be considered, but only if they have an emphasis on the relationship between the nucleus and cytoplasm and/or the structural organization of the eukaryotic cell.

Cover: figure from the article inside by Ngene, C. I. et al. "Genomic portraits: karyotyping of some Nigerian bat species", showing the mitotic metaphase chromosome of *Nycteris arge*.

Caryologia

International Journal of Cytology, Cytosystematics and Cytogenetics

Volume 78, Issue 1 - 2025

Firenze University Press

***Caryologia*. International Journal of Cytology, Cytosystematics and Cytogenetics**
https://riviste.fupress.net/index.php/caryologia
ISSN 0008-7114 (print) | ISSN 2165-5391 (online)

Direttore Responsabile: **Alessio Papini**

Published by Firenze University Press

Firenze University Press
Università degli Studi di Firenze
via Cittadella, 7, 50144 Firenze, Italy
www.fupress.com

Caryologia
International Journal of Cytology, Cytosystematics and Cytogenetics

Firenze University Press
https://riviste.fupress.net/index.php/caryologia

OPEN ACCESS

Citation: Ngene, C. I., Okwuonu, E. S., Ogbonna, I. D., Ukwueze, C. B. & Ejere, V. C. (2025). Genomic portraits: karyotyping of some Nigerian bat species. *Caryologia* 78(1): 3-26. doi: 10.36253/caryologia-3365

Received: March 7, 2025

Accepted: July 16, 2025

Published: October 1, 2025

Data Availability Statement: All relevant data are within the paper and its Supporting Information files.

Competing Interests: The Author(s) declare(s) no conflict of interest.

ORCID
CIN: 0000-0001-6757-8737
VCE: 0000-0003-2657-1912

Genomic portraits: karyotyping of some Nigerian bat species

Chinedu Innocent Ngene[1], Elijah Sunday Okwuonu[1]*, Ifeanyi Damian Ogbonna[2], Chinaza Blessing Ukwueze[1], Vincent Chinwendu Ejere[1]

[1] *Department of Zoology and Environmental Biology, University of Nigeria, Nsukka, Enugu State, Nigeria*
[2] *Department of Plant Science and Biotechnology, University of Nigeria, Nsukka, Enugu State, Nigeria*
*Corresponding author. Email: elijah.okwuonu@unn.edu.ng.

Abstract. Chromosome studies were conducted on bat species in the Nsukka Local Government Area of Enugu State, Nigeria, to determine their karyotypes and assess relatedness. Chromosomes were isolated from the bone marrow and testes of various bat species using 0.4% colchicine for cell division arrest. A calibrated eye-piece graticule was used for counting and measuring chromosomes from prepared slides. Calculations for arm ratios and centromeric indices were performed to categorize chromosomes, and ideograms were created based on these measurements. Standard karyotypes for each species were established using photomicrographs of mitotic metaphase chromosomes. A total of eight bat species were sampled, representing the suborders Yinpterochiropera and Yangochiroptera. The species included *Epomophorus wahlbergi, Epomophorus gambianus, Microteropus pusillus* from Yinpterochiropera, and *Nycteris major, Nycteris grandis, Nycteris arge, Scotophilus diaganii,* and *Scotophilus leucogaster* from Yangochiroptera. The diploid chromosome numbers (2n) and fundamental numbers (FN) were as follows: *Epomophorus wahlbergi* (2n=35, FN=70), *Epomophorus gambianus* (2n=36, FN=79), *Microteropus pusillus* (2n=36, FN=79), *Nycteris major* (2n=40, FN=80), *Nycteris grandis* (2n=42, FN=82), *Nycteris arge* (2n=40, FN=78), *Scotophilus diaganii* (2n=36, FN=45), and *Scotophilus leucogaster* (2n=36, FN=54). Variations in 2n and FN were attributed to centric fission and loss of p arm segments in some chromosomal pairs, leading to different morphological traits observed in the bat species. The study highlights the rich diversity of bat species in Nsukka and supports the use of karyotyping as an effective method for species differentiation.

Keywords: chromosomes, megabats, centric fission, *Epomophorus, Microteropus, Nycteris, Scotophilus.*

INTRODUCTION

Bats, constituting a significant percentage of living mammals, belong to the order Chiroptera, which is the second most diverse order of mammals (Wilson and Reeder 2005; Stevens and Willig 2002; Simmons and Conway 2003). They exhibit unique adaptations such as flight, echolocation, and a

wide range of ecological roles, feeding on various food sources like fish, insects, blood, nectar, and fruit (Fenton et al. 2016; Teeling et al. 2012). Bats play essential ecological roles, including seed dispersal, pest control, and pollination of crops (e.g., agave for tequila production) (McCracken et al. 2012; Bumrungsri et al. 2013).

Bats are also known reservoirs for several deadly viruses, including Ebola, SARS, rabies, and MERS, often remaining asymptomatic (Wang et al. 2011; Drexler et al. 2012; Anthony et al. 2017). Remarkably, they have long lifespans and low cancer rates, which may provide insights into aging and longevity (Austad 2010; Wang et al. 2011).

The taxonomic classification of bats has evolved, with a shift from the "wide" polytypic to the "narrow" monotypic species concept due to advancements in morphological and karyological techniques (Strelkov 2006; Kruskop 2005). Recent taxonomic revisions have identified 14 new Far Eastern bat species (Kruskop et al. 2012; Ruedi et al. 2015). However, African bats remain underresearched, with over 70% of fossil data missing, complicating conservation efforts (Teeling et al. 2012).

This study aimed to investigate the cytotaxonomy of bat species in Nsukka LGA, Enugu State, Nigeria, by determining chromosome numbers and characteristics, constructing karyotypes, and assessing species relatedness, addressing the lack of cytotaxonomic data in this region.

MATERIALS AND METHODS

The study was conducted in the Nsukka Local Government Area (LGA) of Enugu State, Nigeria, within the northern senatorial zone (Figure 1). Nsukka LGA is characterized by its green, steep terrain and includes villages such as Alor-Uno, Ede-Oballa, and Okpuje, covering an area of 1,810 km² with a population of 309,448 (ANON, 2006). The study sites included Obimo, Ibagwa-Ani, Nsukka, and Obukpa (Figure 2).

DATA ANALYSIS

The data collected were analyzed based on observations from Abraham and Prasad (1983) and Adegoke and Ejere (1991). These observations facilitated the classification of chromosomes into four groups: metacentric, submetacentric, subtelocentric, and acrocentric. Additionally, the relationships among the species were determined by measuring the chromosomes' relative lengths and centromeric indices.

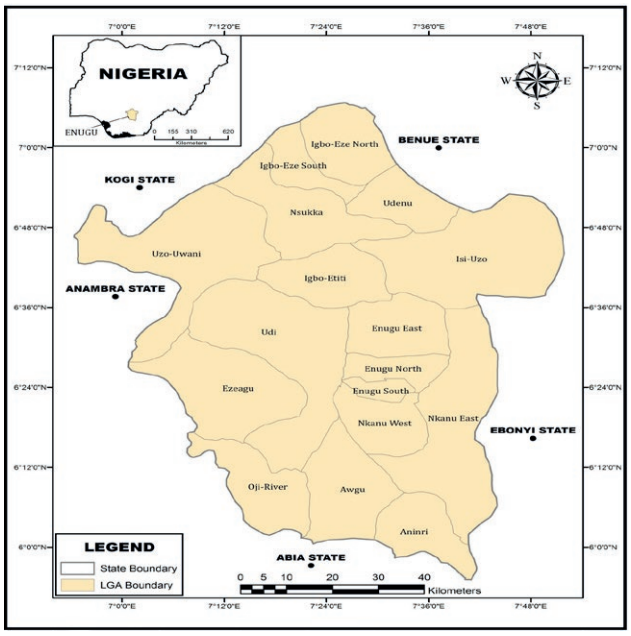

Figure 1. Map of Enugu State showing Nsukka local government area. Source: Geospatial Analysis Mapping and Environmental Research Solution (2018).

Trapping of experimental animals

Bats were trapped using a triple high mist net and a harp trap, following methods from Denys et al. (2013). Traps were set across potential flight paths for one night, checked every 10 to 20 minutes to prevent entanglement. Two bats (one male and one female) from each species were sacrificed for chromosome studies, with an additional specimen kept as a voucher.

Experimental design

The standard colchicine method was employed to prepare metaphase chromosome samples, following the protocol of Ejere and Adegoke (2001) with slight modifications. This procedure involved administering an intraperitoneal injection of 0.1 ml of 0.4% colchicine to each bat species for 2 hours to halt mitotic cell division. After euthanizing the bats with iso-fluorine, the hind leg bones were dissected and trimmed. Bone marrow was extracted using a heparinized syringe containing 3 ml of 0.55% KCl, which was then placed in labeled 15 ml centrifuge tubes, homogenized, and allowed to sit for 15 minutes. The resulting suspensions were centrifuged for 5 minutes at 1500 rpm, and the supernatant was discarded, leaving 0.5 ml of liquid in which the cells were resuspended. The cells were fixed with fresh cold

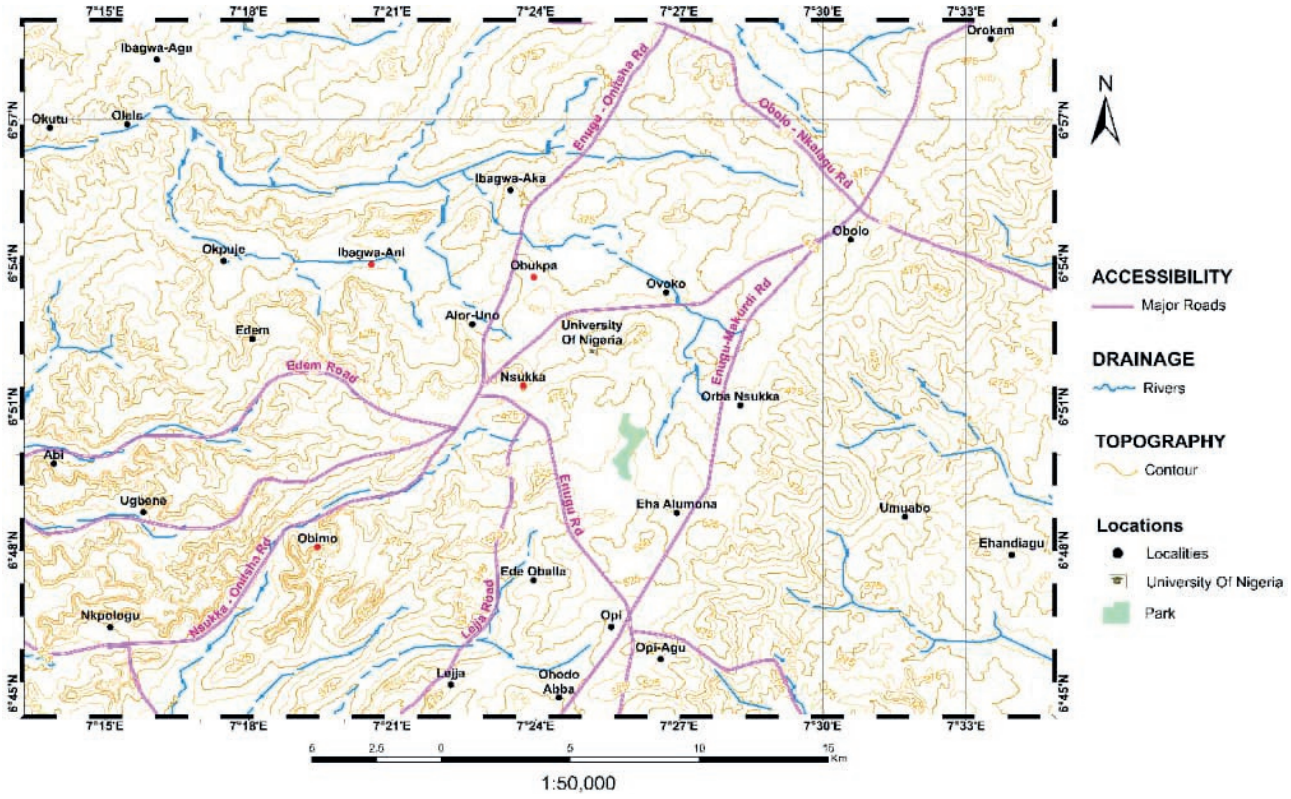

Figure 2. Map of Nsukka Local Government Area showing the study area (Obimo, Ibagwa-ani, Nsukka and Obukpa).

Carnoy's fixative and allowed to sit for about 30 seconds before undergoing centrifugation again, with the supernatant removed. This centrifugation process in the fixative was repeated twice more, after which the cells were resuspended and diluted with the fixative prior to being spread on glass slides. The slides were stained in a Coplin jar with 5 ml of Giemsa stain for 30 minutes, rinsed with tap water, and then placed in a slide warmer at 60 °C for 2 hours. Stained slides were examined for dividing cells under a light microscope at 10x magnification. Well-separated, countable metaphase chromosomes were measured and photographed under oil immersion at approximately 1000x magnification. The resulting photomicrographs were used to construct karyotypes (Adegoke and Ejere 1991; Ejere and Adegoke 2001).

Morphological identification

Morphological identification was performed according to Happold and Happold (2013), and specimens were deposited at the University of Nigeria's Zoology Museum, tagged Ew, Ep, Mp, Nm, Ng, Na, Sa, and Sl.

Ethical approval

Ethical standards were upheld as per the Faculty of Biological Science Ethics and Biosafety Committee, University of Nigeria, Nsukka (Ref. Number: UNN/FBS/EC/1013).

RESULTS

During the study, various species of bats from the families Yinpterochiropera and Yangochiroptera were identified in Nsukka LGA. The Yinpterochiropera family included *Epomophorus wahlbergi, Epomophorus gambianus,* and *Microteropus pusillus,* while the Yangochiroptera family featured *Nycteris major, Nycteris grandis,* and *Nycteris arge.* The Vespertilionidae family included *Scotophilus leucogaster* and *Scotophilus diaganii.* Table 1 presents the chromosomal numbers and fundamental numbers (FN) along with karyotype diagrams.

For each bat species analyzed, distinct karyotypes were established based on size. For example, in *Epomophorus wahlbergi,* the karyotype was categorized into three groups, with group one comprising four large

chromosomes, group two including medium-sized chromosomes, and group three consisting of smaller chromosomes (Table 2). Similarly, *Epomophorus gambianus* and *Microteropus pusillus* displayed comparable karyotypic structures, with varying numbers of chromosomes in each size category (Tables 3 and 4).

Nycteris major, Nycteris grandis, and *Nycteris arge* were also analyzed, revealing three main size groups in their karyotypes (Tables 5, 6 and 7). For *Nycteris major,* it was noted that males and females had distinct chromosome arrangements and FN. Comparisons between species showed that Yinpterochiropteran bats shared similarities, particularly in their larger chromosomes. Notably, *Epomophorus wahlbergi* and *Epomophorus gambianus* had similar chromosome structures, especially in larger and some medium-sized chromosomes.

Scotophilus diaganii and *Scotophilus leucogaster* each had a single large chromosome (Tables 8 and 9), while other species exhibited a range of large and small chromosomes, indicating potential phylogenetic relationships. Differences in chromosomal counts and struc-

Table 1. Diploid chromosome and fundamental numbers of various sampled bat species from Nsukka LGA, Nigeria.

S/N	Bat species	Mitotic metaphase chromosome spread	Karyotype	Diagram	Diploid chromosome number	Funda-mental number (FN)
1.	*Epomophorus wahlbergi*	Plate 1A	Plate 1B	Plate 1C	2n=35	70
2.	*Epomophorus gambianus*	Plate 2A	Plate 2B	Plate 2C	2n=36	79
3.	*Epomophorus* (*Microteropus*) *pusillus*	Plate 3A	Plate 3B	Plate 3C	2n=36	79
4.	*Nycteris major*	Plate 4A & Plate 4B	Plate 4C (male) & Plate 4D (female)	Plate 4E (male) & Plate 4F (female)	2n=40	80
5.	*Nycteris grandis*	Plate 5A	Plate 5B (female)	Plate 5C	2n=42	82
6.	*Nycteris arge*	Plate 6A	Plate 6B	Plate 6C	2n=40	78
7.	*Scotophilus diaganii*	Plate 7A	Plate 7B	Plate 7C	2n=36	45
8.	*Scotophilus leucogaster*	Plate 8A	Plate 8B	Plate 8C	2n=36	54

Table 2. *Epomophorus wahlbergi*'s chromosomal nomenclature based on centromeric indices.

Chromosome Number	Short Arm (S) %	Long Arm (L)	Total Length (C) %	Centromeric Index (I)	Nomenclature
1.	5.40	9.00	14.40	37.50	Nearly submedian (-)
2.	7.20	7.20	14.40	50.00	Median
3.	6.30	7.20	13.50	46.67	Nearly median
4.	4.50	7.20	11.70	38.46	Nearly median
5.	3.60	6.30	9.90	36.36	Nearly submedian (-)
6.	2.80	6.56	9.36	29.91	Nearly submedian (-)
7.	3.60	5.76	9.36	38.46	Nearly median
8.	3.96	5.40	9.36	42.31	Nearly median
9.	3.60	5.40	9.00	40.00	Nearly median
10.	2.60	6.40	9.00	28.89	Nearly submedian (-)
11.	2.50	5.60	8.10	30.86	Nearly submedian (-)
12.	3.60	4.32	7.92	45.45	Nearly median
13.	2.70	3.60	6.30	42.86	Nearly median
14.	2.70	3.60	6.30	42.86	Nearly median
15.	1.80	3.60	5.40	33.33	Nearly submedian (-)
16.	1.80	1.80	3.60	50.00	Median
17.	1.80	1.80	3.60	50.00	Median
X.	3.60	3.60	7.20	50.00	Median

The chromosomal centromeric index (i) was calculated using the method i = 100s/c. In the above table, the chromosome lengths were measured in microns as described under materials and methods, and then individually converted to percentages of total complement

Table 3. *Epomophorus gambianus* chromosomal nomenclature based on centromeric indices.

Chromosome Number	Short Arm (S) %	Long Arm (L)	Total Length (C) %	Centromeric Index (I)	Nomenclature
1.	5.40	7.20	12.60	42.86	Nearly median
2.	6.30	6.30	12.60	50.00	Median
3.	5.40	6.84	12.24	44.12	Nearly median
4.	5.40	6.30	11.70	46.15	Nearly median
5.	3.60	6.30	9.90	36.36	Nearly submedian (-)
6.	2.50	7.40	9.90	25.25	Nearly submedian (-)
7.	3.60	6.30	9.90	36.36	Nearly submedian (-)
8.	3.60	5.40	9.00	40.00	Nearly median
9.	4.50	4.50	9.00	50.00	Median
10.	3.60	5.40	9.00	40.00	Nearly median
11.	3.60	4.50	8.10	44.44	Nearly median
12.	2.70	3.96	6.66	40.54	Nearly median
13.	1.50	3.60	5.40	33.33	Nearly submedian (-)
14.	1.80	3.60	5.40	33.33	Nearly submedian (-)
15.	1.80	3.60	5.40	33.33	Nearly submedian (-)
16.	0.80	2.80	3.60	22.22	Nearly submedian (+)
17.	0.00	3.60	3.60	0.00	Terminal
X.	3.78	3.78	7.56	50.00	Median
X.	3.78	3.78	7.56	50.00	Median

Table 4. The nomenclature of the chromosomes of *Epomophorus* (*Microteropus*) *pusillus* using the centromeric indices.

Chromosome Number	Short Arm (S) %	Long Arm (L)	Total Length (C) %	Centromeric Index (I)	Nomenclature
1.	6.40	8.00	14.40	44.44	Nearly median
2.	7.20	7.20	14.40	50.00	Median
3.	6.30	7.20	13.50	46.67	Nearly median
4.	4.50	5.40	9.90	45.45	Nearly median
5.	4.14	5.40	9.54	43.40	Nearly median
6.	3.60	5.76	9.36	38.46	Nearly median
7.	3.60	5.76	9.36	38.46	Nearly median
8.	1.80	5.76	7.56	23.81	Nearly submedian (+)
9.	2.20	5.36	7.56	29.10	Nearly submedian (-)
10.	3.60	3.96	7.56	47.62	Nearly median
11.	3.60	3.60	7.20	50.00	Median
12.	3.40	3.80	7.20	47.22	Nearly median
13.	2.70	3.60	6.30	42.86	Nearly median
14.	1.80	2.70	4.50	40.00	Nearly median
15.	1.80	2.70	4.50	40.00	Nearly median
16.	1.80	1.80	3.60	50.00	Median
17.	0.00	3.60	3.60	0.00	Terminal
X.	3.60	3.60	7.20	50.00	Median
X.	3.60	3.60	7.20	50.00	Median

tural characteristics were highlighted, with telocentric chromosomes prevalent in the *Scotophilus* species. Table 10 summarizes that all bat species had at least one large chromosome, with specific similarities and differences noted in their karyotypic features (Figure 3).

Table 5. The nomenclature of the chromosomes of *Nycteris major* using the centromeric indices.

Chromosome Number	Short Arm (S) %	Long Arm (L)	Total Length (C) %	Centromeric Index (I)	Nomenclature
1.	5.40	9.90	15.30	35.29	Nearly sub-median (-)
2.	5.40	8.64	14.04	38.46	Nearly median
3.	6.30	6.30	12.60	50.00	Median
4.	5.40	5.40	10.80	50.00	Median
5.	3.60	7.20	10.80	33.33	Nearly submedian (-)
6.	3.60	6.30	9.90	36.36	Nearly submedian (-)
7.	2.40	7.50	9.90	24.24	Nearly submedian (+)
8.	3.60	5.76	9.36	38.46	Nearly median
9.	3.60	5.76	9.36	38.46	Nearly median
10.	3.60	5.40	9.00	40.00	Nearly median
11.	3.60	4.50	8.10	44.44	Nearly median
12.	1.80	6.30	8.10	22.22	Nearly sub median (+)
13.	1.80	5.40	7.20	25.00	Submedian
14.	3.42	3.78	7.20	24.62	Nearly submedian (+)
15.	2.70	3.60	6.30	42.86	Nearly median
16.	2.70	3.60	6.30	42.86	Nearly median
17.	2.70	3.60	6.30	42.86	Nearly median
18.	1.80	3.60	5.40	33.33	Nearly submedian (-)
19.	1.80	3.60	5.40	33.33	Nearly submedian (-)
X.	3.60	3.60	7.20	50.00	Median
X.	3.60	3.60	7.20	50.00	Median
Y.	0.00	3.60	3.60	0.00	Terminal

Table 6. The nomenclature of the chromosomes of *Nycteris grandis* using the centromeric indices.

Chromosome Number	Short Arm (S) %	Long Arm (L)	Total Length (C) %	Centromeric Index (I)	Nomenclature
1.	7.20	9.00	16.20	44.44	Nearly median
2.	7.20	7.20	14.40	50.00	Median
3.	6.75	6.75	13.50	50.00	Median
4.	6.30	6.30	12.60	50.00	Median
5.	6.30	6.30	12.60	50.00	Median
6.	5.40	7.20	12.60	42.86	Nearly median
7.	5.85	5.85	11.70	50.00	Median
8.	4.50	6.84	11.34	39.68	Nearly median
9.	3.96	7.20	11.16	34.14	Nearly submedian (-)
10.	5.04	5.40	10.80	46.67	Nearly median
11.	4.50	5.40	9.90	45.45	Nearly median
12.	3.60	6.30	9.90	36.36	Nearly submedian (-)
13.	1.80	7.20	9.00	20.00	Nearly submedian (+)
14.	3.60	5.40	9.00	36.36	Nearly submedian (-)
15.	2.80	6.20	9.00	31.11	Nearly submedian (-)
16.	1.80	7.20	9.00	20.00	Nearly submedian (+)
17.	3.60	5.40	9.00	36.36	Nearly submedian (-)
18.	2.70	3.60	6.30	42.86	Nearly median
19.	2.70	3.60	6.30	42.36	Nearly median
20.	0.00	2.70	2.70	0.00	Terminal
X.	3.80	3.80	7.60	50.00	Median
X.	3.80	3.80	7.60	50.00	Median

Table 7. The nomenclature of the chromosomes of *Nycteris arge* using the centromeric indices

Chromosome Number	Short Arm (S) %	Long Arm (L)	Total Length (C) %	Centromeric Index (I)	Nomenclature
1.	5.40	9.00	14.40	37.50	Nearly submedian (-)
2.	5.40	7.20	12.60	42.86	Nearly median
3.	3.60	7.20	10.80	33.33	Nearly submedian (-)
4.	5.40	5.40	10.80	50.00	Median
5.	3.96	5.40	9.36	42.31	Nearly median
6.	3.60	5.76	9.36	38.46	Nearly median
7.	3.78	5.40	9.18	41.18	Nearly median
8.	3.60	5.40	9.00	40.00	Nearly median
9.	3.60	5.40	9.00	40.00	Nearly median
10.	3.60	5.04	8.64	41.67	Nearly median
11.	3.60	4.50	8.10	44.44	Nearly median
12.	3.60	4.32	7.92	45.45	Nearly median
13.	3.60	3.60	7.20	50.00	Median
14.	3.00	4.20	7.20	41.67	Nearly median
15.	2.40	4.80	7.20	33.33	Nearly submedian (-)
16.	3.24	3.60	6.84	47.37	Nearly median
17.	2.88	3.60	6.48	44.44	Nearly median
18.	2.70	3.60	6.30	43.86	Nearly median
19.	0.00	3.60	5.40	0.00	Terminal
X.	3.60	3.60	7.20	50.00	Median
X.	3.60	3.60	7.20	50.00	Median

Table 8. The nomenclature of the chromosomes of *Scotophilus diagonal* using the centromeric indices

Chromosome Number	Short Arm (S) %	Long Arm (L)	Total Length (C) %	Centromeric Index (I)	Nomenclature
1.	5.20	5.60	10.80	48.15	Nearly median
2.	3.60	5.40	9.00	40.00	Nearly median
3.	2.20	5.00	7.20	30.56	Nearly submedian (-)
4.	1.80	5.40	7.20	25.00	Submedian
5.	0.00	6.30	6.30	0.00	Terminal
6.	0.00	6.30	6.30	0.00	Terminal
7.	0.00	6.30	6.30	0.00	Terminal
8.	0.00	6.30	6.30	0.00	Terminal
9.	0.00	6.30	6.30	0.00	Terminal
10.	0.00	6.30	6.30	0.00	Terminal
11.	0.00	6.30	6.30	0.00	Terminal
12.	0.00	6.30	6.30	0.00	Terminal
13.	0.00	6.30	6.30	0.00	Terminal
14.	0.00	5.40	5.40	0.00	Terminal
15.	0.00	5.40	5.40	0.00	Terminal
16.	0.00	4.50	4.50	0.00	Terminal
17.	0.00	4.50	4.50	0.00	Terminal
X.	2.80	2.80	5.60	50.00	Median
Y.	0.00	3.60	3.60	0.00	Terminal

Table 9. The nomenclature of the chromosomes of *Scotophilus lecuogaster* using the centromeric indices

Chromosome Number	Short Arm (S) %	Long Arm (L)	Total Length (C) %	Centromeric Index (I)	Nomenclature
1.	5.40	6.30	11.70	46.15	Nearly median
2.	4.50	5.40	9.90	45.45	Nearly median
3.	3.60	5.40	9.00	40.00	Nearly median
4.	1.80	7.20	9.00	20.00	Nearly submedian (+)
5.	2.70	5.40	8.10	33.33	Nearly sub median (-)
6.	0.00	8.10	8.10	0.00	Terminal
7.	0.00	7.20	7.20	0.00	Terminal
8.	0.00	7.20	7.20	0.00	Terminal
9.	0.00	7.20	7.20	0.00	Terminal
10.	0.00	7.20	7.20	0.00	Terminal
11.	3.00	4.20	7.20	41.67	Nearly median
12.	0.00	7.20	7.20	0.00	Terminal
13.	0.00	6.64	6.84	0.00	Terminal
14.	0.00	6.84	6.84	0.00	Terminal
15.	1.80	3.60	5.40	33.33	Nearly submedian (-)
16.	1.80	3.60	5.40	33.33	Nearly submedian (-)
17.	0.00	3.60	3.60	0.00	Terminal
X.	4.05	4.05	8.10	50.00	Median
X.	4.05	4.05	8.10	50.00	Median

Table 10. A table showing the relationship among the bat species using autosomal chromosomes

Chromosome Number	*Epomophorus wahlbergi*	*Epomophorus gambianus*	*Microteropus pusillus*	*Nycteris major*	*Nycteris grandis*	*Nycteris* species	*Nycteris arge*	*Scotophilus diaganii* (yellow-bellied bat)	*Scotophilus lecuogaster* (white-bellied bat)
1.	L, Sm	L, Sm	L, Sm	L, Ac	L, Sm	L, Ac	L, Ac	L, Mc	L, Sm
2.	L, Mc	L, Mc	L, Mc	L, Sm	L, Mc	L, Ac	L, Sm	M, Sm	M, Sm
3.	L, Sm	L, Sm	L, Sm	L, Mc	L, Mc	L, Ac	L, Ac	M, Tc	M, Sm
4.	L, Sm	L, Sm	M, Sm	L, Mc	L, Mc	L, Sm	L, Mc	M, Ac	M, Sm
5.	M, Ac	M, Ac	M, Sm	L, Ac	L, Mc	L, Sm	M, Sm	S, Tc	M, Sm
6.	M, Ac	M, Ac	M, Sm	M, Ac	L, Sm	L, Ac	M, Sm	S, Tc	M, Ac
7.	M, Sm	M, Ac	M, Sm	M, Ac	L, Mc	L, Ac	M, Sm	S, Tc	M, Tc
8.	M, Sm	M, Sm	M, Ac	M, Mc	L, Sm	L, Mc	M, Sm	S, Tc	M, Tc
9.	M, Sm	M, Mc	M, Ac	M, Mc	L, Ac	L, Sm	M, Sm	S, Tc	M, Tc
10.	M, Ac	M, Sm	M, Sm,	M, Mc	L, Sm	M, Ac	M, Sm	S, Tc	M, Tc
11.	M, Ac	M, Sm	M, Mc	M, Mc	M, Sm	M, Sm	M, Sm	S, Tc	M, Tc
12.	M, Sm	S, Sm	M, Sm	M, Ac	M, Ac	M, Sm	M, Sm	S, Tc	M, Tc
13.	S, Mc	S, Ac	M, Ac	M, Ac	M, Ac	M, Sm	M, Mc	S, Tc	S, Tc
14.	S, Sm	S, Ac	S, Sm	M, Ac	M, Ac	M, Sm	M, Sm	S, Tc	S, Tc
15.	S, Ac	S, Ac	S, Sm	S, Sm	M, Ac	M, Sm	M, Sm	S, Tc	S, Ac
16.	S, Mc	S, Ac	S, Sm	S, Sm	M, Ac	M, Sm	S, Sm	S, Tc	S, Ac
17.	S, Mc	S, Tc	S, Tc	S, Sm	M, Ac	M, Sm	S, Sm	S, Tc	S, Tc
18.				S, Ac	S, Sm	S, Sm	S, Sm		
19.				S, Ac	S, Sm	S, Tc	S, Ac		
20.					S, Tc	S, Tc			
21.						S, Tc			

Key: L = Large; M = Medium; S = Small; Submetacentric = Sm; Metacentric = Mc; Acrocentic = Ac; Telocentric =Tc.

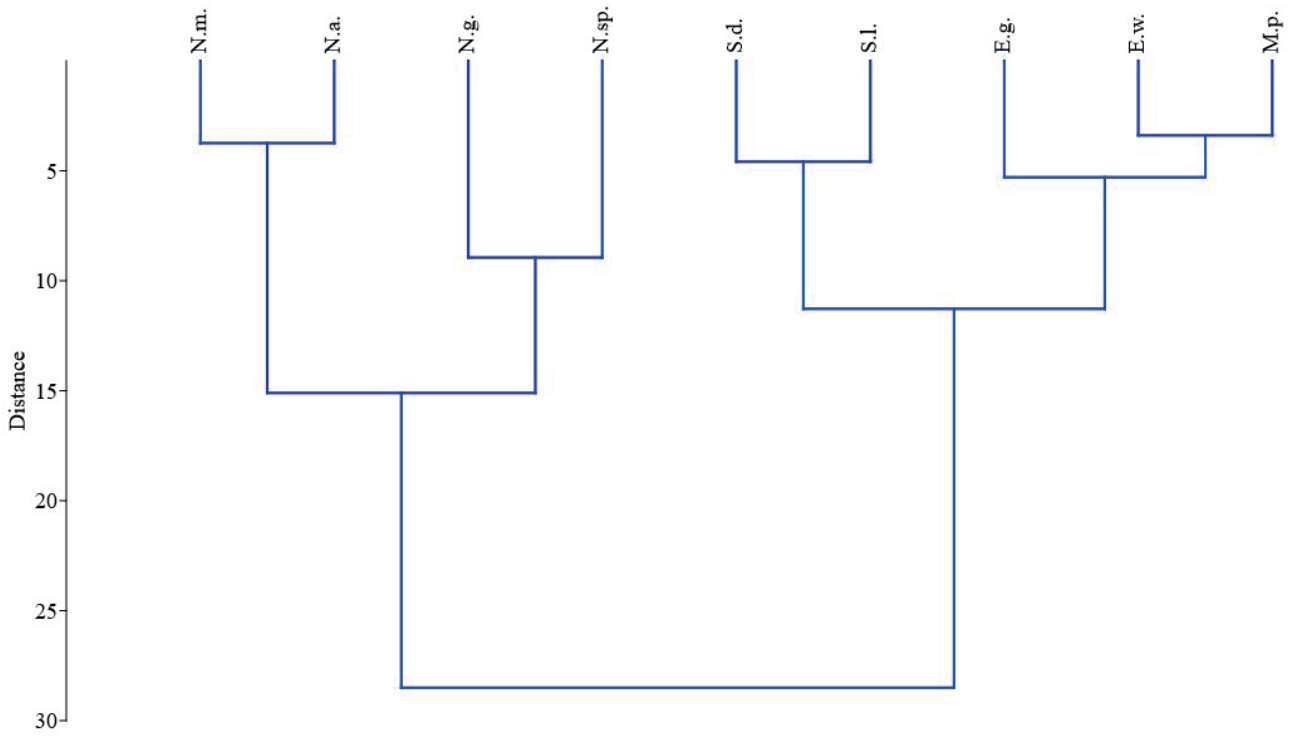

Figure 3. Cluster relationship of the bat species using chromosomal indices.
Key:
- *Epomophorus wahlbergi = E.w.,*
- *Epomophorus gambianus = E.g.,*
- *Microteropus pusillus = M.p.,*
- *Nycteris major = N.m.,*
- *Nycteris grandis = N.g.,*
- *Nyceris arge = N.a.,*
- *Sctotophilus diaganii = S.d.,* and *Scotophilus lecuogaster = s.l*

DISCUSSION

This study identified bat species from the Megachiroptera (frugivorous bats) and Microchiroptera (insectivorous bats), each exhibiting one large chromosome. The diploid chromosome number (2n) of the bat species analyzed ranged from 35 to 42, aligning with the known chromosome diversity in bats (2n=14 to 64) (Cibele et al. 2017). This indicates a high degree of conservation in diploid chromosome numbers among bat groups (Cibele et al. 2017).

The Pteropodidae family (fruit bats) displayed a chromosome range of 35-36, similar to the 2n range of 24-58 reported by Sotero-Caio et al. (2017). Specifically, Epomophorus wahlbergi was found to have 2n=35 and FN=70, differing from Kenyan and Zimbabwean species with 2n=36, FN=68 (Dulic and Mutere 1975; Peterson and Nagorsen 1975). This study confirms *Epomophorus wahlbergi* follows the X0 sex chromosome system. *Epomophorus gambianus* exhibited 2n=36 and FN=70, aligning with the XX system for *Epomophorus* species. *Microteropus pusillus* currently known as *Epomophorus pusillus* also displayed 2n=36 and FN=70, contrasting with prior reports of 2n=35, FN=64 in Cameroon (Haiduk et al. 1981).

The Nycteridae family was characterized by varying diploid numbers, with *Nycteris major* showing 2n=40 (FN=79 for males, FN=80 for females) and Nycteris grandis reported as 2n=42 (FN=82) (Porter et al. 2010). There were notable morphological and chromosomal differences observed among species within this family, which is classified into *Nycteris* with diploid counts ranging from 2n=34 to 42 (Denys et al. 2013).

In the Vespertilionidae family, *Scotophilus diaganii* presented 2n=36 and FN=45, consistent with South African specimens but differing in FN (52 and 50) reported by Schlitter et al. (1980) and Ruedas et al. (1990). *Scotophilus leucogaster*'s karyotype showed 2n=36, FN=54, differing

from reports of 50 for specimens in Namibia and Burkina Faso (Ruedas et al. 1990; Volleth et al. 2006).

The chromosomes of these bat species differ from those of lizards, suggesting genus-specific variations. As research advances to molecular levels, previously misclassified species are being correctly positioned within taxonomic frameworks, revealing geographic influences on chromosomal variations (Foley et al. 2017). Notable patterns of karyotype similarities were identified across species, potentially linked to cryptic species and geographical isolation (Cibele et al. 2017).

In summary, this detailed study of the cytogenetics of bat species in Nsukka reported karyotypes for eight species: *Epomophorus wahlbergi* (2n=35), *Epomophorus gambianus* (2n=36), *Microteropus pusillus* (2n=36), *Nycteris major* (2n=40), *Nycteris grandis* (2n=42), *Nycteris arge* (2n=40), *Scotophilus diaganii* (2n=36), and *Scotophilus leucogaster* (2n=36). Further research utilizing modern cytogenetic techniques is needed to fill knowledge gaps in this field.

AUTHOR CONTRIBUTION STATEMENT

Chinedu Innocent Ngene and Vincent Chinwendu Ejere: conceptualization of the project research; Chinedu Innocent Ngene and Elijah Sunday Okwuonu: data collection; Chinedu Innocent Ngene: lab work; Chinedu Innocent Ngene, Elijah Sunday Okwuonu, Ifeanyi Damian Ogbonna and Chinaza Blessing Ukwueze: manuscript drafting and review

ACKNOWLEDGEMENTS

We thank the Small Mammal Conservation Organization (SMACON) for providing harp traps and mist nets. We also thank Johnmartin Oforkansi, Samson Ugwuanyi, Elijah Okwuonu, Osita Ezeugwu, and Francis Abonyi, for assisting in the field. Finally, we are grateful to Professor Vincent C. Ejere, and the late Prof. Felicia C. Eke, for providing chemicals, equipment, and instructions for chromosomal extractions.

REFERENCES

Abraham Z. & Prasad PN. (1983). A system of chromosome classification and nomenclature. Cytologia, 48, 95–101. https://doi.org/10.1508/cytologia.48.95.

Adegoke JA. & Ejere VC. Description of the chromosomes of three lizard species belonging to the genus, *Mabuya* (Scincidae, Reptilia). Caryologia, 44, 333–342. https://doi.org/10.1080/00087114.1991.10797199.

Anthony SJ, Johnson CK, Greig DJ, Kramer S, Che X et al. (2017). Global patterns in coronavirus diversity. Virus Evolution, 3(1), vex012. https://doi.org/10.1093/ve/vex012.

Austad SN. (2010). Methuselah's zoo: how nature provides us with clues for extending human health span. Journal of Comparative Pathology, 142, S10–S21. https://doi.org/10.1016/j.jcpa.2009.10.024.

Baker RJ. & Bickham JW. (1980). Karyotypic evolution in bats: Evidence of extensive and conservative chromosomal evolution in closely related taxa. Systematic Zoology, 29(3), 239–253. https://doi.org/10.2307/2412660.

Bickman JW. (1979). Banded Karyotypes of 11 Species of American Bats (*Genus Myotis*). Journal of Mammalogy, 60, 350 – 363. https://doi.org/10.2307/1379807.

Brook CE. & Dobson AP. (2015). Bats as "special" reservoirs for emerging zoonotic pathogens. Current Trends Microbiology, 23(3), 172–180.

Bulkina TM. & Kruskop SV. (2009). Search for morphological differences between genetically distinct brown long-eared bats (*Plecotus auritus* s. lato, Vespertilionidae). Plecotus, 11-12: 3–13.

Bumrungsri S, Lang D, Harrower C, Sripaoraya E, Kitpipit K and Racey PA. (2013). The dawn bat, *Eonycteris spelaea* Dobson (Chiroptera: Pteropodidae) feeds mainly on pollen of economically important food plants in Thailand. Acta Chiropterologica, 15(1), 95–104. https://doi.org/10.3161/150811013X667894.

Cibele G. Sotero-Caio, Robert J. Baker, and Marianne Volleth (2017). Chromosomal evolution in Chiroptera. *Genes*, 8, 273. https://doi.org/10.3390/genes8100272.

Denys C, Kadjo B, Missoup AD, Monadjem A and Aniskine V. (2013). New records of bats (Mammalia: Chiroptera) and karyotypes from Guinean Mount Nimba (West Africa). Italian Journal of Zoology, 80(2): 279–290. https://doi.org/10.1080/11250003.2013.775367.

Drexler JF, Corman VM, Muller MA, Maganga GD, Vallo P, Binger T. et al. (2012). Bats host major mammalian paramyxoviruses. Nature Communications, 3, 796. https://doi.org/10.1038/ncomms1796.

Dulic B. & Mutere FA. (1975). Les chromosome de tro's especes, des, megachropteres (mamm ba, chiroptera) d'Afrique orientale. Caryologia, 26, 389–396.

Eick GN, Jacobs DS, Yang F and Volleth M. (2007). Karyotypic differences on sibling species of *Scotophi-*

lus from South Africa (Vespertilionidae, Chiroptera, Mammalia). Cytogenetic and Genome Research, 118(1), 72–77. https://doi.org/10.1159/000106444.

Ejere VC. & Adegoke JA. (2001). Karyological study of banded gecko, *Hemidactylus fasciatus fasciatus* Gray (Gekkonidae, Reptilia). Cytologia, 66, 133–137. https://doi.org/10.1508/CYTOLOGIA.66.133.

Fahr J. (2013). *Rhinolophus maclaudi* Maclaud's horseshoe bat in mammals of Africa. In: Happold M & Happold DCD (Editors). *Mammals of Africa, Volume IV: Hedgehogs, Shrews and Bats*. Bloomsbury, London, England.

Fenton MB, Grinnell AD, Popper AN and Fay RR. (2016). *Bat Bioacoustics*. Springer, New York.

Foley NM, Goodman SM, Whelan CV, Peuchmaille SJ and Teeling T. (2017). Towards navigating the minotaur's labyrinth: cryptic diversity and taxonomic revision within the speciose genus *Hipposideros* (Hipposideridae). Acta Chiropterologica, 19, 1–18. https://doi.org/10.3161/15081109ACC2017.19.1.001.

Geospatial Analysis Mapping and Environmental Research Solution (GAMERS). 2018. Map of Enugu State, Nigeria. Available at: https://www.gamers.com.ng/map-of-enugu-state-nigeria/. Accessed on 22nd August 2019.

Haiduk MW, Baker RJ, Robbins L and Shlitter DA. (1981). Chromosomal evolution in African Megachiraptera: G-and C-band assessment of the magnitude of change in similar standard karyotypes. Cytogenetics & Cell Genetics, 29(4), 221–232. https://doi.org/10.1159/000131573

Happold M. & Happold DCD. (2013). Mammals of Africa. Volume IV: Hedgehogs, Shrews and Bats. Bloomsbury Publishing, London, United Kingdom. 800 pp.

Hsu TC. & Arrighi FE. (1971). Distribution of constitutive heterochromatin in mammalian chromosomes. Chromosoma, 34(3), 243–253. https://doi.org/10.1007/BF00286150.

Kartavtseva IV. (2002). Karyosystematics of Wood and Field Mice (Rodentia: Muridae). Dal'nauka Press, Vladivostok. 144 pp.

Kearney TC, Volleth M, Contrafatto G and Taylor PG. (2002). Systematic implications of chromosome GTG-band and bacula morphology for southern African Eptesicus and Pipistrellus and several other species of Vespertilioninae (Chiroptera: Vespertilionidae). Acta Chiropterologica, 4(1), 55–76. https://doi.org/10.3161/001.004.0107.

Koubinová D, Sreepoda K, Koubek P and Zima J. (2010). Karyotypic variation in rhinolophid and hopposiderid bats (Chiroptera; Rhirolophidae, Hipposideridae). Acta Chiropterologica, 12, 393–400. https://doi.org/10.3161/150811010X537972.

Kruskop SV. (2006). Towards the taxonomy of the Russian Murina. Russian Journal of Theriology, 4(2), 135–140. https://doi.org/10.15298/rusjtheriol.04.2.01.

Kruskop SV. (2012). *Order Chiroptera.* In: Pavlinov, I.Y. & Lissovsky, A.A. (Editors). The Mammals of Russia: A Taxonomic and Geographic Reference. KMK Scientific Press, Moscow. 604 pp. https://doi.org/10.5772/intechopen.78767.

Kruskop SV, Borisenko AV, Ivanova NV, Lim BK and Eger JL. (2012). *Genetic diversity of northeastern Palaearctic bats as revealed by DNA barcodes.* Acta Chiropterologica, 14(1), 1–14. https://doi.org/10.3161/150811012X654222.

Matthey, R. 1973. The chromosome formulae of eutherian mammals. In Cytotaxonomy and Vertebrate Evolution, ed. A. B. Chiarelli and E. Capanna, 531–616. Academic Press: London/New York.

McCracken GF, Westbrook JK, Brown VA, Eldridge M, Federico P and Kunz TH. (2012). Bats track and exploit changes in insect pest populations. PLoS ONE, 7(8), e43839. https://doi.org/10.1371/journal.pone.0043839.

Peterson RL. & Nagorsen DW. (1975). Chromosome of fifteen species of bats (Chiroptera) form kerygad Rhodesia. Life Science Occasional Paper Royals Ontario Museum, 27, 1–14.

Porter CA, Primus AW., Hoffmann FG and Baker RJ (2010). Karyology of five species of bats (Vespertiliondae Hipposideridae, and Nycteridae) from Gabon with comments on the taxonomy of Glauconycteris museum of Texas Tech. University Occasion paper, 295. https://doi.org/10.5962/bhl.title.156992.

Primes A, Harvey J, Guimondou S, Mboumba S, Ngangui R, Hoffmann F, Baker R and Porter CA. (2006). Karyology and chromosome evolution of some small mammals inhabiting the rainforest of the Rabi oil field, Gabon. Bulletin of the Biological Society of Washington, 12, 372–382.

Puig-Montserrat X, Torre I, L´opez-Baucells A, Guerrieri E and Monti MM. (2015). Pest control service provided by bats in Mediterranean rice paddies: linking agroecosystems structure to ecological functions. Mammalian Biology, 80(3), 237–245. https://doi.org/10.1016/j.mambio.2015.03.008.

Rautenbach IL, Bronner GN, Schlitter DA. (1993). Karyotypic data and attendant systematic implications for the bats of Southern Africa. Koedoe, 36, 87–104. https://doi.org/10.4102/koedoe.v36i2.377.

Riccucci M. & Lanza B. (2014). Bats and insect pest control: a review. Vespertilio, 17, 161–169.

Rickart EA, Mercier JA, Henny LR. (1999). Cytogeography of Philippine bats (Mammalia; Chiroptera). Proceedings of the Biological Society of Washington, 112, 453–469. https://doi.org/10.5281/zenodo.13442161.

Ruedas LA, Lee TE, Bickman J and Schlitter DA. (1990). Chromosomes of five species of vespertilionid bats from Africa. Journal of Mammalogy, 71(1), 94. https://doi.org/10.2307/1381324.

Ruedi M, Csorba G, Lin LK and Chou CH. (2015). Molecular phylogeny and morphological revision of Myotis bats (Chiroptera: Vespertilionidae) from Taiwan and adjacent China. Zootaxa, 3920(1), 301–342. https://doi.org/10.11646/zootaxa.3920.2.6.

Schlitter DA, Rautenbach IL, Wohlhuter DA. (1980). Karyotpyes and morphometrics of two species of *Scotophilus* in South Africa (Mammalia: Vespertilionidae). Annals of the Transvaal Museum, 32, 231–239. https://doi.org/10.2307/1381324.

Simmons NB (2005). Order Chiroptera. In: Wilson, D. & Reeder, D.M. (Editors). Mammal Species of the World: A Taxonomic and Geographic Reference. Smithsonian Institution Press, Washington DC.

Simmons NB. & Conway TM. (2003). Evolution of ecological diversity in bats. In: Kunz, T.H. & Fenton, M.B. (Editors). Bat Ecology. University of Chicago Press, Chicago, Illinois. Pp. 493–535.

Sotero CG, Baker RJ, Volleth M. (2017). Chromosomal evolution in Chiroptera. Genes, 8(10), 272. https://doi.org/10.3390/gene8100272.

Sreepada K, Koubinová D, Konecny A, Koubek P, Rab P, Rábová M and Zima J. (2008). Karyotypes of three species of molossid bats (Molossidae, Chiroptera) from India and West Africa. Folia Zoologica, 57, 347–357. https://www.ivb.cz/wp-content/uploads/57_347-357.pdf. ISSN 0139-7893.

Stevens RD. & Willig MR. (2002). Geographical ecology at the community level: perspectives on the diversity of New World bats. Ecology, 83, 545–560. https://doi.org/10.1890/0012-9658(2002)083[0545:GEATCL]2..0.CO;2.

Strelkov PP. (2006). The crisis of the polytypic species concept is illustrated by the genus Plecotus. Plecotus, 9, 3–7.

Teeling EC, Dool S, Springer MS. (2012). Phylogenies, fossils and functional genes: the evolution of echolocation in bats. In: Gunnell, G. and Simmons, N. (Editors). Evolutionary History of Bats: Fossils, Molecules and Morphology. Cambridge University Press, Cambridge. Pp. 1–22. https://doi.org/10.1016/.tree.2006.01.001.

Tiunov MP (2011). Distribution of the bats in the Russian Far East. Proceedings of the Japan-Russia Cooperation Symposium on the Conservation of the Ecosystem. Okhotsk, Sapporo, pp. 359–369. https://doi.org/10.5772/intechopen.78767.

Volleth M. & Heller KG (2012). Variations on a theme: karyotype comparison in Eurasian myotis species and implications for phylogeny. Vespertilio, 16, 329–350.

Volleth M, Heller KG, Fahr J. (2006). Phylogenetic relationships of three "Nycticeiini" genera (Vespertilionidae, Chiroptera, Mammalia) as revealed by karyological analysis. Mammalian Biology, 71(1), 1–12. https://doi.org/10.1016/j.mambio.2005.09.001.

Volleth M, Heller KG, Pfeiffer RA and Hameister HA (2002). A comparison of zoo fish analysis in bats elucidates the phylogenetic relationships between Megachiroptera and five microchiroptera formulas. Chromosome Research, 10, 477–497. https://doi.org/10.1023/a:1020992330679.

Volleth M, Son NT, Wu Y, Li Y, Yu W. et al. (2017). Comparative chromosomal studies in *Rhinolophus formosae* and *R. luctus* from China and Vietnam: elevation of *R. l. lanosus* to species rank. Acta Chiropterologica, 19(1), 41–50. https://doi.org/10.3161/15081109ACC2017.19.1.003.

Wang LF, Walker PJ, Poon LL. (2011). Mass extinctions, biodiversity, and mitochondrial function: are bats "special" as reservoirs for emerging viruses? Current Opinion in Virology, 1(6), 649–657. https://doi.org/10.1016/j.coviro.2011.10.013.

Wilson DE. & Reeder DM. (2005). *Mammal Species of the World: A Taxonomic and Geographic Reference*. 3rd Edition. Johns Hopkins University Press, Baltimore. https://doi.org/10.1644/06-MAMM-R-422.1.

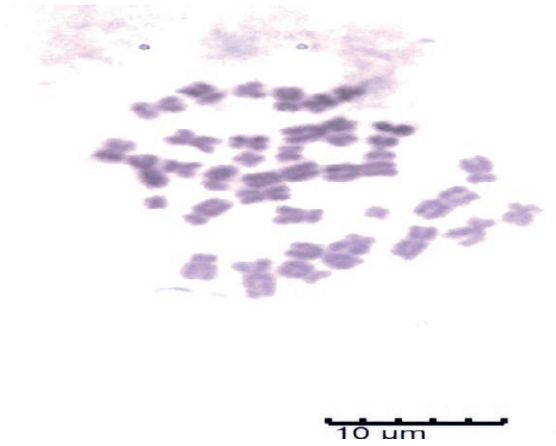

Plate 1A. Mitotic metaphase chromosome of *Epomophorus wahlbergi*;Sex. Female.

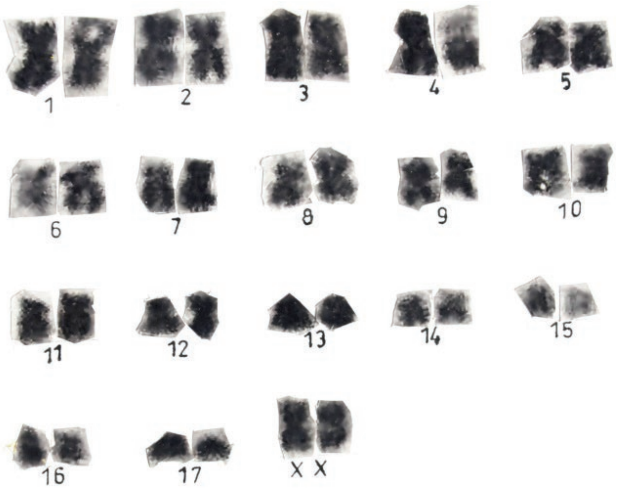

Plate 1B. The karyotype of *Epomophorus wahlbergi.*

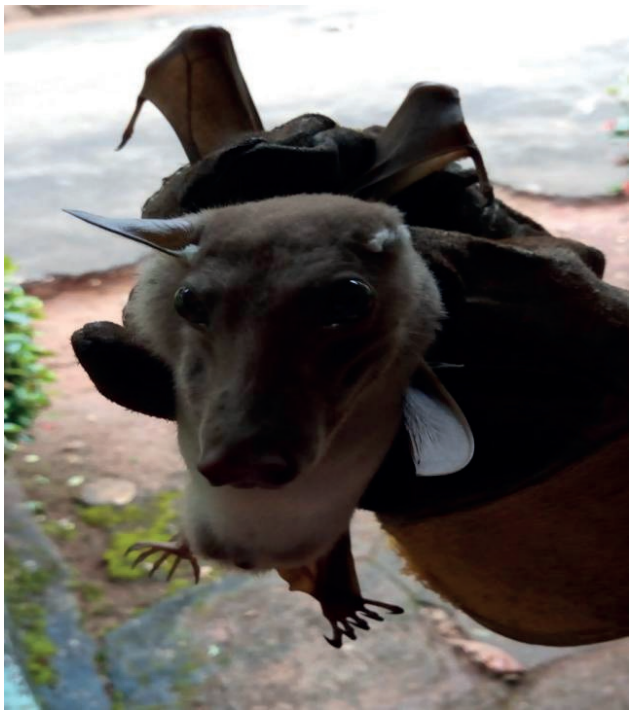

Plate 1C. A diagram of *Epomophorus wahlbergi.*

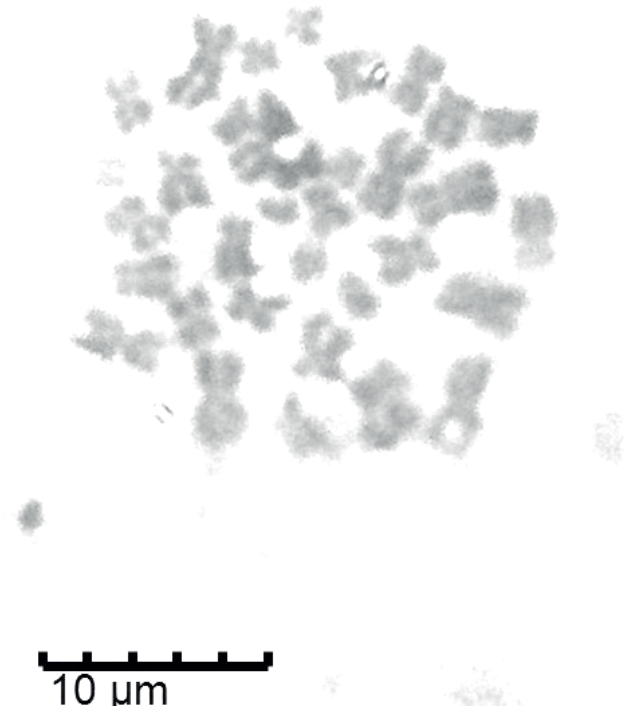

Plate 2A. Mitotic metaphase chromosome of *Epomophorus gambianus*; Sex. Female.

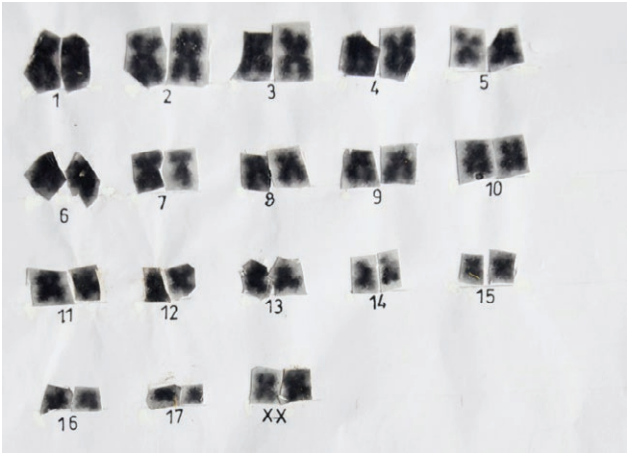

Plate 2B. The karyotype of *Epomophorus gambianus.*

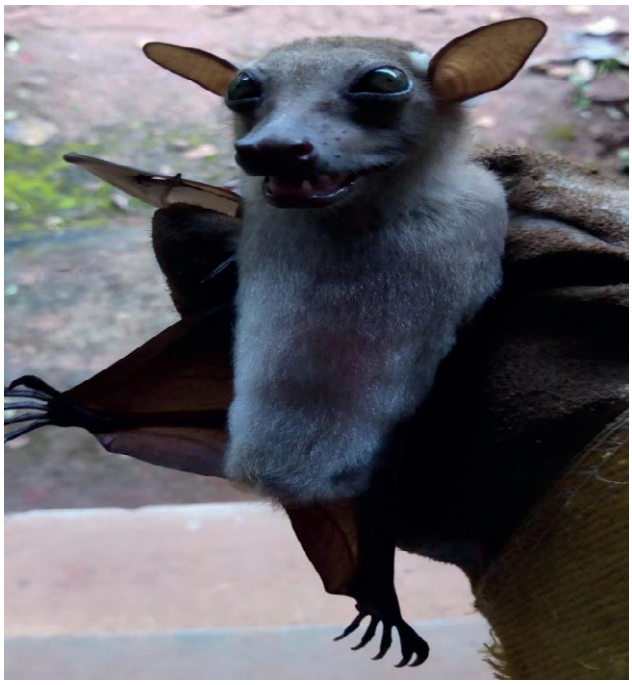

Plate 2C. A diagram of *Epomophorus gambianus.*

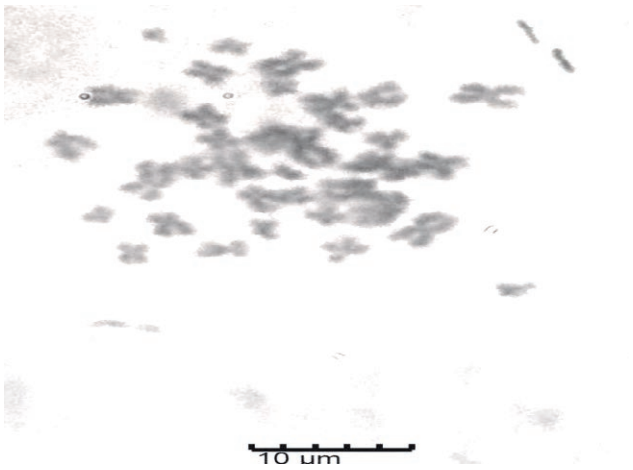

Plate 3A. Mitotic metaphase chromosome of *Microteropus pusillus*; Sex. Female.

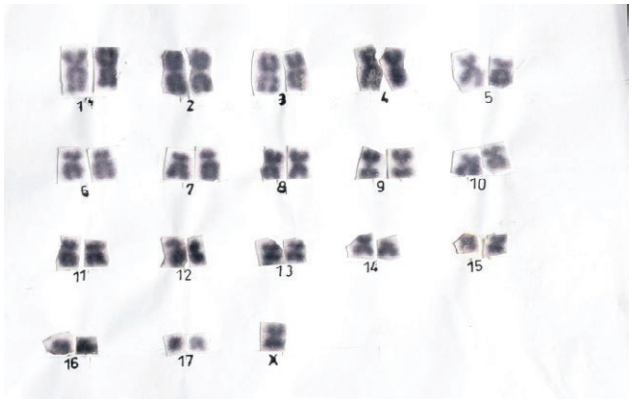

Plate 3B. The karyotype of *Microteropus pusillus.*

Plate 3C. A diagram of *Microteropus pusillus.*

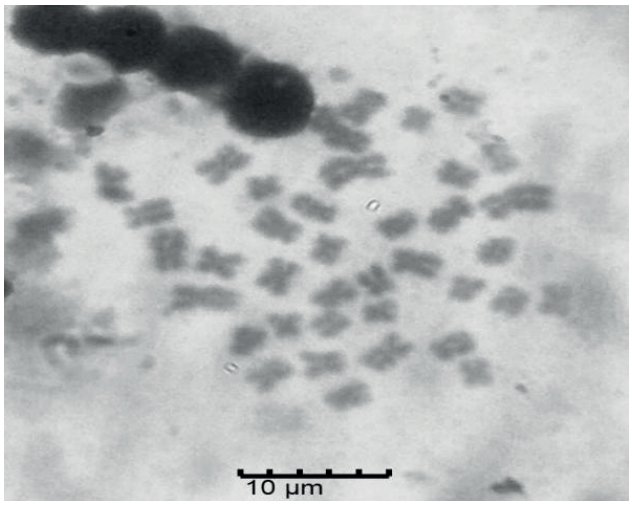

Plate 4A. Mitotic metaphase chromosome of *Nycteris major;* Sex. Male.

Plate 4B. Mitotic metaphase chromosome of *Nycteris major;* Sex. Female.

Plate 4C. The karyotype of *Nycteris major;* Sex. Male.

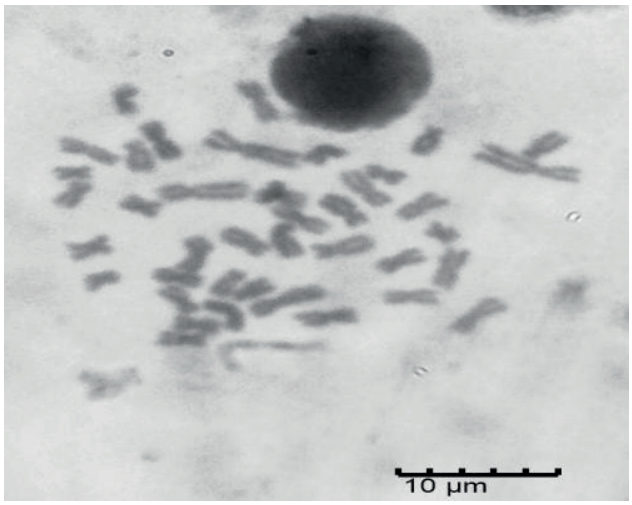

Plate 4D. The karyotype of *Nycteris major;* Sex. Female.

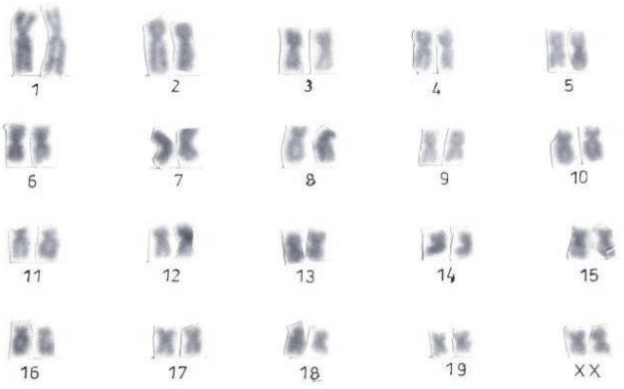

Plate 4E. A diagram of *Nycteris major;* Sex. Male.

Plate 4F. A diagram of *Nycteris major;* Sex. Female.

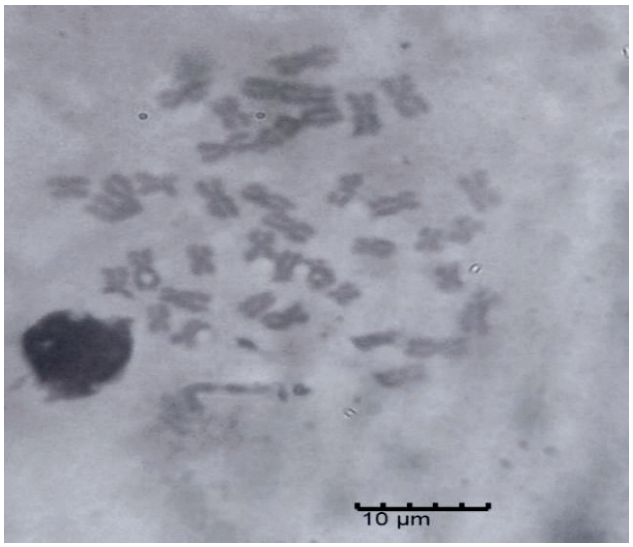

Plate 5A. Mitotic metaphase chromosome of *Nycteris grandis*; Sex**.** Female.

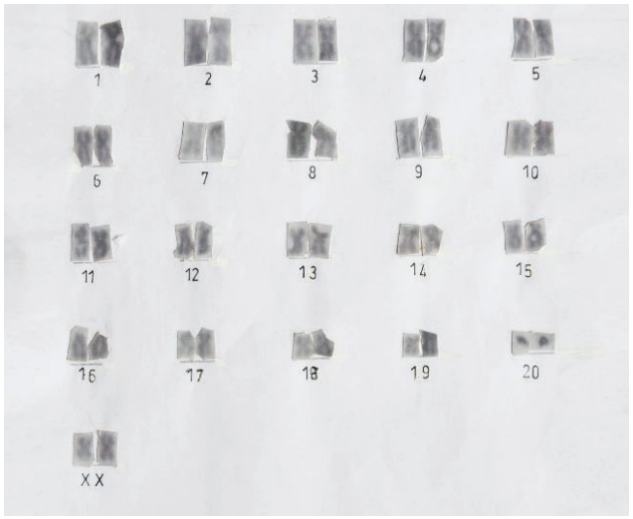

Plate 5B. The karyotype of *Nycteris grandis*; Sex. female.

Plate 5C. A diagram of *Nycteris grandis.*

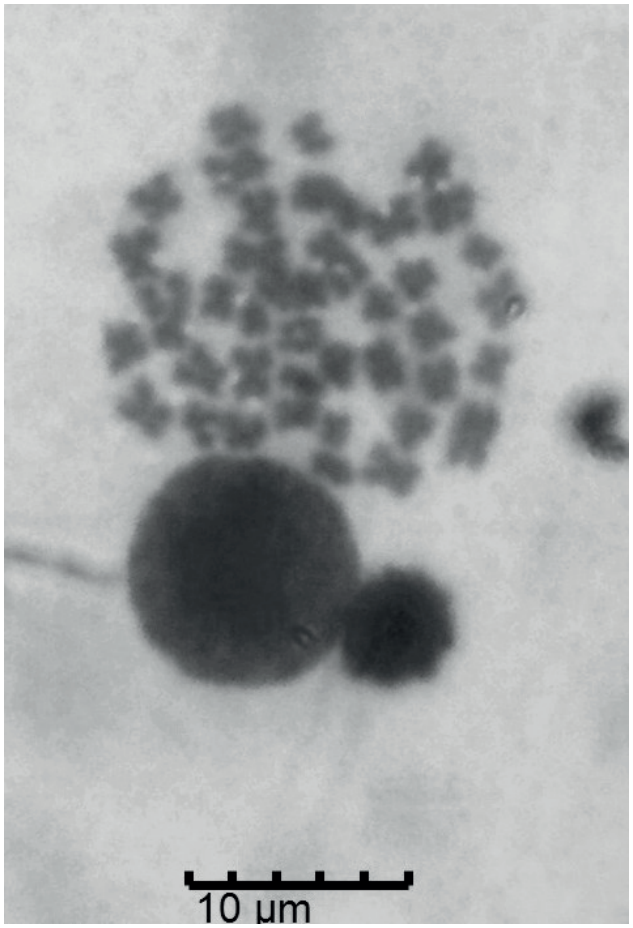

Plate 6A. Mitotic metaphase chromosome of *Nycteris arge;* Sex. Female.

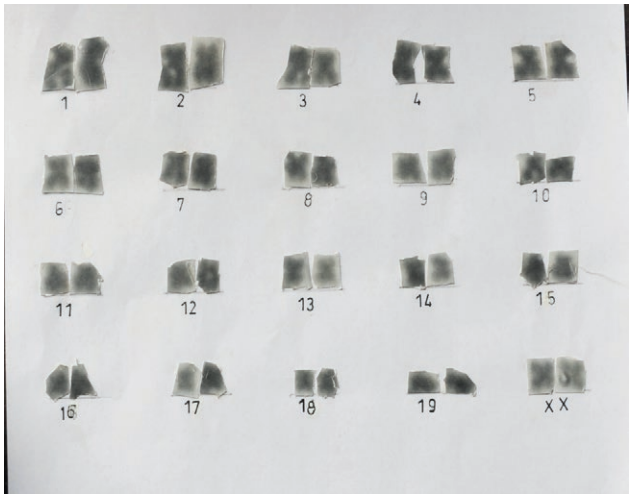

Plate 6B. The karyotype of *Nycteris arge.*

Plate 6C. A diagram of *Nyceris arge.*

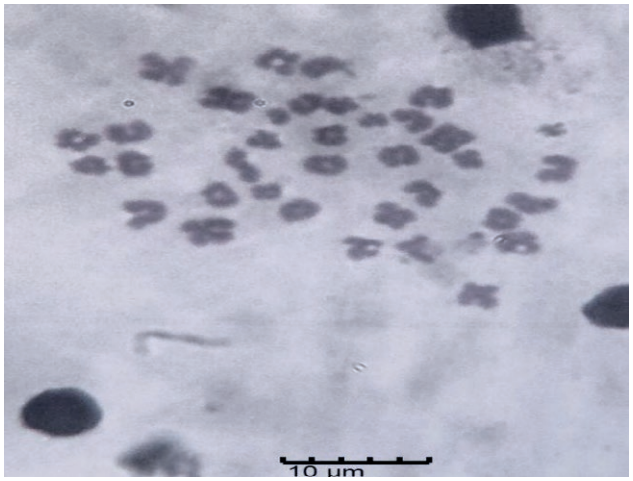

Plate 7A. Mitotic metaphase chromosome of *Scotophilus diaganii*; Sex. Male.

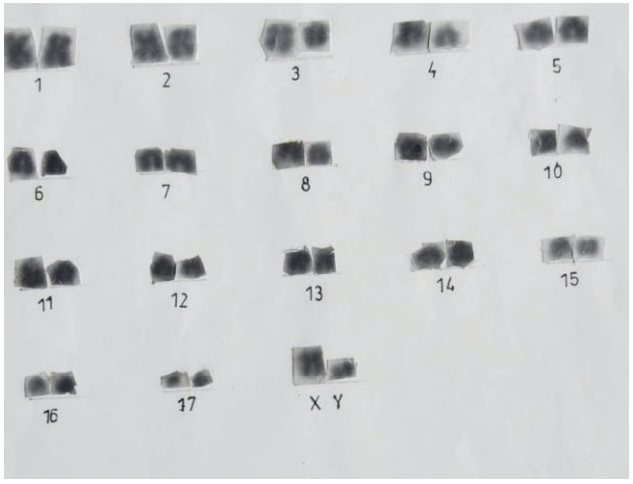

Plate 7B. The karyotype for *Scotophilus diaganii.*

Plate 7C. A diagram of *Sctotophilus diaganii.*

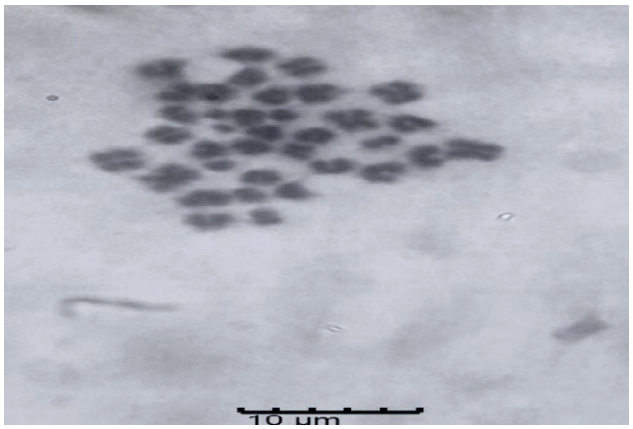

Plate 8A. Mitotic metaphase chromosome of *Scotophilus leucogaster*; Sex. Female.

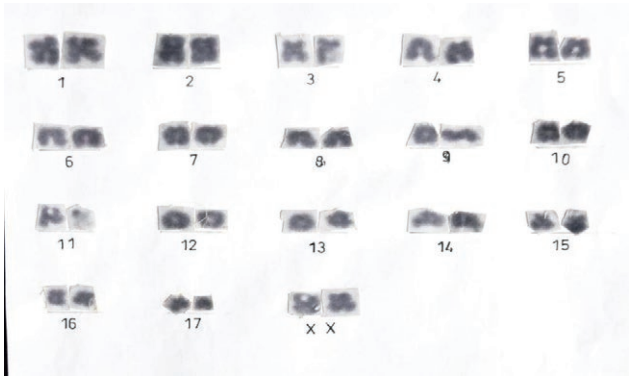

Pate 8B. The karyotype for *Scotophilus leucogaster.*

Plate 8C. A diagram of *Scotophilus leucogaster.*

APPENDIX

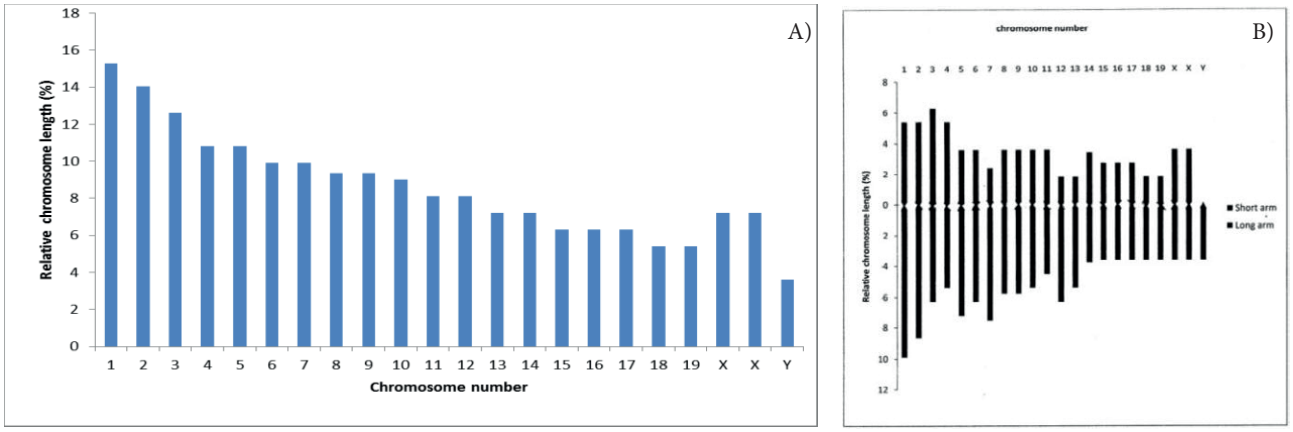

Material 1. Ideogram of the karyotype of *Epomophorus wahlbergi* showing. (A) length variations (xxy shows sex chromosome of the male bat) and (B) centromeric locations.

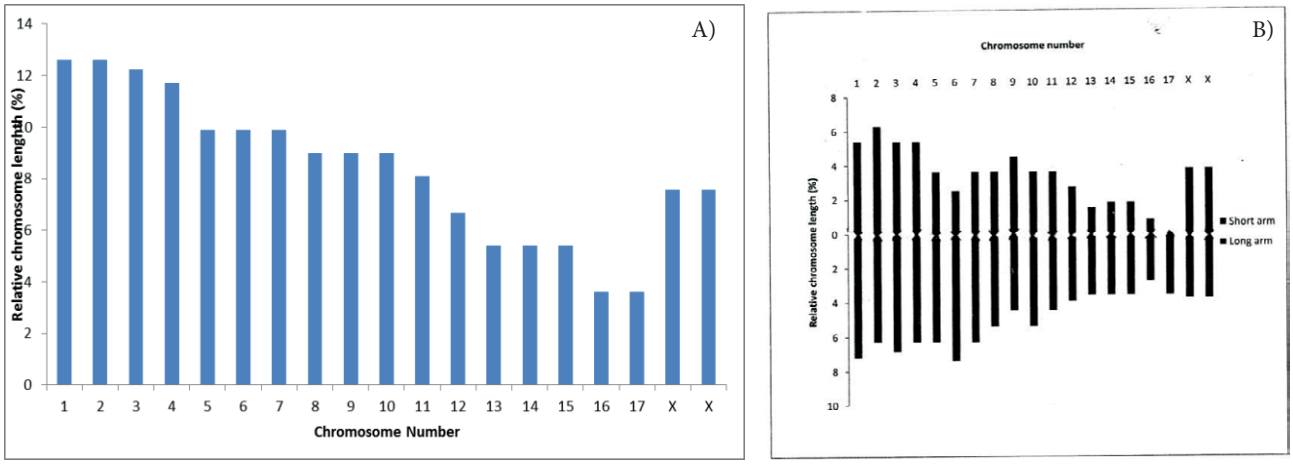

Material 2. Ideogram of the karyotype of *Epomophorus gambianus* showing. (A) length variations (xx shows sex chromosome of the female bat) and (B) centromeric locations.

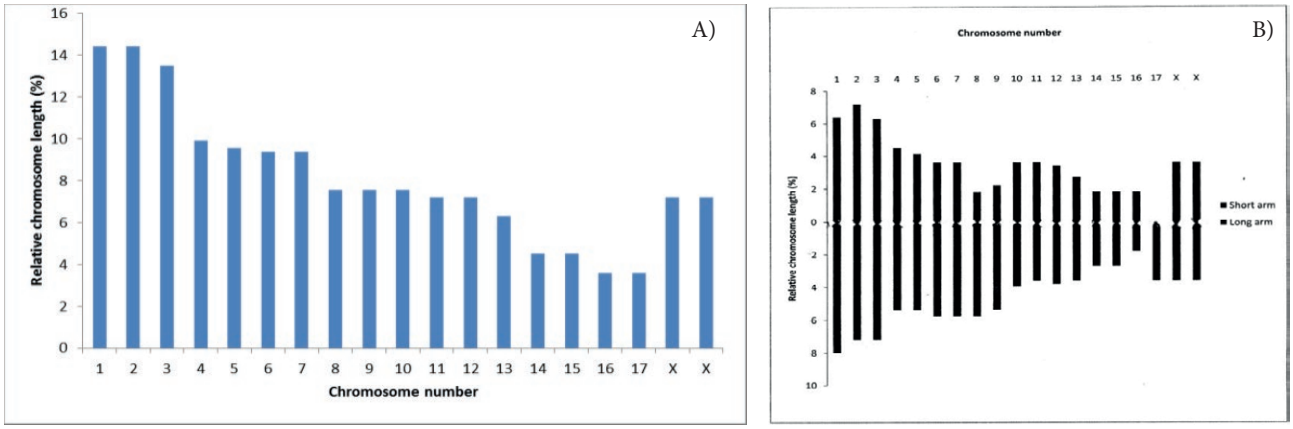

Material 3. Ideogram of the karyotype of *Microteropus pusillus* showing. (A) length variations (xx shows sex chromosome of the female bat) and (B) centromeric locations.

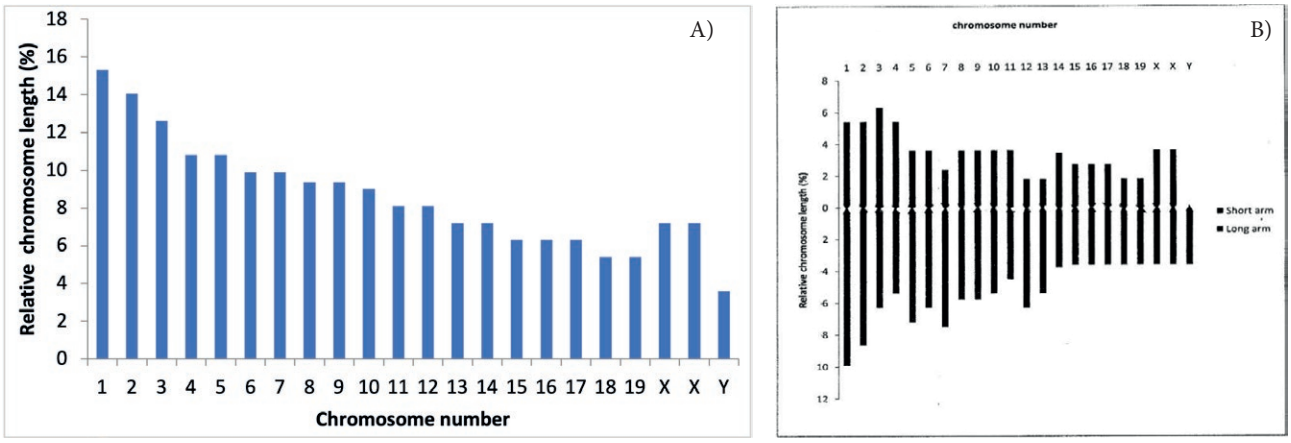

Material 4. Ideogram of the karyotype of *Nycteris major* showing. (A) length variations (xy shows sex chromosome of the male bat) and (B) centromeric locations.

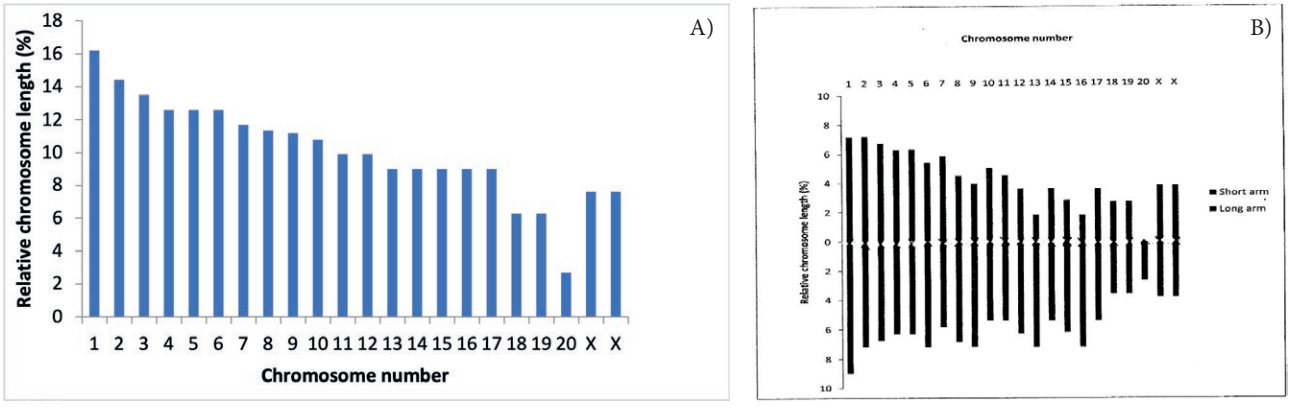

Material 5. Ideogram of the karyotype of *Nycteris grandis* showing. (A) length variations (xx shows sex chromosome of the female bat) and (B) centromeric locations.

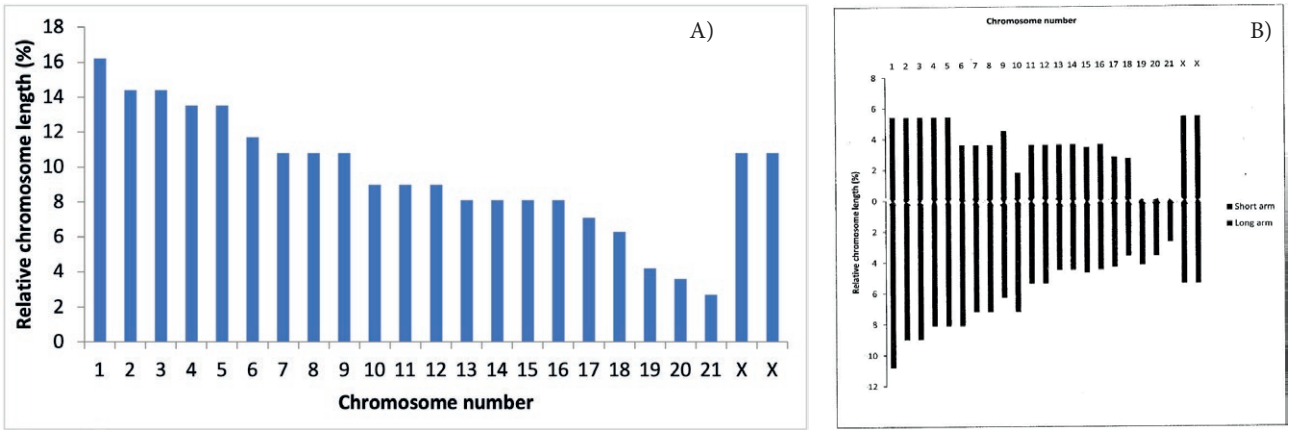

Material 6. Ideogram of the karyotype of *Nycteris* sp. showing. (a) length variations (xx shows sex chromosome of the female bat) and (b) centromeric locations.

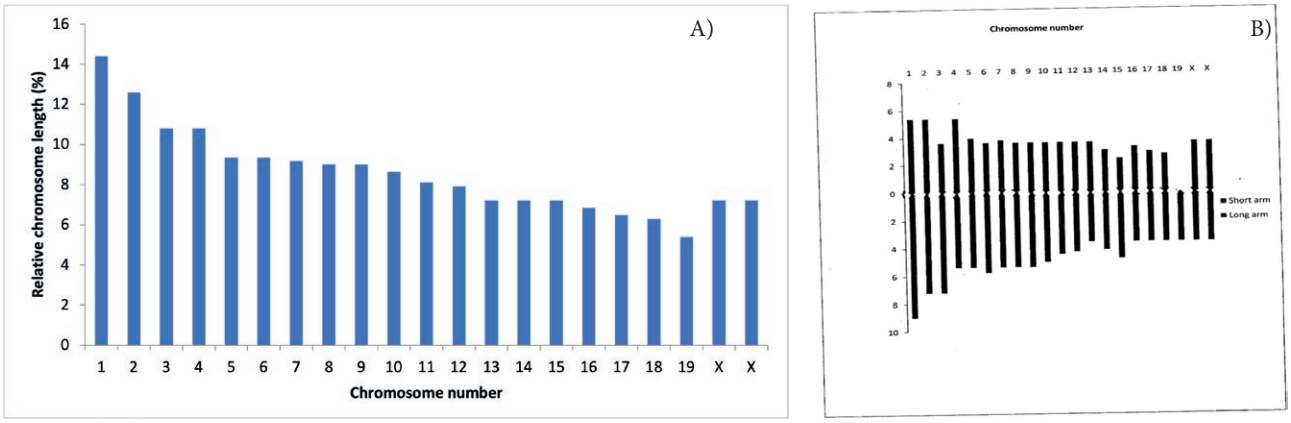

Material 7. Ideogram of the karyotype of *Nycteris arge* showing. (A) length variations (xx shows sex chromosome of the female bat) and (B) centromeric locations.

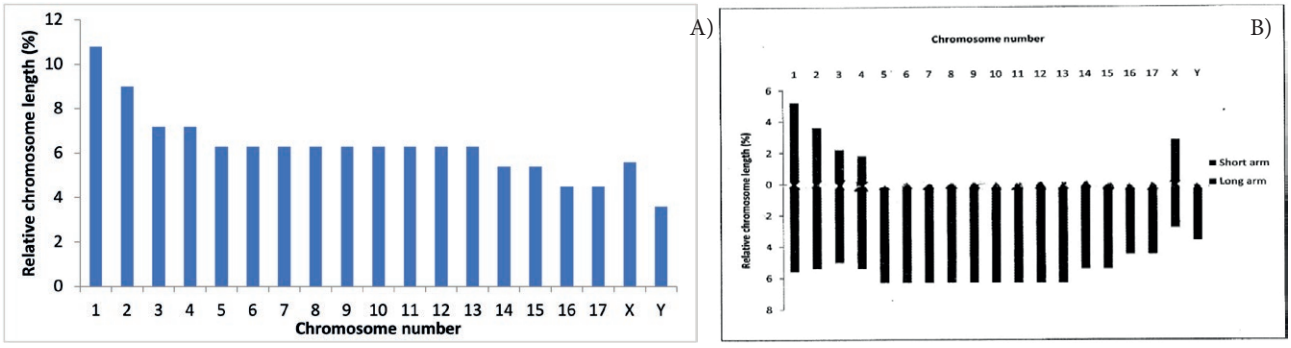

Material 8. Ideogram of the karyotype of *Scotophilus diaganii* showing. (A) length variations (xy shows sex chromosome of the male bat) and (B) centromeric locations.

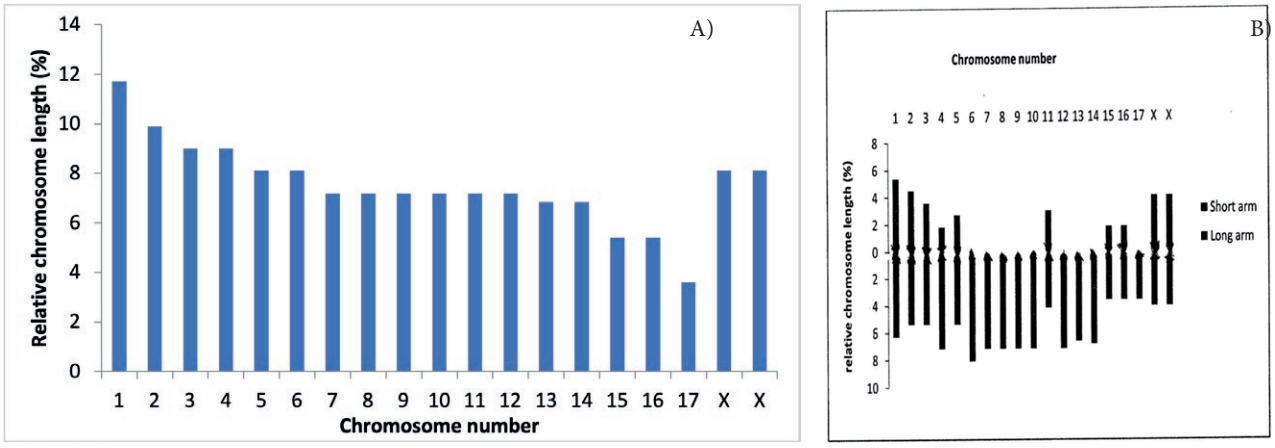

Material 9: Ideogram of the karyotype of *Scotophilus lecuogaster* showing: (A) length variations (xy shows sex chromosome of the male bat) and (B) centromeric locations.

Material 10. Giemsa Stain Preparation.

0.5g of Giemsa powder was dissolved in 33ml glycerol and kept in an Erlmyer bottle in a dark compartment overnight. The next day, it was heated in a water bath set at 60°C for 2 hours and allowed to cool, after which 33 ml of methanol was added and thoroughly mixed. This solution was then stored in an amber-coloured bottle as the stock Giemsa stain. 6% of the stock Giemsa stain was diluted as described below:
3 ml of the Giemsa stain, was diluted to 50 ml in Phosphate buffer, P.H. 6.8. The phosphate buffer was prepared fresh each time before usage by mixing 25 ml each of 9.464g of M/15 Na2HPO4 and 9.073g of M/15 KH2PO4, simultaneously.

Material 11. Chromosome Nomenclature in Relation to Centrometric Indices (Abraham and Prasad, 1982).

Nomenclature	Notation	R1 S/L	R2 L/S	I1 100s/c	I2 100L/C
Median	M	1.00	1.00	50.00	50.00
Nearly median	Nm	0.99–0.61	1.01–1.63	49.99–38.01	50.01–61.99
Nearly submedian	nsm(-)	0.60–0.34	1.64–2.99	38.00–25.00	62.00–74.99
Sub-median	SM	0.33	3.00	25.00	75.00
Nearly submedian	nsm(+)	0.32–0.23	3.01–4.26	24.95–18.20	75.01–81.80
Nearly subterminal	nst(-)	0.22–0.15	4.27–6.99	18.10–12.51	81.81–87.49
Subterminal	ST.	0.14	7.00	12.50	87.50
Nearly subterminal	nst(+)	0.13–0.07	7.01–14.38	12.49–5.01	87.51–94.99
Nearly terminal	nt	0.06–0.01	14.39–19.99	5.00–0.01	95.00–99.99
Terminal	T	0.00	0.00	0.00	100.00

Caryologia
International Journal of Cytology, Cytosystematics and Cytogenetics

Firenze University Press
https://riviste.fupress.net/index.php/caryologia

OPEN ACCESS

Citation: Verma, R., Kushwaha, B., Afaq, U., Baisvar, V. S., Maurya, S., Kumar, M. S., Dasmandal, T., Mishra, A. K., Kumar, R. & Sarkar, U. K. (2025). Bioinformatic analysis and characterization of BAC clones of *Clarias magur* (Hamilton,1822) using FISH and BAC end sequencing. *Caryologia* 78(1): 27-40. doi: 10.36253/caryologia-3196

Received: January 26, 2025

Accepted: June 21, 2025

Published: October 1, 2025

Data Availability Statement: All relevant data are within the paper and its Supporting Information files.

Competing Interests: The Author(s) declare(s) no conflict of interest.

Bioinformatic analysis and characterization of BAC clones of *Clarias magur* (Hamilton,1822) using FISH and BAC end sequencing

Rashmi Verma[1,2], Basdeo Kushwaha[1,*], Uzma Afaq[2,*], Vishwamitra Singh Baisvar[1], Satyamvada Maurya[1], Murali S Kumar[1], Tanwy Dasmandal[1], Akhilesh Kumar Mishra[1] Ravindra Kumar[1], Uttam Kumar Sarkar[1]

[1] *Genomics and Computational Resources Division, ICAR-National Bureau of Fish Genetic Resources, Canal Ring Road, P.O. Dilkusha, Lucknow-226 002, India*
[2] *Department of Biosciences, Integral University, Kursi Road, Lucknow-226 026, India*
*Corresponding authors. Email: basdeo.kushwaha@icar.gov.in; uzmaafaq89@gmail.com; uzmaafaq@iul.ac.in

Abstract. The clones of BAC library combined with FISH are an excellent tool for mapping and identifying full-length genes. The present study was to sequence, mine and characterize the BAC clones of *Clarias magur* (*magur*) genome. The end sequences of the BAC clones were bioinformatically mapped onto the genome scaffolds of *magur* to identify and locate the genes in each clone and FISH was utilized to locate clones on specific chromosomes of *magur*. A total of 13 BAC clones could be mapped using BAC end sequences on 12 genome scaffolds of *magur*. From the 13 clones, 34 genes were mined, annotated and characterized. Physical mapping using BAC-FISH signal was used to localize two clones, 012H23 and 012H7 on 11th and 14th chromosome pairs of *magur*. The gene enrichment analysis revealed involvement of several genes in growth and regulatory processes, such as protein neddylation and metal ion transport. PPI Network analysis revealed two types of interactions among 11 nodes and between 10 edges; and 4 genes (*ash2l, cnot2, lin7c, uba3)* were identified to be important. The study reveals the presence of important genes on the 13 undertaken clones, making this a useful genomic resource. The FISH probe could not only be helpful in generation of basic information of gene location for identification of genes on the chromosomes as a chromosome marker, but also in detection of chromosomal defects arisen due to genetic mutation occurred if any on a particular location of reported genes in *C. magur*.

Keywords: BAC clones, *Clarias magur*, end sequencing, FISH, PPI, SDG, synteny.

INTRODUCTION

Catfish is commercially and economically an important group in aquatics and fisheries. The species *Clarias magur* (magur), which belongs to the Clariidae family, is popular because of its flavor and therapeutic qualities and is found throughout India, Nepal, Bhutan, and Bangladesh (Ng and Kotte-

lat, 2008; Devassy et al., 2009). The species is facing risks from overexploitation, wetland conversion, widespread illegal introduction of invasive *C. gariepinus* species and pesticide use in agricultural areas. According to the IUCN Red List (2010), *magur* is currently listed as endangered species because of several identified and unidentified reasons and most importantly the disappearing breeding habitats and its population in India. A lack of appropriate management strategies may lead to further critical decline for the species in the years to come (Mishra et al.,2019). The United Nation is also concerned towards the people, planet and prosperity and set sustainable development goals (SDGs) as its action agenda. Conservation of fish genetic resources through proper planning, replenishing of fisheries and sustainable utilization of fish as food could be a better way to save our planet earth from over exploitation of water bodies and help in achieving the SDG no. 2 & 14. Owing to the species' commercial significance, the efforts are being made to conserve it through restoration, and enhance its genetic makeup for future expansion.

Genetic characterization is an important step towards the genetic conservation of a species. There are several methodologies for genetic characterization of a fish species and, construction of bacterial artificial chromosome (BAC) library of a fish species is an important genomic resource. Fertility factor (F-) based plasmid vectors are known as bacterial artificial chromosomes (BACs) reproduce steadily at low copy numbers (Woo et al., 1994). According to Shizuya et al. (1992), the BAC clones' large insert capacity allows them to carry whole genes with flanking distant regulatory DNA that provide signals for proper spatiotemporal gene expression. For whole genome sequencing, large insert DNA fragments of an organism between 100 and 300 kb into BAC clones were used in case of human genome project and some of plant species. BAC clones insert DNA are also been used for physical gene mapping in the past in several studies.

For fluorescent in situ hybridization (FISH), BAC clones are useful probes because they can suppress repetitive DNA sequences, making single-copy sequences detectable (Hanson et al., 1995; Jiang et al., 1995). Chromosome mapping, genome sequencing, high-throughput BAC end (BE) sequencing, and other genomic studies can all be performed using BAC extracted DNA (Osoegawa et al., 2001, Osoegawa et al., 2004). Using clone as a probe in FISH is a dependable cytological method for chromosome identification. Genome mapping is vital for identifying and characterizing the genetic basis of phenotypic features in organisms and detecting specific genes of interest. To create a physical connection with unknown targeted sequences, BAC clones provide a practical and trustworthy landmark. BAC-FISH tool will help us assess how well a linkage map may create and covers a saturated genetic map on a broad scale. Some BAC based studies have been reported for *C. magur* but still there is need of expansion more such works to build detailed information on physical localization of genes using BAC library of *C. magur.* The present study aimed to analyze magur BAC clones using their end sequences and whole genome information for gene and SSR mining and pathway analysis which could aid in genomic selection programs or genetic diversity studies and complement aquaculture production.

MATERIAL AND METHODS

BAC library construction

Using genomic high molecular weight DNA from magur blood, the BAC library was built as part of an earlier research initiative supported by the Indian government's Department of Biotechnology in New Delhi. In brief, the *HindIII* restriction enzyme was used to digest genomic DNA, size selection was performed and selected size insert DNA fragments were attached to the pCC1BAC vector (Epicentre Biotechnologies, Madison, WI, USA). Subsequently, approximately 115kb DNA pieces were converted and propagated in Escherichia coli Phage Restraint DH10~ competent cells (Invitrogen, Burlington, ON, Canada). Using a Genetix Qpix 2 Automated Arraying Bacterial Colony Picker (Molecular Devices, Sunnyvale, CA, USA), the modified BAC clones were robotically lifted, put on plates, and kept in Luria Broth (LB) culture.

BAC clone culture, DNA isolation and BAC end sequencing

From the BAC library, consisting of 55,141 clones stored in 144 plates each of 384-well format, a plate (ID: 012A) was chosen at random for BAC end sequencing and BAC-FISH. After thawing the plate, 15 µl of each clone was transferred to 15 ml centrifuge tubes for revival, culture and insert DNA isolation using previously reported methodology (Kumar et al., 2020). T7 forward (5'TAATACGACTCACTATAGGG3') and pbRP1 reverse (5'CTCGTATGTT GTGTGGAATTGTGAGC3') primers were used to sequence both ends of the clones on an ABI 3500 Genetic Analyzer (Thermo Fisher Scientific, USA). The BAC end sequences (BESs) that were produced were then mapped onto the magur genome scaffolds and examined using a custom Perl script and the Blast tool.

For insert DNA isolation and BAC-FISH, the clones that were bioinformatically positioned on the same scaffolds were merged into a single culture.

Chromosome preparation, probe labelling and BAC-FISH

With the help of a fisherman, live and healthy *magur* specimens were collected from a nearby pond in Lucknow, Uttar Pradesh, India, and brought to the lab in a live form. Using a conventional procedure, the metaphase chromosomal spreads were prepared *in vivo* from the anterior kidney cells. To make the DNA probe for BAC-FISH, one μg of isolated BAC insert DNA was taken from every clone. Using the direct labeling "nick translation" method, the DNA was tagged with the red fluorophore tetramethyl-rhodamine-5-dUTP (Roche, Basel, Switzerland) and green fluorescein-12-dUTP (Fermentas, Vilnius, Lithuania). Metaphase chromosomal spreads that were two to three days old were subjected to FISH for 60 minutes at 95 °C (Kumar et al., 2017). VectaShield mounting media (Vector Labs, Burlingame, CA, USA) containing DAPI and antifade was used to counterstain the chromosomes for 60 minutes after hybridization. Two band filters were then used to view the slides under a Leica fluorescence microscope (Wetzlar, Germany): DAPI (excitation at 340–380 nm, emission at 461 nm) for chromosome visualization, I3 (excitation at 450–490 nm) for fluorescein-labeled probe visualization, and N2.1 (excitation at 515–560 nm, emission at 595–605 nm) for rhodamine-labeled probe visualization. For probe signal screening, about 50 metaphase spreads per clone were analyzed. A consensus karyotype was created after establishing karyotypes from good spread for every hybridized clone.

BAC mapped genes and functional description

Four hybridized clones with an e-value of 10-5 on the *magur* genome assembly (NCBI's Genome Acc. No. QNUK00000000) had their BESs aligned using the BLASTN method. For further examination, the BESs that were aligned on the same scaffold were removed. Simple sequence repeats (SSRs) found in the genes identified from the clones were mined using the MISA bioinformatic program.

Comparative genomics and phylogenetics analysis

Ensembl and NCBI databases were searched for *zebrafish (Danio rerio*) and *channel catfish* (*Ictalurus punctatus*) genomes as queries and gene locations as well as chromosome information were retrieved to perform synteny analysis of annotated clone genes. Circos plot (Krzywinski et al., 2009) was used to visualize synteny among 3 fishes *(magur, channel catfish* and *zebrafish*) focusing on genes having same *magur* scaffolds but distinct positions on chromosomes. Phylogenetic study was performed using gene sequences from the *channel catfish, zebrafish* and *magur* scaffolds using MEGA tool (Kumar et al., 2016) and also using interactive tree of life (iTOL) v5.5 tool (Letunic et al., 2019) was used to visualize the evolutionary lineages and DNA sequences phylogenetics structure.

Network analysis of proteins to proteins

The STRING 12.0 (Szklarczyk et al., 2023) database was used to analyze the protein-protein interaction (PPI) networks of the annotated genes, and the Cytoscape v3.6.0 program was used to show the results (Shannon et al., 2003). In order to guarantee interactions with a high degree of confidence and to be included in the interaction network, the network was constructed using a strict confidence score threshold of 0.04.

Functional annotation and enrichment analysis

The identified genes were functionally annotated using Gene Ontology (GO) using BLAST and the UniProtKB/Swiss-Prot databases (http://www.uniprot.org/). The BLOSUM62 substitution matrix with an E-value of less than 1e-4 and a similarity of greater than 80% were the predetermined criteria used to pick BLAST hits. The GO framework was employed to annotate gene sets and KEGG pathway database (Kanehisa & Sato ,2020) was used to obtain information on molecular interactions and network reactions. The PANTHER gene ontology tool was used to perform functional enrichment analysis of the cluster network's nodes in order to uncover functionally enriched gene networks inside the GO Biological Process and to learn more about the biological significance of the genes.

RESULTS

BAC end mapping and gene mining

Sequence quality check resulted in a good quality sequence for 32 clones, out of which only 13 BAC clones could be sequenced with both forward and reverse

end sequences, rest 19 had either forward OR reverse sequence. BESs of these 13 BAC clones were only used for further downstream bioinformatic analysis. Good sequence size was indicated by the 13 clones' forward and reverse end sequence lengths, which varied from 429 bp (forward end sequence of clone ID: 012G22) to 951 bp (reverse end sequence of clone ID: 012A12) (Table 1). The magur genome's BES mapping showed that they were dispersed throughout 12 scaffolds. The size of the scaffolds varied from 4,200,247 bp (ID: 012H23 on Scaffold21) to 340,296 bp (ID: 012H1 on Scaffold657). The lengths of the clones were predicted bioinformatically by aligning both end sequences of the clones on the scaffolds of the magur genome, and the clones size ranged from 45.98 kb (ID: 012J12 on Scaffold22) to 143.307 kb (ID: 012A12 on Scaffold111). A total of 34 genes were identified, annotated and characterized after mapping BESs on magur genome scaffolds (Table 2, Supplementary Table 1). One BAC clone (012H23) contained 5 genes, 2 clones (012H7, 012H21) contained 4 genes, 3 clones (012H8, 012J12, 012G22) contained 3 genes, 5 clones (012H15, 012H1, 012A12, 012B15, 012A15) contained 2 genes, while 2 clones (012A22, 012G24) were found to possess only one gene each. The mean size of all clones was around 113.196 kb. A total of 1275 SSRs could identified from the sequences of all 13 BAC clones using MISA tool (Table 1). BAC clone ID: 012H1 contained maximum SSRs (149), while clone ID: 012J12 contained least SSRs (33).

Chromosomal complements and BAC-FISH

Metaphase chromosomal complements were generated manually with a diploid chromosome (2n) count of 50. According to the morphology and chromosome count, the karyotype was determined to be 14m + 20sm + 8st + 8t with a fundamental arm number (FN) of 90. Clone ID: 012H23, contained maximum 5 genes (Table 1) and labelled with green colour fluorescein-12-dUTP, was mapped on the 11th pair of sub-metacentric chromosomes (Fig. 1), while clone 012H7, contained 4 genes (Table 1) and labelled with red colour rhodamine-5-dUTP, was located on the fourteenth sub-metacentric chromosomal pair. (Fig. 2). The chromosomes' genes were clearly identified, and were compared with zebrafish and channel catfish for the synteny (Fig. 3) which represents the conserveness of the genes across these species.

Functional enrichment and gene ontology analysis

The 'cellular anatomical (GO:0110165)' had the maximum number (13) of GO terms (Fig. 4). There are genes encoding proteins localized to specific molecular function such as the nucleus (e.g. *MIER3A*, *UNC50*), cytoplasmic vesicle membrane (e.g. *SLC39A13*) and lysosomal membrane (e.g. *SPNS1*). Enhancement of cellular constituents such as 'cellular anatomical entity', 'protein-containing complex' point towards cellular structures and protein interactions. Higher-order processes, like 'multicellular organismal process' and 'response to stimulus', hint at responses to environmental cues and organismal functions. Notably, enrichment in 'binding' and 'catalytic activity' suggests significant involvement in these functions within the studied context. Additionally, 'transcription regulator activity' and 'ATP-dependent activity' underscore their regulatory and energy-related roles. In

Table 1. Details of BAC clones end sequences mapped on *Clarias magur* genome.

S. No.	Clone ID	Scaffold mapped on *C. magur* genome	Scaffold length	Sequence length		BAC ends position mapped on *C. magur* scaffold		Estimated BAC size (kb)	Number of SSR on the BAC present	%GC content	No of Genes
1.	012H23	Scaffold 21	4200247	927	900	1536131	1653231	117.101	71	37.72	5
2.	012H7	Scaffold 27	3918154	907	618	1869141	1982924	113.784	81	38.41	4
3.	012H8	Scaffold65	2520177	698	518	1622436	1728132	105.697	120	40.78	3
4.	012H15	Scaffold72	2332806	802	892	603066	716705	113.64	82	38.3	2
5.	012H21	Scaffold222	1147004	573	582	694436	828095	133.66	130	38.65	4
6.	012J12	Scaffold22	4179625	799	898	2020754	2066733	45.98	33	39.11	3
7.	012G22	Scaffold68	2435928	429	310	243382	341745	98.364	62	38.6	3
8.	012H1	Scaffold657	340296	769	897	89407	211638	122.232	149	41.12	2
9.	012A12	Scaffold111	1875956	875	951	1206038	1325900	143.307	123	39.65	2
10.	012B15	Scaffold22	4179625	778	272	1788839	1911851	123.013	138	39.55	2
11.	012A15	Scaffold349	749303	859	338	359629	481144	121.516	68	39.57	2
12.	012A22	Scaffold368	723143	477	774	350497	444907	94.411	128	39.38	1
13.	012G24	Scaffold49	3144600	643	900	1454430	1593272	138.843	90	38.02	1

Table 2. Annotation of genes from Mapped scaffold at *C. magur* genome.

S. No.	From	Protein names	Gene Ontology (biological process)	Gene Ontology (cellular component)	Gene Ontology (molecular function)
1.	tmem17	Transmembrane protein 17	NA	ciliary membrane [GO:0060170]	symporter activity [GO:0015293]
2.	agbl2	Cytosolic carboxypeptidase 2 isoform X1	NA	NA	carboxypeptidase activity [GO:0004180]
3.	agbl2	Cytosolic carboxypeptidase 2 (ATP/GTP-binding protein-like 2) (Protein deglutamylase CCP2)	proteolysis [GO:0006508]	cell projection [GO:0042995]; centriole [GO:0005814]; cytosol [GO:0005829]	metallocarboxypeptidase activity [GO:0004181]; zinc ion binding [GO:0008270]
4.	Cnot2	CCR4-NOT transcription complex subunit 2 isoform X1	NA	NA	NA
5.	washc4	WASH complex subunit 7	NA	WASH complex [GO:0071203]	NA
6.	pdxp	Pyridoxal phosphate phosphatase	NA	NA	NA
7.	mier3a	Mesoderm induction early response protein 3-like	NA	nucleus [GO:0005634]	NA
8.	DAT39_003426	G protein-coupled receptor kinase (EC 2.7.11.-)	phosphorylation [GO:0016310]; signal transduction [GO:0007165]	NA	ATP binding [GO:0005524]; G protein-coupled receptor kinase activity [GO:0004703]
9.	ash2l	Set1/Ash2 histone methyltransferae complex subunit ASH2 isoform X2	methylation [GO:0032259]	Set1C/COMPASS complex [GO:0048188]	methyltransferase activity [GO:0008168]
10.	DAT39_006333	Serine/threonine-protein kinase SBK1-like	phosphorylation [GO:0016310]	NA	ATP binding [GO:0005524]; protein kinase activity [GO:0004672]
11.	nlrc3	NLR family CARD domain-containing protein 3	NA	cytoplasm [GO:0005737]; membrane [GO:0016020]	NA
12	wdr90	WD repeat-containing protein 90	NA	NA	NA
13.	CHIA	Acidic mammalian chitinase-like	carbohydrate metabolic process [GO:0005975]	NA	chitin binding [GO:0008061]; hydrolase activity, hydrolyzing O-glycosyl compounds [GO:0004553]
14.	CHIA	Acidic mammalian chitinase-like	carbohydrate metabolic process [GO:0005975]	NA	NA
15.	CHIA	Acidic mammalian chitinase-like	carbohydrate metabolic process [GO:0005975]	NA	chitin binding [GO:0008061]; hydrolase activity, hydrolyzing O-glycosyl compounds [GO:0004553]
16.	CHIA	Acidic mammalian chitinase-like	carbohydrate metabolic process [GO:0005975]	NA	NA
17.	uba3	NEDD8-activating enzyme E1 catalytic subunit (EC 6.2.1.64)	protein neddylation [GO:0045116]	NA	ubiquitin-like modifier activating enzyme activity [GO:0008641]
18.	mltF	Membrane-bound lytic murein transglucosylase F	NA	NA	NA
19.	lin7c	Protein lin-7 homolog C	exocytosis [GO:0006887]; protein transport [GO:0015031]	anchoring junction [GO:0070161]; plasma membrane [GO:0005886]	NA

(Continued)

Table 2. (Continued).

S. No.	From	Protein names	Gene Ontology (biological process)	Gene Ontology (cellular component)	Gene Ontology (molecular function)
20.	mybpc3	Myosin-binding protein C, cardiac-type (C-protein, cardiac muscle isoform)	NA	NA	NA
21.	slc39a13	Zinc transporter ZIP13 (Solute carrier family 39 member 13) (Zrt- and Irt-like protein 13)	NA	cytoplasmic vesicle membrane [GO:0030659]	metal ion transmembrane transporter activity [GO:0046873]
22.	pcm	Argininosuccinate lyase	NA	membrane [GO:0016020]	lyase activity [GO:0016829]
23.	DAT39_002900	Uncharacterized protein	NA	NA	NA
24	DAT39_002797	Suppressor of cytokine signaling 5-like	intracellular signal transduction [GO:0035556]; negative regulation of signal transduction [GO:0009968]; protein ubiquitination [GO:0016567]	NA	NA
25.	spns1	Protein spinster homolog 1 (Spns1)	NA	lysosomal membrane [GO:0005765]	transmembrane transporter activity [GO:0022857]
26.	DAT39_006477	Ataxin-2-like protein isoform X1	NA	NA	RNA binding [GO:0003723]
27.	pitpnbl	Phosphatidylinositol transfer protein beta isoform-like	NA	endoplasmic reticulum membrane [GO:0005789]; Golgi membrane [GO:0000139]	phospholipid transporter activity [GO:0005548]
28.	unc50	Protein unc-50	NA	nuclear inner membrane [GO:0005637]	NA
29.	slc25a12	Calcium-binding mitochondrial carrier protein Aralar1-like	malate-aspartate shuttle [GO:0043490]	mitochondrial inner membrane [GO:0005743]	calcium ion binding [GO:0005509]
30.	slc25a12	Calcium-binding mitochondrial carrier protein Aralar1-like	malate-aspartate shuttle [GO:0043490]	mitochondrial inner membrane [GO:0005743]	calcium ion binding [GO:0005509]
31.	stk38a	Serine/threonine-protein kinase 38	phosphorylation [GO:0016310]	NA	ATP binding [GO:0005524]; protein serine/ threonine kinase activity [GO:0004674]
32.	prex1	Phosphatidylinositol 3,4,5-trisphosphate-dependent Rac exchanger 1 protein	anatomical structure development [GO:0048856]; intracellular signal transduction [GO:0035556]	NA	guanyl-nucleotide exchange factor activity [GO:0005085]
33.	DAT39_002823	Neurexin-1a isoform X10	anatomical structure development [GO:0048856]	membrane [GO:0016020]	NA
34.	DAT39_002905	Uncharacterized protein	NA	NA	NA
35.	Otogl	Otogelin-like protein	NA	NA	NA
36.	Otogl	Otogelin-like	NA	membrane [GO:0016020]	transmembrane transporter activity [GO:0022857]
37.	Otogl	Otogelin-like protein	L-arabinose metabolic process [GO:0046373]	NA	alpha-L-arabinofuranosidase activity [GO:0046556]
38.	Otogl	Otogelin-like	L-arabinose metabolic process [GO:0046373]	NA	alpha-L-arabinofuranosidase activity [GO:0046556]
39.	ypel1	Protein yippee-like 1	NA	NA	NA
40.	bmp5-1	Bone morphogenetic protein 5	NA	extracellular region [GO:0005576]	growth factor activity [GO:0008083]

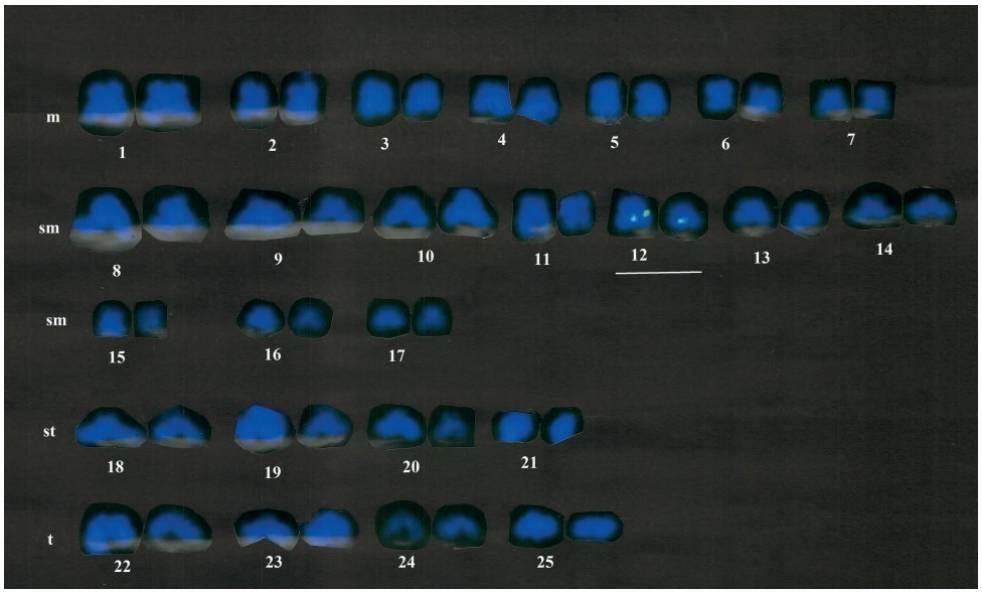

Figure 1. Karyotype of magur showing presence of FISH signals (green) of BAC clone 012H23 on 11th pair submetacentric chromosomes.

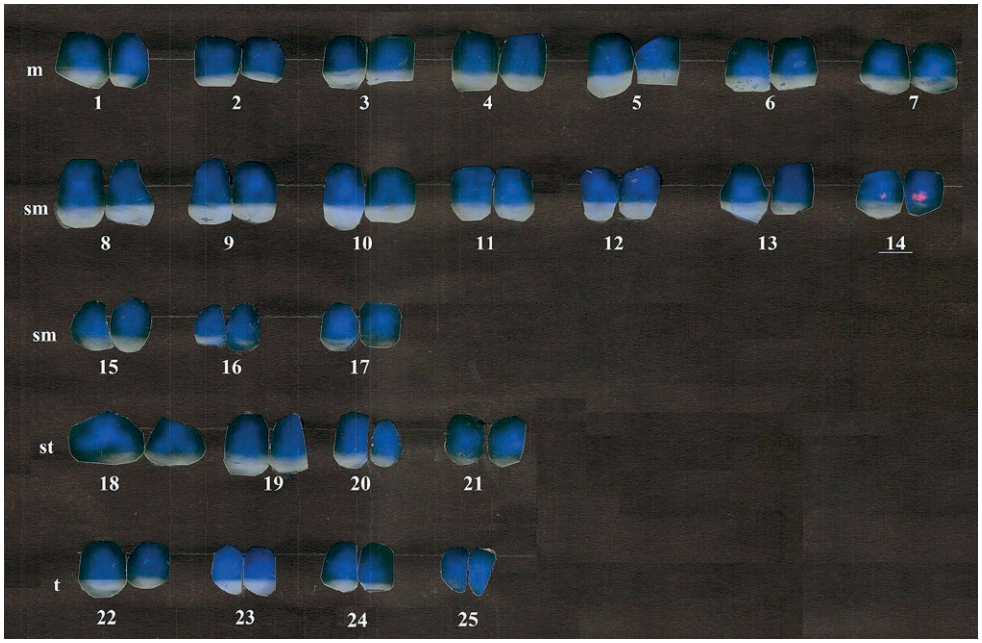

Figure 2. Karyotype of magur showing presence of FISH signals (red) of BAC clone 012H7 on 14th pair submetacentric chromosomes.

biological processes, the enrichment in 'cellular process', 'biological regulation' and 'metabolic process' emphasizes their importance in various cellular activities and regulatory pathways. Overall, these genes represent a wide spectrum of biological functions, from molecular regulation to cellular structural integrity, highlighting the complexity and diversity of cellular processes.

TMEM17 gene encodes a transmembrane protein, primarily situated within the ciliary membrane and facilitating symporter activity. *AGBL2* gene is involved in proteolysis and is predominantly found in the centriole and cytosol, with notable metallo-carboxypeptidase activity and zinc ion binding. *WASHC4* interact with VCP in zebrafish and impacts muscle function as

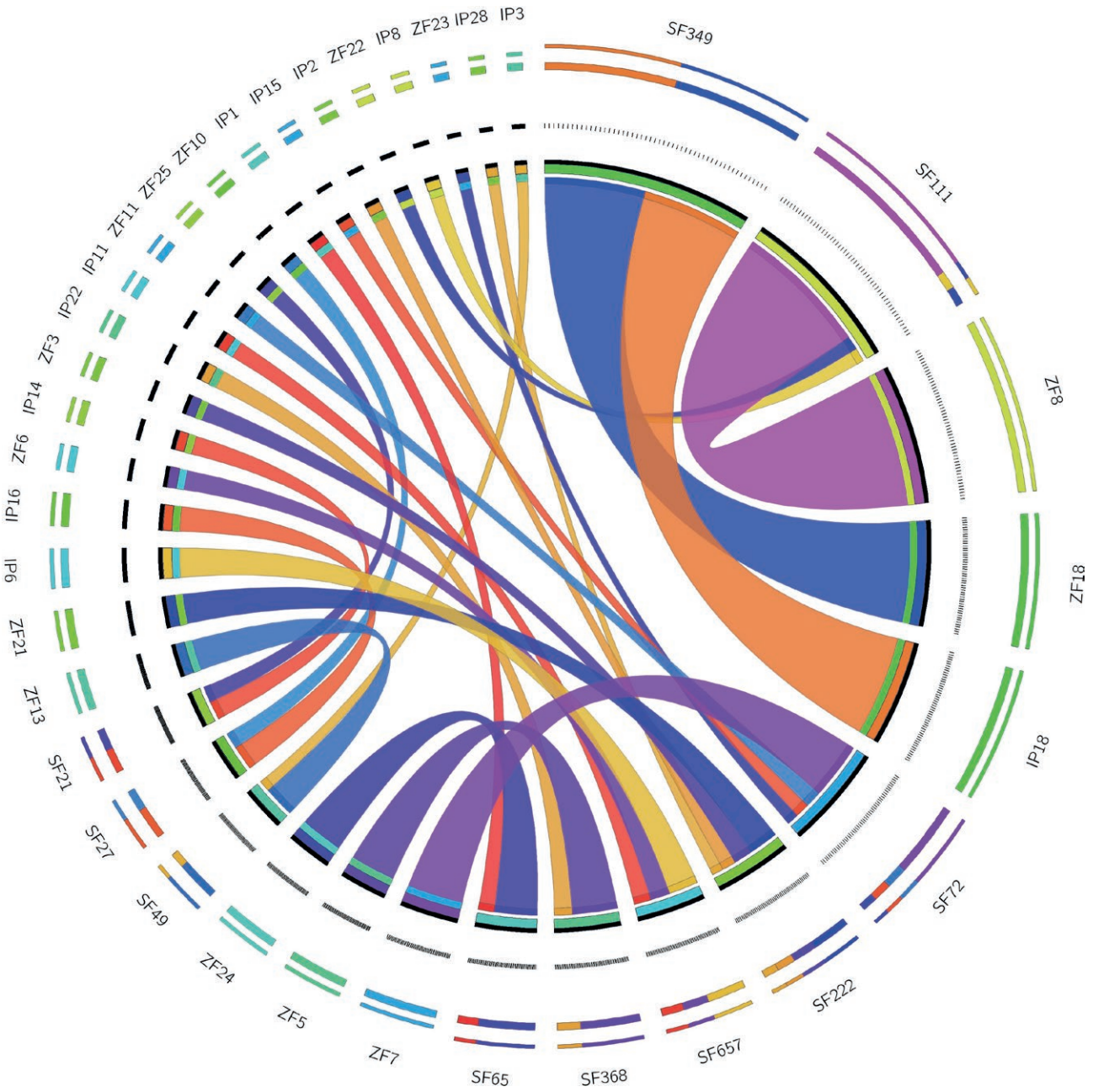

Figure 3. Synteny visualization of 34 genes present on 12 scaffolds of *magur* genome with channel catfish and zebrafish. SF represents scaffold of magur, IP represents channel catfish and ZF is zebrafish on which the gene are present.

well as autophagy with distinct roles in protein degradation and ER stress. *Pitpnb* is crucial for double cone cell maintenance in the zebrafish retina, while *Pitpna* supports early development. Additionally, proteins, like PDXP, PCM and MLPF, contribute to pyridoxal phosphate phosphatase activity, lyase activity in the membrane, and membrane-bound lytic murein transglucosylase activity, respectively. Other proteins are essential for many biological functions, including signal transmission. (DAT39_003426, DAT39_002797), intracellular transport (LIN7C, PITPNBL) and metabolic pathways (CHIA, SLC25A12). Notably, some proteins, like UBA3 and SLC39A13, are engaged in crucial regulatory functions such metal ion transport and protein neddylation, respectively. Moreover, several genes encode proteins with undefined functions (e.g. DAT39_002905,

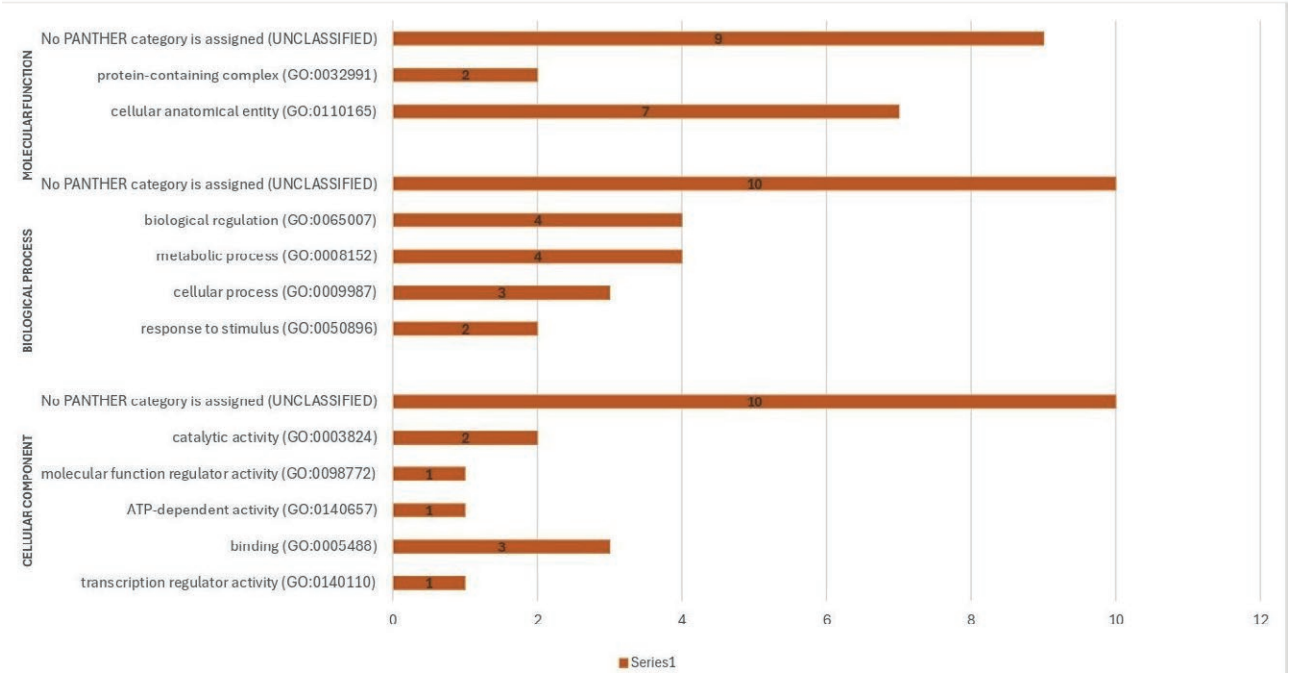

Figure 4. Panther database analysis showing GO terms associated with molecular function, biological process and cellular components.

YPEL1). Overall, this classification illustrates the complexity of biological systems by offering insights into the variety of gene functions across many cellular contexts and pathways.

Four pathways, which provided insights into potential cellular mechanisms, could be predicted using PANTHER, *viz*. Nicotinic acetylcholine receptor signalling pathway (P00044), PI3 kinase pathway (P00048), p53 pathway (P00059) and Ubiquitin proteasome pathway (P00060) (Fig. 5).

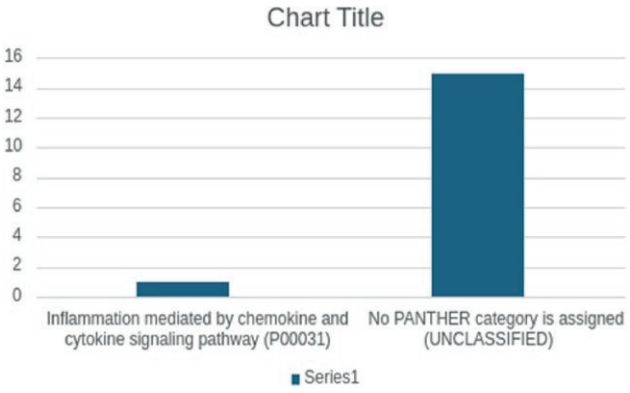

Figure 5. Panther database analysis.

Study of protein-protein interactions

The protein-protein interaction (PPI) network analysis identified 11 genes (mybpc3, prex1, stk38a, tmem17, ash2l, cnot2, lin7c, uba3, agbl2, slc39a13, wdr90) interconnected by 10 edges, representing their interactions. Cluster analysis revealed three distinct clusters represented by red, blue, and green colours. The red cluster includes mybpc3, prex1, stk38a, and tmem17, indicating close interactions likely involved in a shared functional pathway. The green cluster includes uba3, lin7c, cnot2, and ash2l**,** with uba3 acting as a central hub. The blue cluster includes agbl2, slc39a13, and wdr90, showing localized interactions. These clusters may represent distinct functional modules or pathways, providing insights into the biological roles and relationships among these genes and warranting further analysis to explore their functional and regulatory significance. (Fig. 6).

Comparative genomics and phylogenetics analysis

Based on the p-distances, four neighbor-joining (NJ) circular unrooted phylogenetic trees were built to clearly visualize 24 related genes found on the chromosomes of the zebrafish, channel catfish, and *magur* genome scaffolds. *Wash4* gene of zebrafish did not cluster either with *channel catfish* or *magur.* Similarly, *Aash2I* gene of channel catfish did not cluster either with *magur* or *zebrafish.*

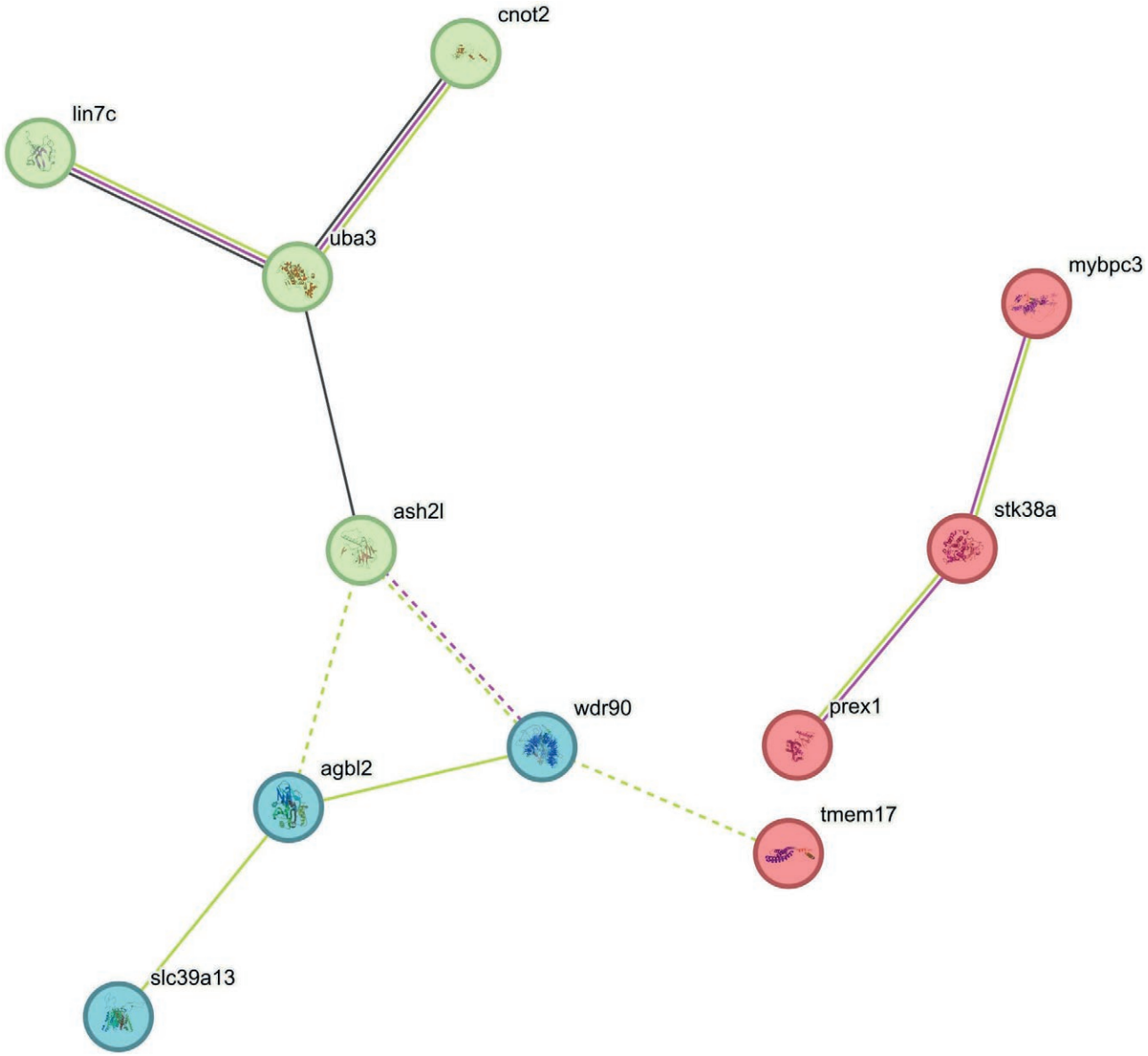

Figure 6. Protein-protein interaction network of 11 genes present on BAC clones. Cluster analysis of 11 genes grouped in three distinct clusters, as represented by red, green and blue colours.

The NJ-phylogeny of genes representing in scaffolds (SF), *SF_21, SF_21, SF_21, SF_21* and *SF_27* combining *magur* with *channel catfish* and *zebrafish* produced two clusters. (Fig. 7a), as similar *SF_27, SF_27, SF_65, SF_65, SF_72, SF_72* (Fig. 7b). Likewise, *SF_22, SF_68, SF_68, SF_222, SF_222, SF_222, SF_222* and *SF_222* generated 4 clusters (Fig. 7c) and *SF_111, SF_111, SF_349, SF_368, SF_657 & SF_657* generated 2 clusters (Fig. 7d). 34 genes located on 13 BAC clones of magur genome were annotated with gene id; protein id; amino acid (AA) and gene size in bp. *Mybpc3* gene present on clone ID: 012H1 contained maximum AAs (1250), while the gene (DAT39_002900) present on clone ID: 012J12 possessed smallest (59 AAs) and rest gene were unannotated (Supplementary Table 1). A total of 14 genes of *magur* (out of 34 genes) were synchronized with zebrafish and channel catfish chromosomes by aligning end sequences of 13 clones (Fig. 3; Supplementary Table 1). Remaining 20 genes present on clones were found in chromosomes of either channel catfish or zebrafish, therefore, not considered for synteny visualization.

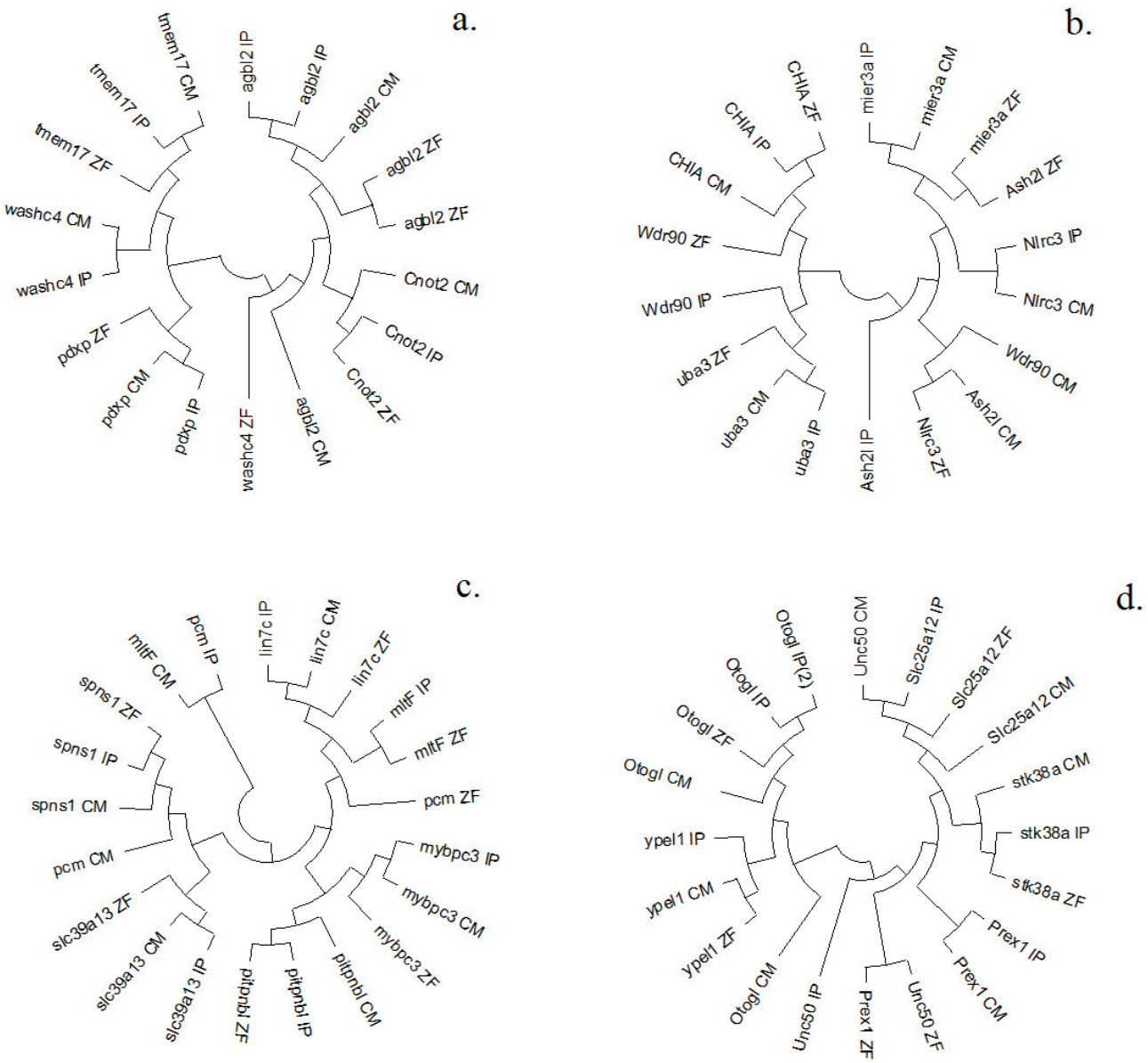

Figure 7. Phylogenetic trees constructed by neighbour-joining method based on p-distance of common genes present on chromosomes of channel catfish and zebrafish with gene present in magur scaffolds: (a) *SF_21, SF_27 (b). SF_27, SF_65, SF_72 (c). SF_22, SF_68, SF_222* (d). *SF_111, SF_349, SF_368, SF_657, SF_657.* CM represents magur, IP represents channel catfish and ZF represents zebrafish.

DISCUSSION

Several studies have been reported where BAC end sequences were utilized for genomic studies in different biological contexts (Meyers et al., 2004; Baisvar et al., 2022), indicating BACs are an important resource of live genetic material. There are several databases of BAC end sequences developed for numerous model species, including human, rice, mouse, and sea urchin (Poulsen et al., 2004). Baisvar et al. (2022) have reported a BAC-based partial physical map of *magur* genome employing whole genome and BAC clones. BAC libraries and their characterization using end sequencing of clones can provide insights into the *magur* genome. In the present study, isolated plasmid DNA of 13 clones of magur genome. Of these, 14 genes were common to *zebrafish* and *channel catfish.*

Metaphase chromosomal complements prepared were of good quality. Similar karyotype results have been obtained by other researchers in magur (Baisvar

et al., 2022; Kumar et al., 2021). Baisvar et al. (2022) employed BAC-FISH as a cytological marker for identifying individual chromosomes. BAC-FISH includes selecting an appropriate clone and obtaining high-quality chromosomal spread for FISH signal detection as well as to distinguish chromosome-based morphology. In the present study, two clones, *viz*. 012H23 (containing 5 genes) and 012H7 (containing 4 genes), were mapped on 11th and 14th sub-metacentric chromosomes pair, respectively.

A network-based method for identifying and ranking potential genes and their functional links is protein-protein interaction analysis. PPI analysis network revealed two interactions among 11 nodes and between 10 edges. These interactions were assessed based on various parameters, including their source in the database, experimental evidence, co-expression patterns and text mining, with a confidence score of 0.004 and PPI enrichment value (*p*-value of 0.000734). Clustering analysis of these 11 genes resulted in three distinct clusters. The red and green clusters contained 4 genes (*mybpc3, prex1, stk38a, tmem17*) and (*ash2l, cnot2, lin7c, uba3*) each, respectively, while the blue colour cluster consisted of 3 genes (*agbl2, slc39a13, wdr90*).

Gene enrichment analysis sheds light on a wide range of molecular and biological processes associated with the gene set under study. Deeper comprehension of the roles of the examined gene set in cellular activities and interactions is made possible by these analyses, which provide thorough insights into the biological processes, molecular functions, and possible pathways connected to the gene set. The GO categorizes genes into molecular functions, biological processes, and cellular components. Among cellular function binding was the most frequent, followed by transcription regulator activity and ATP-dependent activity. For biological processes, metabolic process and biological regulation each were the most prevalent (4), followed by response to stimulus and cellular process. Cellular anatomical entity was the most frequent (7 times), followed by protein-containing complex (twice). The genes in the list cover a wide range of cellular locations and biological roles. Four pathways, *viz*. nicotinic acetylcholine receptor signalling pathway (P00044), PI3 kinase pathway (P00048), p53 pathway (P00059), and ubiquitin proteasome pathway (P00060), could be identified from PANTHER analysis offering glimpses into synaptic transmission, cellular signalling, stress response and protein turnover, respectively. The list also includes the 'Inflammation mediated by chemokine and cytokine signalling pathway (P00031)', highlighting the genes involved in inflammation via chemokine and cytokine signalling. Additionally, there are entries labelled as No PANTHER category (UNCLASSIFIED), occurring ten times for cellular components and biological process, and nine times for molecular function. The presence of unclassified entries suggests potential novel functions requiring further investigation.

CONCLUSION

BAC based genomic library is very useful resource for mapping of genes on the chromosomes using FISH. A total of 9 genes found to be present in two BAC clones of *C. magur* were mapped in this study. The BAC end sequencing of 13 clones and mapping on magur genome scaffolds generated information of a total of 34 genes. This is the first report of physical mapping of these genes in *C. magur*. The PPI network among 11 genes revealed their interaction in three different clusters. This information is valuable for the point of further utilization of BAC resources of *C. magur* .

ACKNOWLEDGMENTS

The present reported work was carried out by the first author at ICAR-NBFGR, Lucknow, for her Ph.D. program. The director of the ICAR-National Bureau of Fish Genetic Resources in Lucknow provided laboratory space and other assistance that the authors needed to complete the Ph.D. research, for which they are grateful. For mapping BAC resources and providing financial assistance for the study, the authors further acknowledge the DBT, New Delhi, and the CABin Scheme of ICAR, which is run by the Division of Agricultural Bioinformatics, ICAR-IASRI, New Delhi. The BAC resource utilized here is the outcome of DBT funded project entitled 'Whole genome sequencing and development of allied genomics resources in two commercially important fish-*Labeo rohita* and *Clarias batrachus* (Sanction Order BT/PR3688/AAQ/3/571/2011 dated 10.09.2013)' and the consumables and other laboratory resources were utilized from the ICAR CABin Scheme sub-project entitled 'Construction of physical map of Clarias magur genome' executed at ICAR-NBFGR, Lucknow, under the 'Network project on Agricultural Bioinformatics and Computational Biology' implemented through Division ,ICAR-IASRI, New Delhi. The authors are also grateful to Integral University for providing necessary guidance and help to the first author. This manuscript is also acknowledged under Integral University Manuscript number-IU/R&D/2024-MCN0002767.

DECLARATION OF INTEREST STATEMENT

The authors state that none of the work described in this study could have been influenced by any known competing financial or non-financial, professional, or personal conflicts.

FUNDING INFORMATION

The authors are thankful to the DBT, New Delhi, and CABin Scheme of ICAR, implemented through Division of Agricultural Bioinformatics, ICAR-IASRI, New Delhi, for providing BAC resource and financial support to the study. The BAC resource utilized here is the outcome of DBT funded project entitled 'Whole genome sequencing and development of allied genomics resources in two commercially important fish- *Labeo rohita* and *Clarias batrachus* (Sanction Order BT/PR3688/AAQ/3/571/2011 dated 10.09.2013)' and the consumables and other laboratory resources were utilized from the ICAR CABin Scheme sub-project entitled 'Construction of physical map of *Clarias magur* genome' executed at ICAR-NBFGR, Lucknow, under the 'Network project on Agricultural Bioinformatics and Computational Biology' implemented through Division of Agricultural Bioinformatics, ICAR-IASRI, New Delhi.

AUTHOR CONTRIBUTION STATEMANT

RV: Experimentation, draft writing and editing; BK: Conceptualization, Project Administration, Data Curation, Investigation, Methodology, Writing -original draft; UA: Project Administration: VSB: Formal Analysis, draft writing, editing; SM: Formal Analysis; MSK: Methodology, Formal Analysis, Writing, reviewing, and editing; TD: Formal Analysis, editing; RK: Project Administration, Resources, Supervision, Writing - review and editing.

REFERENCES

1. Ng HH, Kottelat M. 2008. The identity of *Clarias batrachus* (Linnaeus,1758), with the designation of a neotype *(Teleostei: Clariidae*). *Zoo. J. Lin. Soc.* 153(4): 725–732.
2. Baisvar VS, Kushwaha B, Kumar R, Kumar MS, Singh M, Rai A, Sarkar UK. 2022. BAC-FISH Based Physical Map of Endangered Catfish *Clarias magur* for Chromosome Cataloguing and Gene Isolation through Positional Cloning. Int. J. Mol. Sci. 24:15958. https://doi.org/10.3390/ijms232415958.
3. Mishra BM, Khalid MA, Labh, SN. 2019. Assessment of the effect of water temperature on length gain, feed conversion ratio (FCR) and protein profile in brain of *Labeo rohita* (Hamilton 1822) fed *Nigella sativa* incorporated diets. Intl J Fish Aquatic Studies. 3: 6-13.
4. Osoegawa K, Mammoser AG, Wu C, Frengen E, Zeng C, Catanese JJ, de Jong PJ. 2001. A bacterial artificial chromosome library for sequencing the complete human genome. Geno. Res. 113: 483-96.
5. Osoegawa B, Zhu CL, Shu T, Ren Q, Cao G M, Vessere MM. 2004. BAC resources for the rat genome project. Genome Res. 14(4): 780–785.
6. Kanehisa M, Sato Y. 2020. KEGG Mapper for inferring cellular functions from protein sequences. Prot. Sci. 29(1): 28–35.
7. Meyers B C, Scalabrin S, Morgante M. 2004. Mapping and sequencing complex genomes: Let us get physical. Nat Rev Genet. 5(8): 578–89.
8. Devassy A, Kumar R, Shajitha PP, John R, Padmakumar KG, Basheer V S, Gopalakrishnan A,Mathew L.2016. Genetic identification and Phylogenetic relationships of Indian *clariids* based on mitochondrial COI sequences. Mitoch. DNA 27(5): 3777–3780.
9. Shizuya Hiroaki, Bruce Birren, Ung-Jin Kim, Valeria Mancino, Tatiana Slepak, Yoshiaki Tachiiri, & Melvin Simon. 1992. Cloning and stable maintenance of 300-kilobase-pair fragments of human DNA in Escherichia coli using an F-factor-based vector. *Proc Natl Acad Sci U S A.* 89(18): 8794-8797.
10. Kumar R, Baisvar VS, Kushwaha B, Waikhom G, Nagpur NS. 2017. Cytogenetic investigation of *Cyprinus carpio* (Linnaeus, 1758) using giemsa, silver nitrate, CMA3 staining and fluorescence in situ hybridization. Nuc. 60: 1–8.
11. Kumar R, Baisvar VS, Kushwaha B, Murali S, Singh VK. 2020. Improved protocols for BAC insert DNA isolation, BAC end sequencing and FISH for construction of BAC based physical map of genes on the chromosomes. Mol. Bio. Rep. 47(3): 2405–2413.
12. Kumar S, Stecher G, Tamura K. 2016. MEGA7: Molecular Evolutionary Genetics Analysis Version 7.0 for Bigger Datasets. Mol. Bio. Evol. 33(7): 1870–1874.
13. Derelle E, Ferraz C, Rombauts S, Rouzé P, Worden AZ, Robbens S, Partensky F, Degroeve S, Echeynié S, Cooke R, Saeys Y, Wuyts J, Jabbari K, Bowler C, Panaud O, Piégu B, Ball SG, Ral JP, Bouget FY, Piganeau GDe, Baets B, Picard A, Delseny M, Demaille J, Peer YV, Moreau H.2006. Genome analysis of the smallest free-living eukaryote Ostreococcus tauri unveils many unique features. Proc Natl Acad Sci U S A. 103(31): 11647-52.

14. Hanson RE, Zwick MS, Choi S, Islam-Faridi MN, McKnight TD, Wing RA, Price HJ , Stelly DM .1995. Fluorescent in situ hybridization of a bacterial artificial chromosome. Genome. 38(4): 646-651.
15. Jiang J, Gill BS, Wang G, Ronald PC, Ward DC. 1995. Metaphase and interphase fluorescence in situ hybridization mapping of the rice genome with bacterial artificial chromosomes. Proc Natl Acad Sci USA. 92(10): 4487-4491.
16. Krzywinski M, Schein J, Birol I, Connors J, Gascoyne R, Horsman D, Jones SJ, Marra MA. 2009. Circos: An information aesthetic for comparative genomics. Gen.Res. 19(9): 1639–1645.
17. Letunic I, Bork P. 2019. Interactive Tree of Life (iTOL) v4: Recent updates and new developments. Nucl. Aci.Res. 47(W1): W256–W259.
18. Shannon P, Markiel A, Ozier, O, Baliga NS ,Wang JT, Ramage D, Amin N, Schwikowski B, Ideker T.2003. Cytoscape: a software environment for integrated models of biomolecular interaction networks. Gen. Res. ,13(11): 2498-504.
19. Szklarczyk D, Kirsch R, Koutrouli M, Nastou K, Mehryary F, Hachilif R, Gable AL, Fang T, Doncheva NT, Pyysalo S, Bork P, Jensen LJ, Mering CV. 2023. The STRING database in 2023: protein-protein association networks and functional enrichment analyses for any sequenced genome of interest. Nuc. Ac. Res.51(D1): D638-D646.
20. Woo SS, Jiang J, Gill BS, Paterson AH, Wing RA. 1994. Construction and characterization of a bacterial artificial chromosome library of *Sorghum bicolor*. Nc. Ac. Res.22(23):4922-31.
21. Vishwanath W. 2010.*Clarias magur*. The IUCN Red List of Threatened Species. 2010: e.T168255A6470089. https://doi.org/10.2305/IUCN.UK.2010-4. RLTS. T1682 55A64 70089.
22. Poulsen TS, Johnsen HE, Zhao S, Stodolsky M.2004. BAC End Sequencing. In Methods in Molecular Biology. Bacterial Artificial Chromosomes, Library Construction, Physical Mapping and Sequencing Humana Press Inc. Totowa. 255: 157–161.

Supplentary Table 1.

Stands	Scaffold	Genomic Accession	Protein id	Amino acid
+	Scaffold21	QNUK01000021.1	KAF5907527.1	442aa
-	Scaffold21	QNUK01000021.1	KAF5907528.1	208aa
-	Scaffold21	QNUK01000021.1	KAF5907529.1	772aa
+	Scaffold21	QNUK01000021.1	KAF5907531.1	330aa
-	Scaffold21	QNUK01000021.1	KAF5907532.1	1150aa
-	Scaffold27	QNUK01000027.1	KAF5906889.1	200aa
-	Scaffold27	QNUK01000027.1	KAF5906891.1	364 aa
+	Scaffold27	QNUK01000027.1	KAF5906892.1	495aa
-	Scaffold27	QNUK01000027.1	KAF5906893.1	521aa
-	Scaffold65	QNUK01000065.1	KAF5903982.1	149aa
+	Scaffold65	QNUK01000027.1	KAF5906893.1	521aa
+	Scaffold65	QNUK01000065.1	KAF5903985.1	295aa
-	Scaffold72	QNUK01000072.1	KAF5903458.1	292aa
+	Scaffold72	QNUK01000072.1	KAF5903460.1	336aa
-	Scaffold222	QNUK01000222.1	KAF5897751.1	83aa
+	Scaffold222	QNUK01000222.1	KAF5897752.1	200aa
-	Scaffold222	QNUK01000222.1	KAF5897753.1	1250aa
+	Scaffold222	QNUK01000222.1	KAF5897754.1	376aa
-	Scaffold22	QNUK01000022.1	KAF5907406.1	64aa
+	Scaffold22	QNUK01000022.1	KAF5907407.1	59aa
-	Scaffold22	QNUK01000022.1	KAF5907408.1	552aa
+	Scaffold68	QNUK01000068.1	KAF5903764.1	926aa
-	Scaffold68	QNUK01000068.1	KAF5903765.1	883aa
+	Scaffold68	QNUK01000068.1	KAF5903766.1	256aa
+	Scaffold657	QNUK01000657.1	KAF5890715.1	250aa
+	Scaffold657	QNUK01000657.1	KAF5890716.1	608aa
+	Scaffold111	QNUK01000111.1	KAF5901503.1	369aa
+	Scaffold111	QNUK01000111.1	KAF5901504.1	1125aa
+	Scaffold22	QNUK01000022.1	KAF5907397.1	711aa
-	Scaffold22	QNUK01000022.1	KAF5907398.1	135aa
+	Scaffold349	QNUK01000349.1	KAF5894936.1	912aa
+	Scaffold349	QNUK01000349.1	KAF5894937.1	327aa
+	Scaffold368	QNUK01000368.1	KAF5894553.1	178aa
+	Scaffold49	QNUK01000049.1	KAF5905006.1	269aa

Caryologia
International Journal of Cytology, Cytosystematics and Cytogenetics

Firenze University Press
https://riviste.fupress.net/index.php/caryologia

Anther structure and pollen development in *Jurinea kilaea* Azn. (Asteraceae)

Nuran Ekici

Trakya University, Faculty of Education, Department of Mathematics and Science Education, Edirne, Turkey
E-mail: nuranekici@yahoo.com

OPEN ACCESS

Citation: Ekici, N. (2025). Anther structure and pollen development in *Jurinea kilaea* Azn. (Asteraceae). *Caryologia* 78(1): 41-51. doi: 10.36253/caryologia-2965

Received: September 29, 2024

Accepted: June 25, 2025

Published: October 1, 2025

Data Availability Statement: All relevant data are within the paper and its Supporting Information files.

Competing Interests: The Author(s) declare(s) no conflict of interest.

ORCID
NE: 0000-0003-2005-7293

Abstract. In this study, anther wall structure and the embryological features of male gametophyte development in *Jurinea kilaea* from Asteraceae family are described for the first time. Capitula of different sizes containing young flower buds of *J. kilaea* was collected from Tekirdağ, Saray - Kastro coast in July 2022 – 2024. Anthers separated according to their sizes under a stereo microscope were passed through arising alcohol series and embedded in Hisstore. Toluidine blue O solution was used to stain the sections. Slides were examined with light microscope and photographed by an Olympus E330 camera. In *J. kilaea*, anthers are tetrasporangiate. Anther wall consists of the outermost epidermis, the endothecium, the middle layer and the innermost tapetum layer. Tapetum cells appear to have 1 or 2 nuclei. Tapetum is plasmodial type and, tapetum cells begin to degenerate towards the end of the tetrad phase. Microsporogenesis and pollen mitosis are generally regular. Asynchrony is observed during meiosis in young anther loci. Generally, decussate type tetrad was observed. Rarely pentads were also observed. Cytoplasmic channels were observed between microspores at different stages of microsporogenesis. The mature pollen grains of *J. kilaea* are generally composed of three nuclei and have a normal structure. However, there have been instances where pollen grains exhibit an abnormal structure. Pollen sterility ratio was found to be 12.1%.

Keywords: *Jurinea kilaea,* Asteraceae, anther wall, microsporogenesis, pollen development.

INTRODUCTION

The Asteraceae family is one of the largest flowering plant families, has 12 subgenera and 43 tribes, which contain ca. 24,000–30,000 species placed within 1,600 genera (Susanna et al. 2019; Bona 2020; Rolnik and Olas 2021). It is represented in Turkey with a total of 1438 taxa, of which 152 genera, 1230 species, 133 subspecies and 75 varieties (Yıldırımlı 1999). Therefore, Asteraceae family needs more data about the additional taxonomic characters such as anther and pollen development (Çetinbaş and Ünal 2015).

The Asteraceae family members are widely distributed in the world, except for the Antarctic region, especially in tropical and subtropical semi-arid regions

such as the Mediterranean Region, Mexico and South Africa, in the forested regions of Africa, South America and Australia, in the prairies and in bush formations (Heywood 1978). They are annual, biennial or perennial herbs; rarely shrubs, trees or climbing woody plants; their tissues may or may not carry latex (Saday 2005).

Its most well-known taxa are daisies, dandelion, lettuce, endive, and artichokes. For ages, people have been using plants from the Asteraceae family for their nutritional and medicinal benefits. The majority of the family's members share a similar chemical makeup despite their great diversity. For instance, all species are good sources of inulin, a naturally occurring polysaccharide with potent prebiotic qualities. They also possess potent antibacterial, anti-inflammatory, and antioxidant qualities in addition to diuretic and wound-healing capabilities (Rolnik and Olas 2021). Family Asteraceae as a sustainable planning tool in phytoremediation and its relevance in urban areas was studied by Nikolic and Stevovic (2015). Kartal (2016) examined calcium oxalate (CaOx) crystals in the tissues and organs of eighteen species in the Cardueae tribe (Asteraceae).

Jurinea which is represented by about 300 species on earth, is mainly distributed in Central Asia, the Mediterranean basin, Iran, and Turkey (Szukala et al. 2019). In Turkey *Jurinea* is represented by 18 species in Turkey. 6 of these species are endemic to Turkey. The distributions of the endemic taxa are as follows: *J. brevicaulis* and *J. cadmea* have local distribution; *J. alpigena, J. ancyrensis* and *J. cataonica* have regional, and *J. pontica* has larger distribution. The distribution of the species according to the phytogeographic regions is as follows: 10 species of Irano-Turanian; 2 types of Mediterranean; It is an element of 5 types of Euxine (2 types of Balkans, 1 type of Caucasian, 1 type of Turkey in Europea-Thrace) (Davis 1975). They are usually herbaceous plants that can live for several years. Despite the richness of its species, only a few analyses on a regional scale have so far attempted to clarify the phylogenetic relationships within *Jurinea* (Doğan et al. 2010; Szukala et al. 2019; Bona 2020)

Jurinea kilaea is a rhizomatous plant that grows in the foredunes of Turkey (Avcı et al. 2015). *J. kilaea* has been studied more systematically (Gülez et al. 2007; Özhatay et al. 2013; Özhatay and Öztekin 2015; Kutbay et al. 2017; Tuncay and Akalın 2018; Sürmen et al. 2019; Uslu and Keçeli 2019; Ağır et al. 2016; 2017; 2021; Valcheva et al. 2020; Karaduman and Sağıroğlu 2021). Phylogenetic analysis of *Jurinea* (Compositae) species in Turkey based on ITS sequence data was performed. These include *Jurinea kilaea* (Doğan et al. 2010). Pappus and achene characteristics of *J. kilaea* is studied by Bona (2020). Morphological features of *J. kilaea* were studied by Saday in 2005. There are also biochemical studies with *J. kilaea*. The antioxidant activity and capacity of *J. kilaea* were investigated. Phenolic, flavonoid substance, antioxidant and antimicrobial properties were studied (Kılıç 2020). Fatty acid and amino acid profiles of *J. kilaea* was studied by Taç and Özcan (2019).

Although there are many systematic studies on Asteraceae, there are very few cytoembryological studies. Some of these were made by Sun and Ganders (1987) on nine gynodioecious taxa of Hawaiian bidens, by Meriç et al. (2004) on *Helianthus annuus* L., by Yurukova-Grancharova and Dimitrova (2006) on *Crepis bithynica* Boiss., by Li et al. (2010) on *Chrysanthemum morifolium* Ramat., by Kaur et al. (2010) on *Inula cuspidata* C.B. Clarke, by Liu et al. (2012) on *Ambrosia artemisiifolia* L., by Kaur et al. (2019) on some species of *Lactuca* L., by Gupta et al. (2017) on 45 species of Asteraceae from Parvati Valley in Kulu district, India, and by Chehregani and Salehi (2016) on *Achillea tenuifolia.* Palynological studies were carried out by Wortley et al. (2012), Chehregani and Salehi (2016) and Gupta et al. (2017).

In this study, *Jurinea kilaea* Azn, which is not endemic but can be considered endangered nationally and worldwide, was studied cyto-embryologically for the first time. This study will contribute to systematic and cyto-embryological studies on the Asteraceae family.

MATERIAL AND METHODS

As the study material, capitulums (8-13 mm) containing young flower buds (1,5 -8 mm) of *Jurinea kilaea* was collected from Tekirdağ, Saray - Kastro coast in July 2022 and July 2024. After being fixed in Carnoy's fixative (1acetic acid: 3 absolute alcohol), it was washed in 96% ethanol and stored in 70% ethyl alcohol. Anthers (1-6 mm) separated according to their sizes under a stereo microscope were passed through arising alcohol series and embedded in Hisstore (Leica, Historesin-embedding kit) according to the manufacturer's instructions (http://www.leicabiosystems.com/specimen-preparation/consumables/mounting-edia-section-adhesive/details/product/historesin-1/). Sections of 4 μm thickness were taken with a tungsten carbide blade on a Leica RM2255 model rotary microtome. Sections were kept in 0.5% Toluidine blue O solution (O'Brien et al. 1964) prepared in 0.1 M phosphate buffer (pH 6.8) for 2 minutes, washed in distilled water for 30 seconds and dried in air. It was closed with Entellan and made into a continuous preparation (Kartal 2015). Pollen taken at the time of flowering of *J. kilaea* was stained with Aniline blue (Merck). It was left at room temperature for half an hour. 1000 pollens were

evaluated by counting whether they were stained or not. Slides were examined with an Olympus CX31 microscope and were photographed by an Olympus E330 camera.

RESULTS

Androecium

Androecium of *Jurinea kilaea* consists of 5 stamens. Anther structure is caudate type. Anthers are united, tube-shaped, purple, basifix, filaments are free and white. In *J. kilaea*, anthers are tetrasporangiate. Pollen sacs are interconnected with connective tissue containing a vascular bundle (Figure 1). When the anthers mature, the microsporangia split open from their stomium.

Anther wall

The anther wall was also examined during pollen development in *J. kilaea*. Young anther wall consists of the outermost epidermis, the endothecium, the middle layer and the innermost tapetum layer. Endothecium thickenings are not seen in the young anther wall. Epidermis and endothecium cells are almost cubic in shape, and they have large nuclei relative to the cell size. Under the endothecium, there is a middle layer consisting of a very thin, single layer of flat cells. Tapetum cells appear to have 1 or 2 nuclei. The number of cells undergoing nuclear division is high. Asynchrony is observed during meiosis in young anther loci. The first stages of meiosis can be seen in one locus, and the tetrad stage can be seen in the other locus (Figure 1a).

Layers, the epidermis and the endothecium, remain intact in the mature anther wall. The epidermis layer consists of a single row of flat cells. It is seen that the cells of the endothecium layer are highly developed and increase in size compared to the other layers. It is also observed that fibrous thickenings develop in the cells of the endothecium layer. It is seen that the middle layer, which consists of a very thin and flat single layer of cells in the young anther, is completely degenerated in the mature anther. Tapetum is plasmodial type and, tapetum cells begin to degenerate towards the end of the tetrad phase. Then tapetal remnants from the degenerating tapetum are seen in the mature anther locus The asynchronization between loci seen in the young anther also disappears in the mature anther (Figure 1b).

Microsporogenesis

In this study, microsporogenesis stages in *J. kilaea* were examined for the first time. In sections taken from the anther during the interphase phase, the nuclei of the pollen mother cells are of similar size and the nucleoli are conspicuous. There is no callose wall around the pollen mother cells (Figure 2a). During the leptotene stage, callose wall begins to form around the microspore mother cells (Figure 2b). In the zygotene stage, the chromatin material is in a loose state (Figure 2c). In pachytene, homologous chromosomes come together. The nucleus is pulled towards the edge of the cell. This phase is also called the bouquet phase (Figure 2d). During the diplotene phase, the lengths of bivalent chromosomes begin to shorten. Callose wall formation is completed at

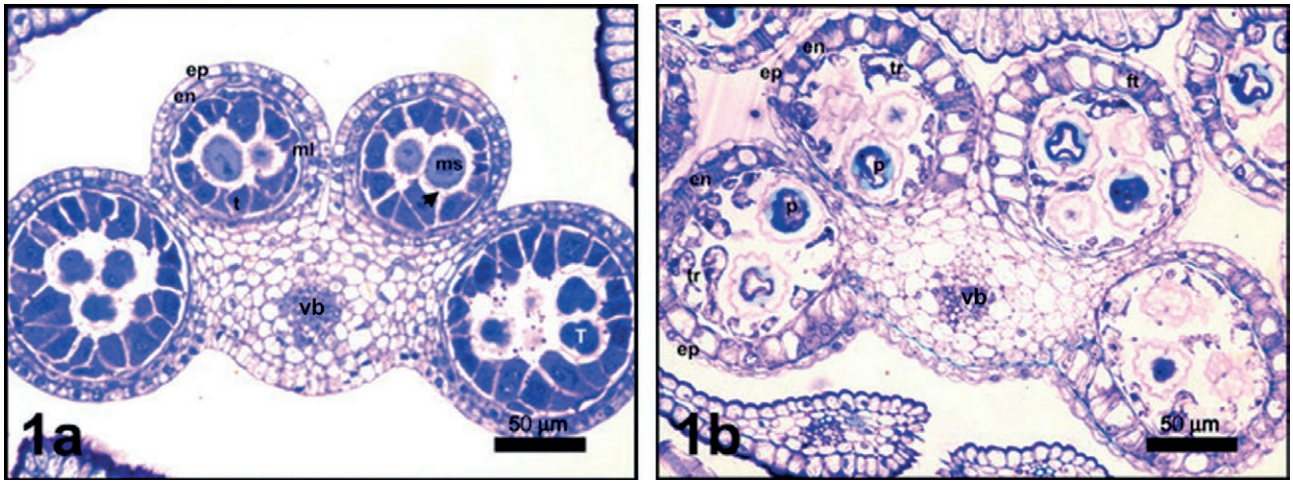

Figure 1. Anther structure in *J. kilaea.* (a) young anther; (b) mature anther (arrowhead, callose; en, endothecium; ep, epidermis; ft, fibrous thickenings; ml, middle layer; ms, microspore; p, pollen; T, tetrad; t, tapetum; tr, tapetal remnants; vb, vascular bundle).

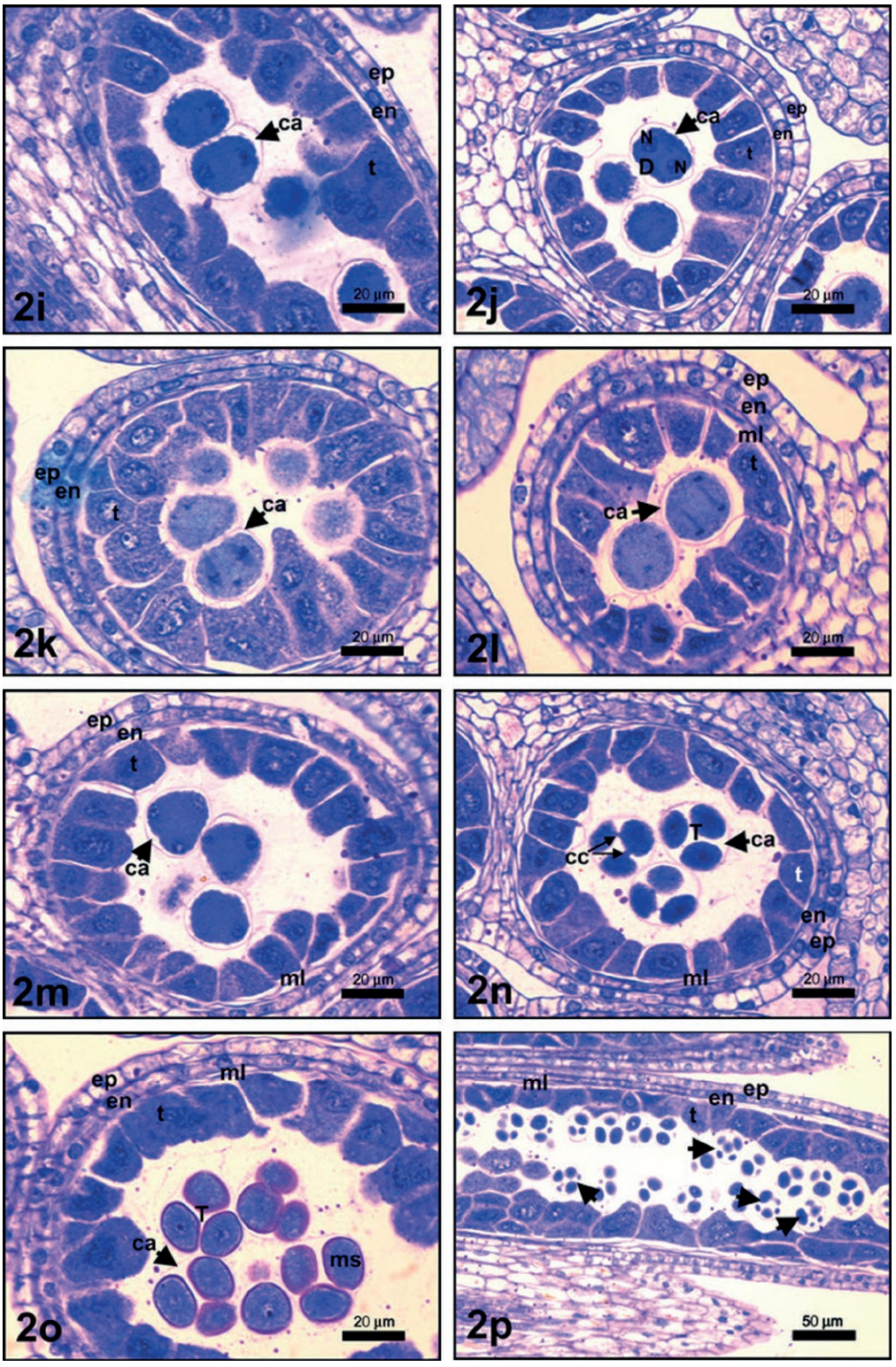

Figure 2. Microsporogenesis in pollen mother cells of *J. kilaea*. (a) interphase; (b) leptotene; (c) zygotene; (d) pachytene (bouquet stage); (e) diplotene; (f) diakinesis; (g) metaphase I; (h) anaphase I; (i) telophase I; (j) dyad phase; (k) metaphase II; (l) anaphase ll; (m) telophase II; (n) early tetrad phase; (o) late tetrad phase; (p) anomalies in tetrad phase (arrowheads, tetrad anomalies; ca-arrowheads, callose; cc; cytoplasmic channels; D, dyad; en, endothecium; ep, epidermis; ml; middle layer; ms, microspore; N; nucleus; Nu; nucleolus; PMC, pollen mother cell; t, tapetum; T, tetrad).

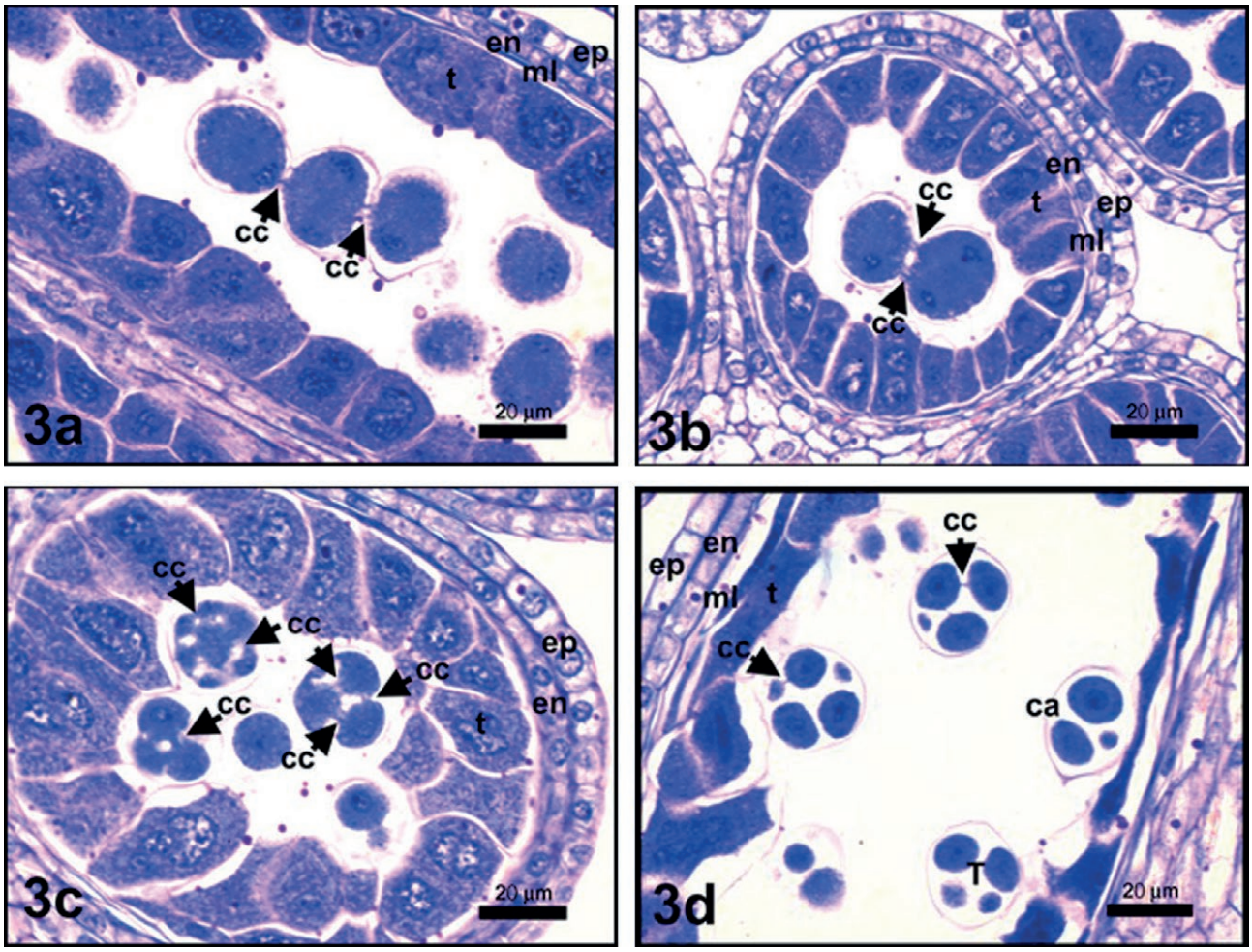

Figure 3. Cytoplasmic channels in some phases of microsporogenesis in *J. kilaea*. (a) early telophase I; (b) early dyad phase; (c) early tetrad phase; (d) late tetrad phase (ca, callose; cc-arrowheads, cytoplasmic channels; en, endothecium; ep, epidermis; ml, middle layer; t, tapetum; T, tetrad).

this stage (Figure 2e). During the diakinesis phase, chromosome shortening continues (Figure 2f). In metaphase I, the chromosomes line up on the equatorial plate and appear to be connected by spindle fibers (Figure 2g). In anaphase I, homologous chromosomes are pulled to the poles (Figure 2h). In telophase I, chromosomes lose their dense shape and return to their thread-like form. An intermediate lamella begins to form between the two nuclei, from the middle of the cell to the edges (Figure 2i). Dyad occurs with successive type of cytokinesis (Fig. 2j). In metaphase II, chromosomes align on the equatorial plate (Figure 2k). In anaphase II, sister chromatids are pulled to the poles with the help of spindle fibers (Figure 2l). It is observed that in telophase II, nuclei 4 are formed at the edges. Cytokinesis is simultaneous type at tetrad phase (Figure 2m). Cytoplasmic channels were seen between microspores in the early tetrad phase. There is a well-developed callose wall around the tetrads (Figure 2n). In later stages, the callose wall around the microspores breaks down and the microspores are released (Figure 2o). Generally, decussate type tetrad was observed. In *J. kilaea*, pentads as well as tetrads were observed in the anther locus - arrowheads (Figure 2p). Cytoplasmic channels were observed between microspores at different stages of microsporogenesis, such as telophase I (Figures 3a, 3b), early tetrad (Figure 3c) and tetrad stage (Figure 4d).

Microgametogenesis

In J. kilaea, it is observed that the microspores released after the callose wall degeneration in the tetrad stage are tricolpate and the intine layer begins to form

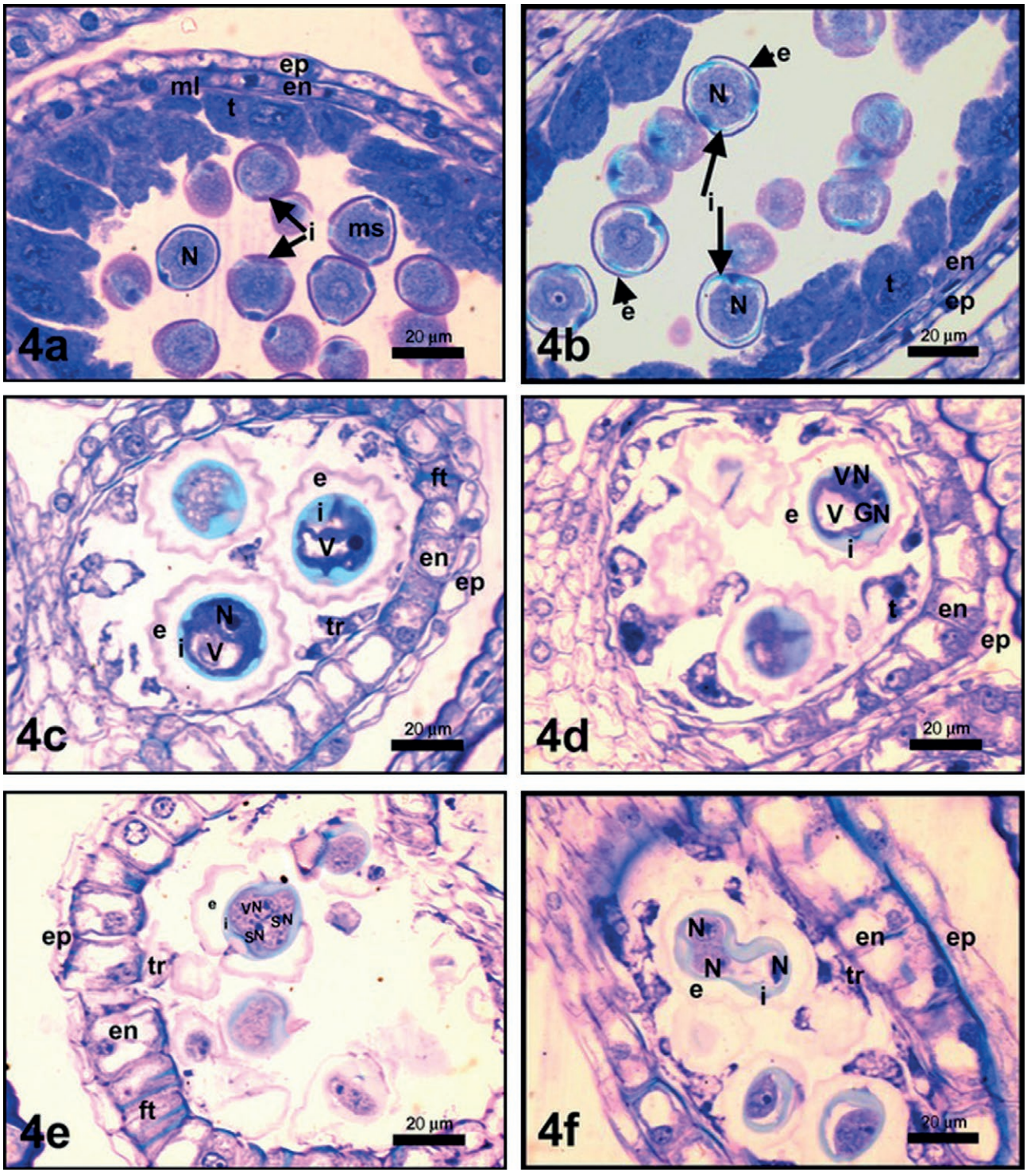

Figure 4. Pollen development in *J. kilaea*; (a) one-nucleated microspore phase after callose deposition; (b) wrinkled microspore phase (c) vacuolated microspore phase; (d) two-celled pollen phase, (e) three-celled mature pollen, (f) abnormal shaped pollen (en, endothecium; ep, epidermis; e; exine; ft, fibrous thickenings; gn, generative nucleus; i; intine (arrows); ml, middle layer; ms microspore; N, nucleus; sn, sperm nucleus; t, tapetum; tr, tapetal remnants; V, vacuole; vn, vegetative nucleus).

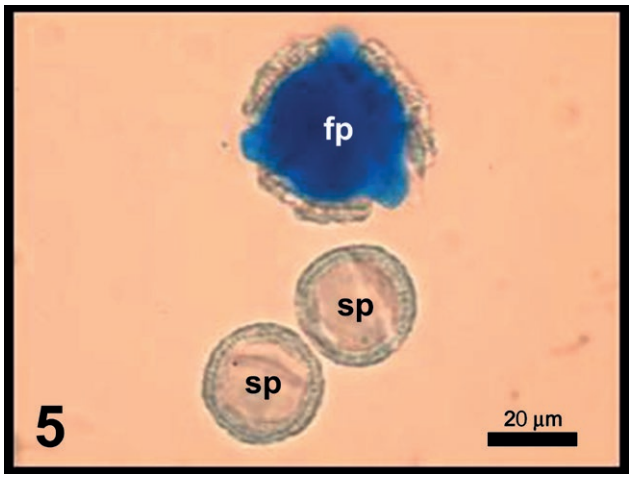

Figure 5. Pollen viability in *J. kilaea* (fp, fertile pollen; sp, sterile pollen).

around them (Figure 4a). Then, it is seen that the exine layer begins to form over the intine (Figure 4b). After the formation of the exine layer is completed in the single-nucleated stage, a vacuole that covers most of the cell is formed and the nucleus migrates to the pole where pollen mitosis will occur (Figure 4c). After first mitosis vegetative and generative nuclei are formed (Figure 4d). As the generative nucleus undergoes mitosis, sperm nuclei are formed and the three-nucleated mature pollen grain in *J. kilaea* completes its development (Figure 4d). Pollen grains of *J. kilaea* generally have a normal structure, and very rarely pollen grains with an abnormal structure have been observed (Figure 4e).

Pollen viability

Pollen viability in *J. kilaea* was examined using a light microscope. It was observed that pollens were generally stained well. Pollens were stained with aniline blue (Merck) prepared in lactophenol were considered fertile, others were considered as sterile pollen grains (Figure 5). 1000 pollens were counted. Pollen sterility rate was determined as 12.1%. Mature pollens are tricolpate and trinucleated.

DISCUSSION

In this study, the anther wall structure, and the developmental stages of the male gametophyte in *Jurinea kilaea*, which grows naturally on the coast of Tekirdağ-Saray, were examined. The embryological studies on *J. kilaea* and the Asteraceae family, especially the genus *Jurinea*, are quite limited so the findings regarding the anther wall structure and microsporogenesis are discussed with the characteristics of other species belonging to this family.

In *J. kilaea*, the androecium consists of 5 stamens, as in *Aster subulatus* Michx., *Kalimeris indica* (Linn.) Sch.-Bip., *Heteropappus arenarius* Kitamura, *Erigeron annuus* (Linn.) Pers. (Ao et al. 2009), male fertile and sterile *Chrysanthemum morifolium* Ramat. (Li et al. 2010), *Ambrosia artemisiifolia* L. (Liu et al. 2012), *Helianthus annuus* L. (Çetinbaş and Ünal 2015) from Asteraceae. Anthers of *J. kilaea* are united, tube-shaped, purple, basifixed, filaments are free and white. They are structurally like anthers of *H. annuus* (Çetinbaş and Ünal 2015). They differ only in color. Anther appendage of *J. kilaea* is apiculate like *Ainsliaea latifolia* (D. Don) Schultz-Bipontinus (Shekhar and Pandey 2009) and *Ainsliaea qianiana* (Shi et al. 2011) from Asteraceae family. When the anthers mature, the microsporangia split open from their stomium.

Anthers are tetrasporangiate in *J. kilaea*. The pollen sacs are interconnected with connective tissue containing a vascular bundle as in *C. bithynica* (Yurukova-Grancharova and Dimitrova 2006), *A. subulatus, K. indica, H. arenarius, E. annuus* (Ao et al. 2009), *C. morifolium* (Li et al. 2010), *A. artemisiifolia* (Liu et al. 2012).

In *J. kilaea*, the young anther wall, as in *Bidens cervicata* Sherff (Sun and Ganders 1987), *C. bithynica* (Yurukova-Grancharova and Dimitrova 2006), *A. subulatus, K. indica, H. arenarius, E. annuus* (Ao et al. 2009) *C. morifolium* (Li et al. 2010), *A. artemisiifolia* (Liu et al. 2012) *H. annuus* (Meriç et al. 2004; Çetinbaş and Ünal 2015) consists of epidermis, endothecium, intermediate layer and tapetum, consisting of single-row cells from outside to inside. In the young anther, the cell sizes of the epidermis and endothecium layers are similar. Fibrous thickenings of the endothecium have not yet developed in the early stage. In the mature anther, transverse expansion occurs in the epidermis cells. The epidermis remains intact until the end of pollen development in *J. kilaea*.

The endothecium layer has single-nucleated and rather larger cells than the epidermis in mature anther. It contains fibrous thickenings in the mature anther wall of *J. kilaea* as in *C. bithynica* (Yurukova-Grancharova and Dimitrova 2006) and *C. morifolium* (Li et al. 2010). In *A. subulatus, K. indica, H. arenarius, E. annuus* (Ao et al. 2009), *A. artemisiifolia* L. (Liu et al. 2012), *H. annuus* (Çetinbaş and Ünal 2015) no thickenings were seen in endothecium layer.

In the young anther of *J. kilaea*, the middle layer consists of a very flattened single layer of cells between the

endothecium and tapetum, as in *B. cervicata* (Sun and Ganders 1987), *C. bithynica* (Yurukova-Grancharova and Dimitrova 2006), *C. morifolium* (Li et al. 2010), *A. artemisiifolia* L. (Liu et al. 2012), *H. annuus* (Meriç et al. 2004; Çetinbaş and Ünal 2015). In *J. kilaea*, the middle layer is not seen in the mature anther because it degenerates at the end of microsporogenesis - the beginning of pollen mitosis. In *B. cervicata*, the middle layer becomes vacuolated immediately after differentiation and appears more flattened with further development of the anther wall. It is not evident before the formation of the plasmodial tapetum (Sun and Ganders 1987). In *C. bithynica* the middle layer is generally degenerates towards the end of prophase I of meiosis in PMCs, but occasionally stains darkly during metaphase I – anaphase I, degenerating parts of this structure can be observed (Yurukova-Grancharova and Dimitrova 2006). In *C. morifolium*, the middle layer flattened during meiosis and was still observable at the late mononuclear pollen grain stage but degenerated at the binucleate stage (Li et al. 2010). In *H. annuus*, the middle layer disappears when the pollen mother cells reach the tetrad stage (Çetinbaş and Ünal 2015).

There is a tapetum layer under middle layer in the innermost part of the anther wall. Some studies have summarized the different functions that tapetum cells can perform regarding the development of the pollen grain (Pacini et al. 1985). Some of these are the production and release of callase enzyme; transfer of polysaccharides into the locule provides the energy required during microsporogenesis and microgametogenesis cell divisions by the hydrolysis of these polysaccharides. In addition, from the synthesis of exine precursors to the formation of viscin threads; Tapetal cells are also responsible for the formation of a membrane resistant to acetolysis, the formation of orbicules or Ubisch bodies, the synthesis of sporophytic proteins, the production of trypsin, which covers the pollen grains and consists of a fibro-granular and a lipidic component, and the development of pollenkitt (Gotelli et al. 2023).

Although tapetum cells carry a single nucleus in the early stages of microsporogenesis, most of them have 2 or more nuclei in later stages. Normal mitosis, secondary nuclear divisions and nuclear fusion were observed in the tapetum cells of the anther wall in *J. kilaea*. Tapetum cells of *J. kilaea* usually have one or two nuclei. Polyploidy was observed in the tapetum cells of *Achillea tenuifolia*, from the Asteraceae family (Chehregani and Salehi 2016). The tapetum cells of *A. subulatus, K. indica, H. arenarius, E. annuus* (Ao et al. 2009) have uni- or binucleated, as in *J. kilaea*.

Programmed cell death is a physiological cell death that selectively destroys cells that are no longer needed or have no function. Although programmed cell death has been studied primarily and mostly in animal cells, it has been shown to also occur in plant cells in recent years. The occurrence of programmed cell death in the cells of the tapetum layer, which is the innermost layer of the anther wall, has been examined in studies conducted with transmission electron microscopy. While entering from the tetrad stage to the free microspore stage, it was shown that the tapetum cells lost their geometric shape and microtubules disappeared in the cytoplasm, in *Tillandsia albida*, *Lobivia rauschii* by Papini et al. (1999). According to many ontogenetic palynologists, the tetrad stage is very important in determining the exine pattern (Gabarayeva et al. 2019). It was observed that the tapetum cells began to degenerate at the same stage in *J. kilaea*.

It was observed that microsporogenesis stages were generally regular in pollen mother cells (PMC) in *J. kilaea*. Simultaneous type of cytokinesis was observed in *C. bithynica* (Yurukova-Grancharova and Dimitrova 2006), *A. subulatus*, *K. indica*, *H. arenarius* (Ao et al. 2009), *C. morifolium* (Li et al. 2010), *H. annuus* (Çetinbaş and Ünal 2015), *Galinsoga quadriradiata* Ruiz & Pav. (Kolczyk et al. 2015), *Ambrosia trifida* (Gabarayeva et al. 2019), as generally seen in dicots. *In E. annuus,* successive cytokinesis was observed in the dyad stage and simultaneous cytokinesis was observed in the tetrad phase (Ao et al. 2009). Two types of cytokinesis were observed *in J. Kilaea,* as in *E. annuus*. Successive type of cytokinesis was observed in *A. artemisiifolia*, as in monocots (Liu et al. 2012). As seen in many angiosperms, the callose wall in the PMCs of *J. kilaea* begins to form in the leptotene and disintegrate in the tetrad phase.

Asynchrony is observed during meiosis in young anther loci of *J. kilaea* as in *K. indica*, *E. annuus* (Ao et al. 2009). In one locus, the first stages of meiosis were observed, and in the other, the tetrad stage was observed in *J. kilaea*. The loci where the early stages of meiosis are seen are smaller in size than the loci where the tetrad stages are seen. It is thought that the asynchrony occurring in the anther loci is related to the transmission of nutritional materials.

In the early stages of microsporogenesis, although the cells were surrounded by the cell wall and there was callose accumulation, connections between the pollen mother cells were seen. These connections are called cytoplasmic/cytomictic channels. They represent a different type of cell wall channels from plasmodesmata. They do not have an internal structure like desmotubules and have relatively large openings compared to them (Baquar and Husain 1969; Mursalimov et al. 2010; Kolczyk et al. 2015). Cytoplasmic channels provide inter-

cellular exchange of nutrients, water, ions, various macromolecules and metabolites according to their reaction to environmental stimuli in plants (Wang et al. 2006).

Cytomixis has been considered as an abnormality in previous studies due to occurrence of pathology (Morisset 1978) or traumatic injury of plants (Takats 1959). Recently, it is generally accepted as a normal but rare cytological phenomenon. According to Mursalimov et al (2013), the absolute majority of cytomixis cases are recorded in microsporogenesis of angiosperms. Cytomixis has been described in more than 400 plant species belonging to 84 families. Among the Asteraceae family, this process has been observed in *Helianthus* (Whelan 1974), *Artemisia* (Malik and Kumari 2010), *Galinsoga* (Kolczyk et al. 2015) and *Ambrosia* (*Gabarayeva* et al. 2019). This is the first report of the genus *Jurinea*. Cytoplasmic channels are seen between cells in the stages starting from the leptotene stage of meiosis I prophase and ending with the tetrad stage in *J. kilaea*.

In *J. kilaea*, decussate type tetrads are generally formed at the end of microsporogenesis. Besides these, rarely pentads were also seen. In *H. annuus* (Çetinbaş and Ünal 2015), *E. annuus, H. arenarius* (Ao et al. 2009), *C. morifolium* (Li et al. 2010), *Achillea tenuifolia* (Chehregani and Salehi 2016) pollen mother cells produce tetrahedral microspore tetrads. *H. arenarius* (Ao et al. 2009) also produce decussate type tetrads as in *J. kilaea*. PMC of *C. Bithynica* generally produce also tetrahedral, rarely isobilateral tetrads (Yurukova-Grancharova and Dimitrova 2006).

Mature pollens of *J. kilaea* are tricolpate and trinucleated with echinate exine as in *C. bithynica* (Yurukova-Grancharova and Dimitrova 2006). In *J. kilaea*, sterile pollen grains are transparent, smaller in size than normal pollen grains, and have a smooth structure because the exine layer is undeveloped. Sterile pollen grains of *C. bithynica* are of normal size (Yurukova-Grancharova and Dimitrova 2006). In *A. subulatus, K. indica, H. arenarius and E. annuus 3-celled pollen grains were seen* (Ao et al. 2009). Pollens of *Allittia, Lorandersonia* and *Pembertonia*, classified in Astereae, are also echinates (Wortley et al. 2012).

Pollen viability was investigated in some *Lactuca* species (Asteraceae) by Kaur et al. (2019). In *L. orientalis*, 54-62% sterile pollen grains were observed because of chromosome bridges and nondisjunction during microsporogenesis. In *L. serriola*, *L. dissecta*, *L. dolichophylla and L. macrorhiza* 100% fertile pollen was produced because of the normal distribution of bivalents (Kaur et al. 2019). In *J. kilaea*, the sterile pollen rate was determined as 12.1%. Cytoplasmic channels that seen during microsporogenesis and chromosome transitions occurred in those channels might be the reason for this sterility rate in *J. kilaea*.

In conclusion, the anther wall structure, pollen development and pollen viability of *J. kilaea*, which grows naturally in a very limited area in Turkey and Bulgaria, were examined for the first time. The data obtained from this study will contribute to the cytological and embryological features used in the taxonomy of the Asteraceae family in recent years.

ACKNOWLEDGEMENT

I would like to thank to Prof. Dr. Çiler Kartal for her help in the preparation of the material and for sharing her valuable insights and, Dr. Necmettin Güler for his contributions to the collection of plant material during this study.

Part of this work was presented at the "VI. International Agricultural, Biological and Life Sciences Conference (AGBIOL 2024)" to be held on September 18-20, 2024.

FUNDING

This study is supported by Trakya University Scientific Research Project TUBAP 2024/18.

REFERENCES

Ağır SU, Kutbay HG, Sürmen B. 2016. Plant diversity along coastal dunes of the Black Sea (North of Turkey). Rend Lincei 27: 443-453.

Ağır SU, Kutbay HG, Sürmen B, Elmas E. 2017. The effects of erosion and accretion on plant communities in coastal dunes in north of Turkey. Rend Lincei. 28: 203-224.

Ağır SU, Sürmen B, Kutbay HG, İmamoğlu A. 2021. Species importance in coastal dune ecosystems in Northern Turkey. Ann Bot. 13-32.

Ao C, Wang L, Liang L, Wang X. 2009. Anther wall formation, microsporogenesis and male gametogenesis of four closely related species in Astereae (Asteraceae): description, comparison and systematic implications. Nord J Bot. 27(4): 292-297.

Avcı M, Avcı S, Akkurt S. 2015 (October). Coastal dune vegetation in Turkey: a geographical perspective. In *International Conference on the Mediterranean Coastal Environment MEDCOAST* pp. 6-10.

Baquar SR, Husain SA. 1969. Cytoplasmic channels and chromatin migration in the meiocytes of *Arnebia hispidissima* (Sieb.) DC. Ann Bot. 33(4): 821-831.

Bona M. 2020. Systematic importance of achene macro-micromorphological characteristics in selected species of the genera *Crupina, Jurinea*, and *Klasea* (Asteraceae) from Turkey. Microsc Res Tech. 83(11): 1345-1353.

Çetinbaş A, Ünal M. 2015. Anther ontogeny and microsporogenesis in *Helianthus annuus* L. (Compositae). Not Sci Biol. 7(1): 52-56.

Chehregani A, Salehi H. 2016. Male and female gametophyte development in *Achillea tenuifolia* (Asteraceae). P Bio Sci. 6(1): 85-94.

Davis PH. 1975. Flora of Turkey and the East Aegean Islands. Vol.5, Edinburg University Press, Edinburg, Great Britain, pp. 1-43: 370-381.

Doğan B, Hakkı EE, Duran A. 2010. A phylogenetic analysis of *Jurinea* (Compositae) species from Turkey based on ITS sequence data. Afr J Biotechnol. 9(12): 1741-1745.

Gabarayeva N, Polevova S, Grigorjeva V, Severova E, Volkova O, Blackmore S. 2019. Suggested mechanisms underlying pollen wall development in *Ambrosia trifida* (Asteraceae: Heliantheae). Protoplasma 256: 555-574.

Gotelli M, Lattar E, Zini LM, Rosenfeldt S, Galati B. 2023. Review on tapetal ultrastructure in angiosperms. Planta 257(6): 100.

Gülez S, Kaya LG, Dönmez S, Çetinkale SG, Koçan N. 2007. A study on the landscape design for the mugada coastal land. BAROFD. 9(12): 1-10.

Gupta H, Gupta RC, Kumar R, Singhal VK. 2017. A profile of chromosome counts, male meiosis and pollen fertility in 45 species of Asteraceae from Parvati Valley in Kullu district, Himachal Pradesh. Caryologia 70(2): 128-140.

Heywood VH. 1978. Flowering Plants of the World. Oxford University Press, Oxford, UK, pp. 263-268.

http://www.leicabiosystems.com/specimen-preparation/consumables/mounting-media-section-adhesive/details/product/historesin-1/

Karaduman D, Sağıroğlu M. 2021. Flora of Acarlar Longoz (Floodplain) (Sakarya) and its surroundings. Sakarya Univ J of Sci. 25(1): 252-274.

Kartal Ç. 2015. Microsporogenesis, microgametogenesis and in vitro pollen germination in the endangered species *Fritillaria stribrnyi* (Liliaceae). Caryologia 68(1): 36-43.

Kartal Ç. 2016. Calcium oxalate crystals in some species of the tribe Cardueae (Asteraceae). Bot Sci. 94(1): 107-119.

Kaur D, Singhal VK, Gupta RC. 2010. Male meiosis, microsporogenesis and pollen grain study in *Inula cuspidata* CB Clarke (Asteraceae). Cytologia 75(4): 363-368.

Kaur D, Tantray YR, Singhal V K. 2019. Cytological study in some species of *Lactuca* L. (Asteraceae) from high altitudinal regions of Kinnaur district, Himachal Pradesh, India. Taiwania 64(2): 111.

Kılıç O. 2020. Determination of total phenolic, flavonoid substance, antioxidant and antimicrobial properties of *Allium rumelicum, Jurinea kilaea, Peucedanum obtusifolium* plants growing in Thrace region. Master's Thesis, Tekirdağ Namık Kemal University, TURKEY.

Kolczyk J, Tuleja M, Płachno B. 2015. Histological and cytological analysis of microsporogenesis and microgametogenesis of the invasive species *Galinsoga quadriradiata* Ruiz & Pav. (Asteraceae). Acta Biol Cracov Bot. 57(2): 89-97.

Kutbay HG, Sürmen B, Ağır ŞU, Kılıç DD. 2017. Samsun ili kıyı kumullarında tespit edilen yabancı bitkiler. Turk J Weed Sci. 20(2): 19-27.

Li F, Chen S, Chen F, Teng N, Fang W, Zhang F, Deng Y. 2010. Anther wall development, microsporogenesis and microgametogenesis in male fertile and sterile *Chrysanthemum* (*Chrysanthemum morifolium* Ramat., Asteraceae). Sci Hortic (Amsterdam). 126(2): 261-267.

Liu JX, Wang M, Chen BX, Jin P, Li JY, Zeng K. 2012. Microsporogenesis, microgametogenesis, and pollen morphology of *Ambrosia artemisiifolia* L. in China. Pl Syst Evol. 298: 43-50.

Malik RA, Kumari S. 2010. Genetic diversity in different populations of *Artemisia absinthium* Linn. from Kashmir Himalaya. Cytologia 75(3): 273-276.

Meriç C, Dane F, Olgun G. 2004. Histological aspects of anther wall in male fertile and cytoplasmic male sterile *Helianthus annuus* L. (Sunflower) Asian J Plant Sci. 3:145-150.

Morisset P. 1978. Cytomixis in pollen mother cells of *Ononis* (Leguminosae). Can J Genet Cytol. 20(3): 383-388.

Mursalimov SR, Baiborodin SI, Sidorchuk YV, Shumny VK, Deineko EV. 2010. Characteristics of the cytomictic channel formation in *Nicotiana tabacum* L. pollen mother cells. Cytol Genet. 44: 14-18.

Mursalimov SR, Sidorchuk YV, Deineko E. 2013. New insights into cytomixis: specific cellular features and prevalence in higher plants. Planta 238: 415–423.

Nikolić M, Stevović S. 2015. Family Asteraceae as a sustainable planning tool in phytoremediation and its relevance in urban areas. Urban For Urban Green. 14: 782–789.

O'Brien T, Feder NMEM, McCully ME.1964. Polychromatic staining of plant cell walls by toluidine blue O. Protoplasma 59: 368-373.

Özhatay N, Akalın E, Güler N, Ersoy H, Yeşil Y, Demirci S. 2013. Floristic richness and conservation priority sites in the northwest of European Turkey: Mt Yıldız-Kırklareli. Phytol Balc. 19(1): 77-88.

Özhatay N, Öztekin M. 2015. Plant biodiversity and unique yew stands of Istranca (Yıldız) mountains in European Turkey. In *YEW Workshop 2015*. Düzce-Turkey, pp. 76.

Pacini E, Franchi GG, Hesse M. 1985. The tapetum: its form, function, and possible phylogeny in Embryophyta. Pl Syst Evol.149: 155-185.

Papini A, Mosti S, Brighigna L. 1999. Programmed-cell-death events during tapetum development of angiosperms. Protoplasma 207, 213–221.

Rolnik A, Olas B. 2021. The plants of the Asteraceae family as agents in the protection of human health. Int J Mol Sci. 22(6): 3009.

Saday S. 2005. *Jurinea* Cass. (*Compositae*) *Üzerinde Morfolojik, Palinolojik ve Anatomik Araştırmalar* (PhD. Thessis, Marmara Universitesi -Turkey).

Shekhar S, Pandey AK. 2009. Anther appendages and anther collar in Asteraceae and their taxonomic significance. Pleione 3(2): 212-218.

Shi Z et al. [total: 33 co-authors] 2011. Asteraceae (Compositae) [family introduction, glossary, systematic list, and key to tribes]. Pp. 1–8 in: Wu ZY, Raven PH, Hong D Y eds., Flora of China Volume 2021 (Asteraceae). Science Press (Beijing) & Missouri Botanical Garden Press (St. Louis).

Sun M, Ganders FR. 1987. Microsporogenesis in male-sterile and hermaphroditic plants of nine gynodioecious taxa of Hawaiian Bidens (Asteraceae). Am J Bot. 74(2): 209-217.

Susanna A, Baldwin BG, Bayer RJ, Bonifacino JM, Garcia-Jacas N, Keeley SC, ... Stuessy TF. 2020. The classification of the Compositae: A tribute to Vicki Ann Funk (1947–2019). Taxon 69(4): 807-814.

Sürmen B, Şenay ULU, Kutbay HG. 2019. Rare dune plant species in Samsun Province, Turkey. Ant J Bot. 3(2): 34-39.

Szukala A, Korotkova N, Gruenstaeudl M, Sennikov AN, Lazkov GA, Litvinskaya SA, ... von Raab-Straube E. 2019. Phylogeny of the Eurasian genus *Jurinea* (Asteraceae: Cardueae): Support for a monophyletic genus concept and a first hypothesis on overall species relationships. Taxon 68(1): 112-131.

Taç S, Özcan T. 2019. Fatty acid and amino acid profiles in some dune vegetation species from İstanbul. Süleyman Demirel Univ Fen Bilim Enst Derg. 23(3): 892-903.

Takats ST. 1959. Chromatin extrusion and DNA transfer during microsporogenesis. Chromosoma 10: 430-453.

Tuncay HO, Akalın UE. 2018. Endemism in İstanbul plants. Eur J Biol. 77(1): 38-41.

Uslu M, Keçeli T. 2019. İğneada Longoz Ormanları Milli Parkı (Demirköy-Kırklareli) Ciğerotları (Marchantiophyta) Florası. Anatolian Bryol. 5(2): 114-129.

Valcheva M, Sopotlieva D, Apostolova I. 2020. Current state and historical notes on sand dune flora of the Bulgarian Black Sea Coast. Flora 267: 151594.

Wang CY, Li X, Wu QF, Wang XY. 2006. Cytoplasmic channels and their association with plastids in male meiocytes of tobacco, onion and lily. Cell Biol Int. 30(5): 406-411.

Whelan ED. 1974. Discontinuities in the callose wall, intermeiocyte connections, and cytomixis in angiosperm meiocytes. Canad J Bot. 52(6): 1219-1224.

Wortley AH, Blackmore S, Chissoe WF, Skvarla JJ. 2012. Recent advances in Compositae (Asteraceae) palynology, with emphasis on previously unstudied and unplaced taxa. Grana 51(2): 158-179.

Yıldırımlı Ş. 1999. The chorology of the Turkish species of Asteraceae family. *Ot Sist Bot*. 6(2): 75-123.

Yurukova-Grancharova P, Dimitrova D. 2006. Cytoembryological study of *Crepis bithynica* (Asteraceae) from Bulgaria. Flora Mediterr. 16: 33-43.

Caryologia
International Journal of Cytology, Cytosystematics and Cytogenetics

Firenze University Press
https://riviste.fupress.net/index.php/caryologia

OPEN ACCESS

Citation: Mumbrú, M., Garnatje, T., & Vallès, J. (2025). Methods of internal standards' preservation for genome size assessments: a comparative study. *Caryologia* 78(1): 53-58. doi: 10.36253/caryologia-3323

Received: February 16, 2025

Accepted: March 25, 2025

Published: October 1, 2025

Data Availability Statement: All relevant data are within the paper and its Supporting Information files.

Competing Interests: The Author(s) declare(s) no conflict of interest.

ORCID
MM: 0009-0005-8699-3473
TG: 0000-0001-6295-6217
JV: 0000-0002-1309-3942

Methods of internal standards' preservation for genome size assessments: a comparative study

Màrius Mumbrú[1], Teresa Garnatje[2,3], Joan Vallès[1,4,*]

[1] *Laboratori de Botànica—Unitat Associada CSIC, Facultat de Farmàcia i Ciències de l'Alimentació—Institut de Recerca de la Biodiversitat IRBio, Universitat de Barcelona (UB), Av. Joan XXIII 27-31, 08028 Barcelona, Catalonia, Spain*
[2] *Institut Botànic de Barcelona, IBB (CSIC-CMCNB), Passeig del Migdia s.n. 08038 Barcelona, Catalonia, Spain*
[3] *Jardí Botànic Marimurtra - Fundació Carl Faust, Passeig de Carles Faust, 9, 17300 Blanes, Catalonia, Spain*
[4] *Secció de Ciències Biològiques, Institut d'Estudis Catalans, Carrer del Carme, 47, 08001 Barcelona, Catalonia, Spain*
*Corresponding author. Email: joanvalles@ub.edu

Abstract. Assessing genome size in plant species using flow cytometry requires fresh plant material from both the target species and appropriate internal standards. The use of fresh material from the standards is sometimes difficult. For this reason, a research about three preservation methods and their results when using the plants in flow cytometry has been conducted. We have focused on four of the most used internal standards in flow cytometry to estimate the nuclear DNA amount. Our results pointed out that the best method of conservation was lyophilisation. The conservation method based on drying with silica gel is more advisable to establish the ploidy level than to provide an absolute value of nuclear DNA content. Finally, ultrafreezing is not an appropriate preservation method.

Keywords: flow cytometry, freezing, genome size, internal standards, lyophilisation, silica gel preservation.

INTRODUCTION

The genome size, also named the nuclear DNA amount or 2C value, is a parameter that can be related to many other characteristics of an organism and its environment (Wakamiya et al. 1993; Wang et al. 2021). The term 'C-value' was coined by Swift (1950), the 'C' accounting for 'constancy' and referring to the DNA content of an unreplicated haploid chromosome complement. Later, several studies have established the influences of environmental factors on the variation of this parameter, although it was initially proposed as a constant of the organism and even of the species (Greilhuber et al. 2005). Other studies pointed out that some genuine variation exists, even within a species (Šmarda and Bureš 2010; Díez et al. 2013; Kolář et al. 2017; Boutte et

al. 2020; Becher et al. 2021), and that this can be due to intrinsic (ploidy level, aneuploidy, recombination rates, tandem repeats) or extrinsic (altitude, latitude, soil type, etc.) factors. Genome size information is crucial as the base to perform whole genome sequencing (WGS) and thus further research on this parameter, still unknown for a huge percentage of plant species, is needed (Pellicer et al. 2022). Despite there are many studies devoted to the importance of protocols and their effect on the accuracy of measurements, often highlighting the constancy of the value, the relative proximity to the genome size of the studied plants, the absence of some interfering cytosol metabolites or the possibility of producing low coefficients of variation in the measurements (Jedrzejczyk and Sliwinska 2010; Suda and Leitch 2010; Temsch et al. 2022), very few studies have been performed focused on methods of preservation and storage of plant material (Čertner et al. 2021; Tang et al. 2023), and even less on this aspect applied to internal standards.

The most commonly used technique to estimate genome size is flow cytometry (FCM), which allows estimating the amount of nuclear DNA by the relationship of the intensity of the measured fluorescence of the studied plants and the internal standard (Doležel and Bartos 2005; Hare and Johnston 2011). The quantification of the DNA of plant cells by flow cytometry basically requires fresh plant material from the target species and internal standards, and this need complicates the transfer and the storage of the samples (Doležel and Bartos 2005). The possibility of using fresh material from the standards is sometimes difficult, because the plant is not always available in its optimal state when the collected samples are analysed, although cultivation makes it possible in many cases. The same, and more complicated when dealing with wild plants, goes for the target plants, either because they were collected long time ago and are pending to be processed or because of slow processing. Storing plants in a conventional cold room at 4 °C, or freezing them at -18 °C, does not prevent their degradation, at least after a more or less long period of time. The temperature above 4 °C causes the breaking of the hydrogen bonds between the nitrogenous bases. Even environmental water can separate the two DNA chains by hydrolysis. A good conservation system would be necessary to avoid problems arising from the poor condition of the target plants and standards when there are delays in their processing that may be due to different reasons.

Facing the difficulty to standardize a preservation method for the great diversity of existing species, here we have focused on four of the most used internal standards in flow cytometry to assess the nuclear DNA amount of plants: *Lycopersicon esculentum, Petunia hybrida, Pisum sativum*, and *Triticum aestivum*, with the aim of testing different preservation methods, lyophilisation (also known as freeze drying), drying in silica gel and freezing at ultra-low temperature, and comparing the results obtained.

MATERIALS AND METHODS

Plant material and preservation treatments

Fresh material from leaves of tomato [*Lycopersicon esculentum* Mill. 'Montfavet 63/5' (2C=1.99 pg, Marie and Brown 1993)], petunia [*Petunia hybrida* Vilm. 'PxPc6' (2C=2.85 pg, Marie and Brown 1993)], common pea [*Pisum sativum* L. 'Express long' (2C=8.37 pg, Marie and Brown 1993)] and wheat [*Triticum aestivum* L. 'Triple Dirk' (2C=30.9 pg, Marie and Brown 1993)] were obtained from seeds and grown in a greenhouse at the Faculty of Pharmacy and Food Sciences (University of Barcelona), and treated with three conventional preservation systems usually used at the laboratories: lyophilisation, drying in silica gel and freezing at ultra-low temperature. Freezing was performed at -85 °C in a freezer Sanyo Electric Corporation (Moriguchi City, Osaka, Japan). The lyophilisation was carried out with a lyophiliser, FTS Systems Inc. (Stone Ridge, New York, USA) preserving the plant material into airtight glass jars by following the steps: 1) 2 minutes in liquid nitrogen 2) immersion of the sample in crushed ice and, 3) lyophilisation during 48 hours under vacuum < 500 mTorr. For the silica gel drying, the samples were kept in silica gel at room temperature for one month before the measurement (time 0).

The water percentages were obtained by drying in an oven until constant weight.

Flow cytometry assessments

Pisum sativum was used as standard to assess the genome size of *Triticum aestivum, Petunia hybrida* and *Lycopersicon esculentum,* while *Petunia hybrida* was the standard chosen to establish the nuclear DNA amount of *Pisum sativum*. Five individuals by each of the three treatments of the four standards and two samples of each individual were measured. To carry out the measurements, the standard with a DNA content closest to the theoretical value of the target standard has been chosen. When used as internal standards in this research, the leaf materials were always fresh.

An amount of 40-50 mg of young leaf tissue was used for sample preparation. Leaf material of each inter-

nal standard studied together with the leaf material of the plant used here as internal standard, as mentioned above, was submerged in 1,200 µL of isolation buffer LB01 (Doležel et al. 1989), supplemented with 100 µg/mL of ribonuclease A in a Petri dish, and mechanically chopped using a razor blade. The extract obtained was filtered to 20 µm pore nylon mesh, and stained with 36 µL of propidium iodide (1 mg/mL). Samples remained on ice until analysis.

The DNA measurements were carried out in a flow cytometer Epics XL (Coulter Corporation, Hialeah, Florida, USA). The cytometer used has an air-cooled argon-ion laser tuned at 15 mW and 488 nm of wave length excitation with forward scatter (FS) and side scatter (SS). FS measures the particle size and SS measures the particle complexity. Fluorescence was collected to 620 nm band pass filter (red). Two replicates of five different leafs of each plant were analysed. Acquisition was automatically stopped at 8,000 nuclei counts. The results were acquired by the System II Software version 3.0 (Coulter Electronics). Prior to analysis, the instrument was checked with standard fluorescent beads (Coulter Electronics).

For all the target plants, measurements were carried out immediately after the treatment (t0) and after six months (t6) in the same individual.

Statistical analyses

The variation of the cytometric measurements is usually expressed as the half peak coefficient of variation (HPCV). This parameter, expressed in percentage, indicates the dispersion of fluorescence intensities as the ratio of the standard deviation to the mean measured at 50% peak height. In addition, the mean, standard deviation, coefficient of variation (CV) and confidence interval (CI) were also calculated for each standard and treatment. A paired sample t-test was carried out to determine whether the mean difference between the GS values between t0 and t6 is zero for each treatment and standard. Previously, a Shapiro-Wilk test of normality was carried out for all samples.

Statistical analyses were performed using XLSTAT 2023.1.1 (Lumivero 2023), Excel 16.0.4266 by Microsoft Office (Microsoft Corporation).

RESULTS AND DISCUSSION

The results of descriptive statistics are included in the Table 1. No genome size measurements have been obtained for *Triticum aestivum* lyophilized for six months.

The calculated parameters (mean, SD, CV and CI) reveal a great dispersion of values in the assessments of genome size of the standards. In fact, in many cases the established value of the standard (Marie and Brown 1993) does not fall within the confidence interval calculated from the average and standard deviation of each subset of data. In the lyophilized material, only in *Pisum sativum* (t6) and *Lycopersicon esculentum* (t0) the established values for both internal standards fall outside the interval, while for the remaining treatments (silica gel and freezing), almost all standards values fall out, excepting for the frozen material of *Petunia hybrida* (t6) and *Lycopersicon esculentum* (t0) (Table 1). These results point out that the best treatment to preserve samples is the lyophilisation, while silica gel preservation is the least recommended, despite the results for frozen wheat are missing, probably due to DNA degradation during the freezing process.

Results of p-values from the Paired t-test are displayed in Table 2. Shapiro-Wilk test reveals that 2C values of most data subsets follow a normal distribution. P-values below 0.05 (Table 2) indicate that there are statistically significant differences between the genome size measurements at t0 and t6 into the same standard and treatment. In this case, the different standards behave differently over time, which allows us to assert that some characteristics of the plant species and, in particular, of their leaves, influence their state of conservation. Thus, we note that *Triticum aestivum* and *Pisum sativum*, with a lower water content (74.35% and 80.22%, respectively) are the species showing less genome size variation over time, while *Petunia hybrida* (87.97%) and *Lycopersicon esculentum* (85.53 %) are more time sensitive.

Although a considerable effort has been dedicated to defining the characteristics of the internal standards employed in quantifying DNA, one of the relevant ones being the easy availability (Temsch et al. 2022), the studies on the preservation of plant material for flow cytometry are very scarce. Some authors (Tang et al. 2023) have investigated for alternative solutions such as the use of spores and pollen as internal standards. These authors claim that these standards are ready-to-use, easy to handle, and include long-term storage compared to traditional fresh leaf standards.

Čertner et al. (2021) have analysed the advantages and limitations of different strategies and material storage, but they have not specifically focused on internal standards. The authors conclude that frozen plants can be stored for up to months or years, and silica gel-dried material for up to two years, in both cases only for ploidy level determinations. In fact, these authors only consider as viable materials for genome size estimation

Table 1. Descriptive statistics for the 2C values of the internal standards immediately after the treatment (t0) and after six months preserved (t6).

	Triticum aestivum	*Petunia hybrida*	*Pisum sativum*	*Lycopersicon esculentum*	
2C (pg)	30.9	2.85	8.37	1.99	
H_2O content (%)	74.35	87.97	80.22	85.53	
	t0				
Mean (x̄)±SD	30.914±0.671	2.882±0.028	8.321±0.164	2.092±0.076	
Coefficient of variation (CV)	2.171	0.970	1.976	3.651	
Confidence interval (CI)	[30.080; 31.747]	[2.847; 2.917]	[8.117; 8.525]	[1.997; 2.187]*	Lyophilised
	t6				
Mean (x̄)±SD	31.537±0.596	2.903±0.073	8.050±0.149	1.963±0.050	
Coefficient of variation (CV)	1.890	2.515	1.846	2.569	
Confidence interval (CI)	[30.797; 32.278]	[2.812; 2.994]	[7.866; 8.235]*	[1.900; 2.026]	
	t0				
Mean (x̄)±SD	31.841±0.523	3.144±0.024	7.979±0.171	2.037±0.031	
Coefficient of variation (CV)	1.644	0.779	2.140	1.523	
Confidence interval (CI)	[31.191; 32.491]*	[3.113; 3.174]*	[7.767; 8.191]*	[1.998; 2.075]*	Silica gel-preserved
	t6				
Mean (x̄)±SD	32.004±0.206	2.587±0.164	8.044±0.112	1.404±0.131	
Coefficient of variation (CV)	0.643	6.352	1.396	9.332	
Confidence interval (CI)	[31.749; 32.260]*	[2.383; 2.791]*	[7.905; 8.184]*	[1.242; 1.567]*	
	t0				
Mean (x̄)±SD	34.165±0.362	2.690±0.029	7.424±0.056	2.092±0.091	
Coefficient of variation (CV)	1.059	1.088	0.752	4.353	
Confidence interval (CI)	[33.716; 34.615]*	[2.653; 2.726]*	[7.354; 7.493]*	[1.979; 2.205]	Frozen
	t6				
Mean (x̄)±SD	missing	2.784±0.233	7.680±0.356	2.412±0.112	
Coefficient of variation (CV)	missing	8.360	4.634	4.645	
Confidence interval (CI)	missing	[2.495; 3.074]	[7.238; 8.122]*	[2.273; 2.551]*	

Table 2. p-values from the paired t-test. *Statistically significant differences in 2C values between immediately after the treatment (t0) and after six months preserved (t6).

	Triticum aestivum	*Petunia hybrida*	*Pisum sativum*	*Lycopersicon esculentum*
Llyophilised	p=0.222	p=0.558	p=0.070	p=0.023*
Silica gel preserved	p=0.537	p=0.002*	p=0.539	p=0.000*
Freezing	-	p=0.414	p=0.198	p=0.017*

in absolute fresh tissue units freshly germinated seedlings (which consist also of fresh tissue), and glycerol-preserved nuclei, with silica gel-desiccated tissue, dry seeds, frozen tissue and chemically-fixed tissue as apt for ploidy level determination. Concerning dried material, this agrees with the evidences of usefulness of such tissues for ploidy level determination brought by Suda and Trávníček (2006). Indeed, Sliwinska et al. (2021) recommend to avoid preserved (herbarium vouchers, silica gel-dried tissue, frozen tissue) or fixed samples for a robust genome size assessment in plants. Bourge et al. (2018) state that measurements in dried samples could be less precise and even need correction factors. Conversely, Wang and Yang (2016) affirm that desiccated tissues that remain green (without brown or yellow marks), and stored at -80 °C for less than six months are suitable for genome size estimations with absolute values.

According to the present results, we can add lyophilisation, which is not included in any of previous mentioned studies, as another preservation method allowing nuclear DNA content assessment in absolute units, and confirm the non-suitability of silica gel-desiccated and frozen materials for such precise estimations, although they can be appropriate for ploidy level determination.

Concluding remarks

The optimal conservation method among the three evaluated is lyophilisation. At the initial time point, the values align closely with those of the fresh material, and even after six months, there are no noteworthy differences between both values. Lyophilisation emerges as a more convenient and cost-effective option for sample preservation, when compared to the commonly used cryogenic technique involving liquid nitrogen in situ (Čertner et al. 2021), which is not always practical in field work.

Drying with silica gel stands as a generally acceptable conservation method. However, its effectiveness diminishes in tissues with higher water content, as evidenced by an increase in the coefficient of variation of results. This technique is better suited for determining ploidy levels than providing an absolute DNA content value.

On the other hand, ultrafreezing proves to be the least effective preservation method among the three tested. This inferiority is likely attributed to the freezing process allowing ample time for structural water to degrade a portion of the DNA.

In summary, lyophilisation stands out as the best choice, offering comparable values to fresh material at time 0 and maintaining consistency over a 6-month period. The current results allow to add lyophilisation to the other systems of preservation (apart from using fresh tissue, which is ideal whenever possible) proposed to date to estimate genome size, whereas freezing and silica gel-drying are confirmed to be useful to preserve plant materials for ploidy level establishment, but not for nuclear DNA content assessment in absolute units.

ACKNOWLEDGEMENTS

We thank Jaume Comas, Ricard Álvarez, Rosario González and Sonia Ruiz (Centres Científics i Tecnològics, Universitat de Barcelona) for the assistance given in flow cytometric measurements and Laboratory of Plant Physiology (Faculty of Pharmacy and Food Sciences, University of Barcelona) for lyophilisation facilities. This research was supported by projects 2017SGR1116 and 2021SGR00315 from the Generalitat de Catalunya.

REFERENCES

Becher H, Powell RF, Brown MR, Metherell C, Pellicer J, Leitch IJ, Twyford AD. 2021. The nature of intraspecific and interspecific genome size variation in taxonomically complex eyebrights. Ann Bot. 128(5):639–651. https://doi.org/10.1093/aob/mcab102

Bourge M, Brown SC, Siljak-Yakovlev S. 2018. Flow cytometry as tool in plant sciences, with emphasis on genome size and ploidy level assessment. Genet App. 2(2):1–12. https://doi.org/10.31383/ga.vol2iss2pp1-12

Boutte J, Maillet L, Chaussepied T, Letort S, Aury J-M, Belser C, Boideau F, Brunet A, Coriton O, Deniot G, et al. 2020. Genome Size Variation and Comparative Genomics Reveal Intraspecific Diversity in *Brassica rapa*. Front Plant Sci. 11:577536. https://doi.org/10.3389/fpls.2020.577536

Čertner M, Lučanová M, Sliwinska E, Kolář F, Loureiro J. 2021. Plant material selection, collection, preservation, and storage for nuclear DNA content estimation. Cytometry Part A. 1–12. https://doi.org/10.1002/cyto.a.24482

Díez CM, Gaut BS, Meca E, Scheinvar E, Montes-Hernandez S, Eguiarte LE, Tenaillon MI. 2013. Genome size variation in wild and cultivated maize along altitudinal gradients. New Phytol. 199(1):264–276.

Doležel J, Binarová P, Lucretti S. 1989. Analysis of nuclear DNA content in plant cells by flow cytometry. Biol Plantarum 31:113–120.

Doležel J, Bartoš J. 2005. Plant DNA Flow Cytometry and Estimation of Nuclear Genome Size. Ann Bot. 95(1):99–110. https://doi.org/10.1093/aob/mci005

Hare EE, Johnston JS. 2011. Genome size determination using flow cytometry of propidium iodide-stained nuclei. Methods Mol Biol. 772:3–12. https://doi.org/10.1007/978-1-61779-228-1_1

Jedrzejczyk I, Sliwinska E. 2010. Leaves and Seeds as Materials for Flow Cytometric Estimation of the Genome Size of 11 Rosaceae Woody Species Containing DNA-Staining Inhibitors. J Bot. 930895. https://doi.org/10.1155/2010/930895

Kolář F, Čertner M, Suda J, Schönswetter P, Husband BC. 2017. Mixed-ploidy species: progress and opportunities in polyploid research. Trends Plant Sci. 22(12):1041–1055.

Lumivero. 2023. XLSTAT statistical and data analysis solution. New York, USA. https://www.xlstat.com/es.

Marie D, Brown SC. 1993. A Cytometric Exercise in Plant DNA Histograms, with 2C-Values for 70 Species. Biol Cell. 78(1-2):41–51.

Pellicer J, Hidalgo O, Vallès J, Garnatje T. 2022. Sobre la necessitat d'estudiar trets genètics que influeixen en l'organització i l'estructura del genoma en projectes de seqüenciació de plantes. Treballs Soc Cat Biol. 72:10–15. https://raco.cat/index.php/TreballsSCBiologia/article/view/409868

Sliwinska E, Loureiro J, Leitch IJ, Šmarda P, Bainard J, Bureš P, Chumová, Z, Horová L, Koutecký

P, Lučanová M, et al. 2021. Application-based guidelines for best practices in plant flow cytometry, Cytometry Part A. 101(9):749–781. https://doi.org/10.1002/cyto.a.24499

Šmarda P, Bureš P. 2010. Understanding intraspecific variation in genome size in plants. Preslia 82(1):41–61.

Suda J, Trávníček P. 2006. Reliable DNA Ploidy Determination in Dehydrated Tissues of Vascular Plants by DAPI Flow Cytometry—New Prospects for Plant Research. Cytometry Part A. 69A: 273–280. https://doi.org/10.1002/cyto.a.20253

Suda J, Leitch IJ. 2010. The quest for suitable reference standards in genome size research. Cytometry Part A. 77: 717–720. https://doi.org/10.1002/cyto.a.20907.

Swift H. 1950. The constancy of desoxyribose nucleic acid in plant nuclei. Proc Nat Acad Sci USA 36:643–654.

Tang SK, Lee PH, Liou WT, Lin CH, Huang YM, Kuo LY. 2023. Fern Spores-"Ready-to-Use" Standards for Plant Genome Size Estimation Using a Flow Cytometric Approach. Pl ants 12(1):140. https://doi.org/10.3390/plants12010140

Temsch EM, Koutecký P, Urfus T, Šmarda P, Doležel J. 2022. Reference standards for flow cytometric estimation of absolute nuclear DNA content in plants. Cytometry Part A. 101:710–724. https://doi.org/10.1002/cyto.a.24495

Wakamiya I, Newton RJ, Johnston JS, Price HJ. 1993. Genome size and environmental factors in the genus *Pinus*. Amer J Bot 80:12351241. https://doi.org/10.1002/j.1537-2197.1993.tb15360.x

Wang G, Yang Y. 2016. The effects of fresh and rapid desiccated tissue on estimates of Ophiopogoneae genome size. Plant Div. 38:190–193. https://doi.org/10.1016/j.pld.2016.08.001

Wang D, Zheng Z, Li Y et al. 2021. Which factors contribute most to genome size variation within angiosperms? Ecol Evol. 11:2660–2668. https://doi.org/10.1002/ece3.7222

Caryologia
International Journal of Cytology, Cytosystematics and Cytogenetics

Firenze University Press
https://riviste.fupress.net/index.php/caryologia

OPEN ACCESS

Citation: Rocha, R. B., Benzaquem, D. C., Passos, P. S., Silva, E. K. C., Carvalho, N. D. M., Neves, D. B. S., Silva, P. R. L., & Fantin, C. (2025). Cytogenetic diagnosis of patients with suspected premature ovarian failure in Manaus, Brazil. *Caryologia* 78(1): 59-66. doi: 10.36253/caryologia-3030

Received: September 20, 2024

Accepted: June 21, 2025

Published: October 1, 2025

Data Availability Statement: All relevant data are within the paper and its Supporting Information files.

Competing Interests: The Author(s) declare(s) no conflict of interest.

Cytogenetic diagnosis of patients with suspected premature ovarian failure in Manaus, Brazil

Ruan Barboza Rocha[1], Denise Corrêa Benzaquem[1], Paloma de Sousa Passos[1], Evellyn Karine Cruz da Silva[1], Natália Dayane Moura Carvalho[2], Daria Barroso Serrão das Neves[3], Paula Rita Leite da Silva[3], Cleiton Fantin[1,*]

[1] *Laboratório de Citogenética Humana, Universidade do Estado do Amazonas, Manaus, Brasil*
[2] *Instituto de Saúde e Biotecnologia, Universidade Federal do Amazonas, Coari, Brasil*
[3] *Departamento de Ginecologia, Universidade do Estado do Amazonas, Manaus, Brasil*
*Corresponding author. Email: cfantin@uea.edu.br

Abstract. Premature ovarian failure (POF) is a clinical syndrome that is characterized by loss of ovarian function in women of childbearing age and generally occurs before the age of 40. Genetic causes account for about 20 to 25% of cases of POF. However, in many cases, the origin of the condition remains idiopathic. The objective of this study was to perform cytogenetic research in a group of patients affected by POF in order to identify the type and frequency of chromosomal alterations. Fifteen patients were referred to the Human Cytogenetics Laboratory of the Amazonas State University (UEA) by gynecology specialists from two public health institutions in Manaus, Amazonas, Brazil, for chromosomal analysis. The analysis was performed via peripheral blood lymphocyte culture using the GTG banding method. The karyotypes were assembled with the help of the GeneAll-HD® software and the results were interpreted according to the ISCN 2016 standards. Of the fifteen patients analyzed, nine (60%) had no chromosomal abnormalities, while six (40%) exhibited chromosomal abnormalities. Of the alterations identified, three patients (20%) presented numerical alterations of the X chromosome with mosaicism, two patients (13%) showed autosomal numerical alterations involving chromosomes 15 and 21, both with mosaicism, and one patient (7%) exhibited a structural alteration in the form of terminal deletion of the long arm of the X chromosome. The results obtained in this study have the potential to improve the accuracy of the diagnosis, assist in medical decisions, provide adequate prognoses and facilitate reproductive management through genetic counseling.

Keywords: Premature Ovarian Failure, G-band karyotype, chromosomal alterations, X chromosome, medical diagnosis.

INTRODUCTION

Premature ovarian failure (POF) is a clinical syndrome that is defined by the loss of ovarian function in women of childbearing age, generally before

the age of 40. The main symptoms of POF are menstrual disorders such as amenorrhea or oligomenorrhea, as well as having high levels of gonadotropins and low levels of estradiol. These symptoms result in hypoestrogenic and hypergonadotropic clinical pictures (Goswami and Conway 2005; Eshre 2016; Chon 2021). The first reports of this syndrome were made in 1942 by Fuller Albright, who named the condition "primary ovarian failure" (Albright 1942).

The overall incidence of POF is estimated to be approximately 1% in women aged under 40 and 0.1% in women under 30 (Rahman and Panay 2021). In the mid and long term, this condition can cause an increase in cardiovascular diseases, a decrease in bone mineral density with a risk of osteoporosis, and a progressive decline in fertility with neurological effects, resulting in a general reduction in the woman's life expectancy (Podfigurna-Stopa et al. 2016; Wesevich 2020).

The etiology of POF is highly heterogeneous and causes can be genetic, autoimmune, metabolic, infectious and iatrogenic (Jiao et al. 2012; Qin 2015). Genetic causes account for approximately 20 to 25% of patients with POF (Ayed et al. 2014; Qin 2015; Luo et al. 2023). The most common genetic cause of POF is alterations involving the X chromosome. These changes can be of the numerical type, such as monosomy X, trisomy X, mosaicism X, or structural changes, such as deletions X, X-autosome translocations and isochromosomes (Holland 2001; Baronchelli et al. 2011).

In the diagnosis of POF, a complete gynecological evaluation is carried out with physical, biochemical and imaging examinations, which mainly include the measurement of high gonadotropin levels and low estradiol levels in patients under the age of 40 years who have symptoms of oligomenorrhea or amenorrhea lasting at least 4 months. The specialist can ascertain this condition when examining women with menstrual disorders. In cases of secondary amenorrhea, it is necessary to exclude pregnancy by examining serum levels of betahCG. After confirming the diagnosis of POF through physical and biochemical examinations, due to its heterogeneity, it becomes necessary to request complementary examinations, such as cytogenetic analyses including karyotyping, in order to determine the etiology (Eshre 2016; Jankowska 2017).

Cytogenetic and molecular investigations of these alterations have allowed us to identify two critical regions in the long arm of the X chromosome, in Xq13-q21 and Xq26-27 (Powell et al. 1994; Sala et al. 1997). Although chromosomal alterations primarily involve the X chromosome, an increasing number of alterations involving autosomal chromosomes have been reported in the literature (Goswami and Conway 2005). Chromosomal abnormalities have long been recognized as a frequent cause of POF, with widely varying percentages reported in the literature in both primary and secondary amenorrhea, thus suggesting the need for cytogenetic analyses (Lakhal et al. 2010; Ceylaner et al. 2010; Kalantari et al. 2013; Ayed et al 2014). Nonetheless, in most cases, the etiopathogenesis of this condition still remains idiopathic (Rudnicka et al. 2018).

Given the strong impact of the disease on the quality of life of these women, it is important to highlight the value of cytogenetic investigations, including karyotyping, which can be requested for women affected by POF, in order to detect the presence of chromosomal alterations that may be associated with this condition (Di-Battista 2020). In Brazil, most studies involving the cytogenetic diagnosis in women affected with POF are concentrated in the southern and southeastern regions of the country and cytogenetic investigations related to POF in the state of Amazonas have not yet been carried out.

Therefore, the purpose of this study was to conduct cytogenetic analyses in patients affected by this condition. The results obtained have the potential to offer crucial information to the medical and scientific community of the northern region of Brazil. These findings not only fill a gap in current knowledge, but also have the potential to drive the development of more effective prevention and treatment strategies for POF.

MATERIALS AND METHODS

Patients

A prospective study was conducted in patients with suspected premature ovarian failure who were seen at two public health institutions in Manaus, Amazonas, Brazil: the department of Climacteric, Gynecology and Mastology in the Araújo Lima outpatient clinic at the Getúlio Vargas University Hospital (HUGV), and the department of Gynecology and Obstetrics at the Codajás Polyclinic.

The inclusion criteria for the study were as follows: patients treated by the Unified Health System (SUS) in Manaus, Amazonas, and affected by POF according to the guidelines of the European Society of Human Reproduction and Embryology ESHRE (Eshre 2016). Criteria for diagnosis of POF included: (I) primary or secondary oligo/amenorrhea for at least four consecutive months before the age of 40. (II) high levels of FSH >25 IU/mL and low levels of estradiol <20 pg/mL in the blood, (III) in two dosages more than 4 weeks apart. Patients with conditions known to induce POF, such as chemotherapy or radiotherapy and ovarian surgery, were excluded.

The study was approved by the Ethics Committee of the Universidade do Estado do Amazonas (UEA), under CAAE number 95704617.0.0000.5016. The participation of the patients was voluntary and an informed consent form was signed by all the participants. A total of 15 patients were referred to the Human Cytogenetics Laboratory of the Universidade do Estado do Amazonas, where 5 mL of peripheral blood was collected by venipuncture with a disposable sterile syringe for subsequent culture of lymphocytes.

Cytogenetic analysis

The karyotype analysis was performed using peripheral blood lymphocyte cultures following the methodology described by Moorhead et al. (1960), with modifications. The GTG-banding technique was performed according to Seabright (1973), with modifications. The resolution obtained was 400-500 bands per genome. The karyotype was determined using an optical microscope (Coleman® Trinocular N126T-Infinito Plano Led), with 30 metaphases per patient being analyzed and, in cases of suspected mosaicism, this number was increased to 50 metaphases. The metaphases were photographed using ScopeImage software (version 9.0) and karyotyped using GeneAll-HD software. The results obtained from the GTG-banding were interpreted according to the norms present in the International System for Human Cytogenetic Nomenclature ISCN (McGowan-Jordan 2016).

Statistical analysis

Statistical analyses were performed based on data obtained from patient records, which were compiled and analyzed using Microsoft Excel® software. The relative frequency of the following parameters were obtained: distribution of the results of the normal and altered karyotypes involved (autosomal or sexual); and were relative to the frequency of chromosomal analyses in POF patients.

RESULTS

Between April 2022 and February 2023, chromosomal analyses were conducted at the Laboratory of Human Cytogenetics (UEA) in 15 patients suspected of premature ovarian failure (POF). The results revealed that nine of these patients (60%) presented a normal karyotype 46,XX, without any numerical or structural chromosomal alterations, representing the majority of the cases analyzed. However, in six patients (40%), numerical or structural chromosomal alterations involving autosomal chromosomes and the X chromosome were identified (Table 1).

The prevalence of chromosomal alterations found in patients with POF was as follows: 20% of the patients presented numerical alterations of the monosomy type of the X chromosome with mosaicism, while 13% demonstrated numerical alterations in autosomal chromosomes, including pairs 15 and 21, both with mosaicism (Figure 1). In addition, 7% of patients exhibited a structural alteration characterized by a terminal deletion in the long arm of the X chromosome (Figure 2).

DISCUSSION

According to Chen et al. (2023), the cytogenetic analysis of blood lymphocytes, using the karyotype, is an important tool in the detection of chromosomal alterations, both numerical and structural, and plays a crucial role in understanding the underlying genetic causes of POF.

This work is the first cytogenetic study using peripheral blood of a population of women affected by POF in the northern region of Brazil, since most studies involving cytogenetic diagnosis in women with POF are performed in the southern and southeastern regions of the country. In our study, six patients with POF were identified as having numerical or structural chromosomal alterations involving both autosomal chromosomes and the X chromosome, with these alterations representing 40% of the total number of cases.

Table 1. Chromosomal abnormalities found in patients with POF.

Nº	Age	Alterations	Chromosome	Karyotype
001	19	Numerical-Monosomy-Mosaic	Sexual	45,X[4]/46,XX[46]
002	36	Numerical-Monosomy-Mosaic	Sexual	45,X[3]/46,XX[47]
003	37	Numerical-Monosomy-Mosaic	Sexual	45,X[4]/46,XX[46]
004	34	Numerical-Monosomy-Mosaic	Autosomal	45,XX,-15[6]/46,XX[44]
005	34	Numerical-Monosomy-Mosaic	Autosomal	45,XX,-21[5]/46,XX[45]
006	22	Structural-Deletion-Non-mosaic	Sexual	46,X,del(X)(q22-24;qter)

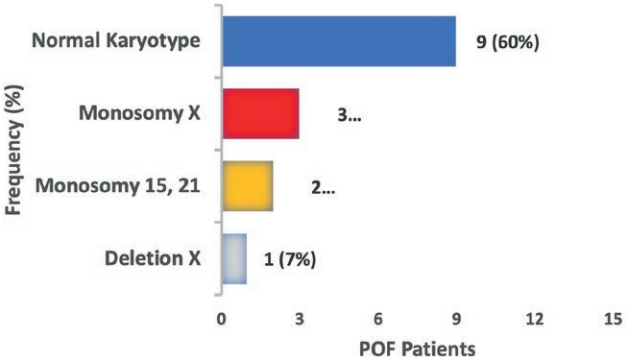

Figure 1. Frequency of the results from the karyotypic analyses in POF patients.

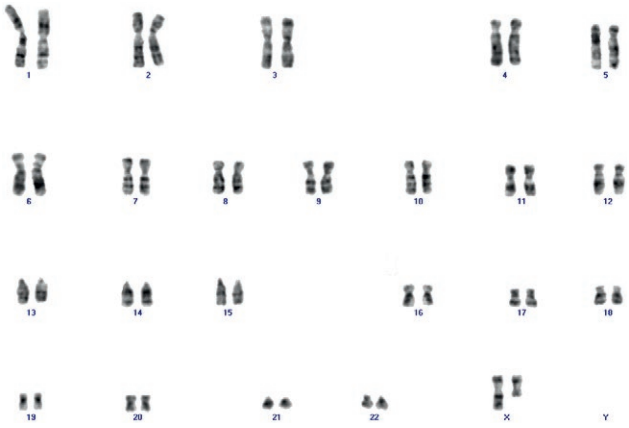

Figure 2. Karyotype with deletion on the long arm of the X chromosome, 46,X,del(X)(q22-24;qter).

One study conducted in patients affected by POF who were submitted to karyotype examinations in a public community genetics service in the state of Rio Grande do Sul, Brazil, demonstrated that 41 (29%) of the 141 confirmed cases presented numerical and structural alterations related to the X chromosome (Rosa et al. 2008). In another retrospective study involving 43 women affected by POF, conducted in public genetic services of the southern region of the country, Besson et al. (2023) identified, mainly in the X chromosome, numerical and structural chromosomal alterations in 14 (32.6%) of the participating women.

Our results also resemble those of a Turkish cytogenetic study involving women affected by POF, which identified a prevalence of chromosomal alterations in 39 (52%) of the 75 participating patients (Ceylaner et al. 2010). On the other hand, in another Turkish cytogenetic study, a lower prevalence of numerical and structural chromosomal alterations involving both autosomal chromosomes and the X chromosome was identified in 44 (25%) of the 175 cases analyzed in women with POF (Geckinli et al. 2014). In an Egyptian cytogenetic study involving 30 women with POF, it was observed that seven cases (23.3%) had chromosomal alterations, including numerical and structural alterations in the X chromosome (Issa and Elhady 2022).

In a Chinese cytogenetic study, chromosomal alterations were present in 64 (12.1%) of the 531 cases of POF analyzed (Jiao et al. 2012). In addition, a study involving Tunisian women with POF showed that 10.8% (108) of the 1,000 patients submitted to karyotype analysis had chromosomal alterations, mainly numerical ones of the X chromosome (Lakhal et al. 2010). Significant differences in the percentage of chromosomal alterations identified in various studies involving POF may be associated with ethnicity (Luborsky 2003). Luborsky et al. (2003) conducted a multi-ethnic epidemiological study and identified variations in the occurrence of POF, with the largest differences observed in Caucasian, African American and Hispanic women. Thus, the prevalence of POF may present ethnical differences, as well as regional ones due to lifestyle and environmental factors, which still need to be more fully investigated (Ishizuka 2021).

In our study, we identified that the highest prevalence of chromosomal abnormalities was of X chromosome monosomy, with a low frequency of mosaicism in three patients, representing 20% of the cases analyzed. The result obtained here is in line with what was found in a study that investigated women with POF and identified a 21.9% prevalence of chromosomal alterations with the presence of low frequency mosaicism of the X chromosome in the cases analyzed (Gersak and Veble 2011).

The most common chromosomal alteration in a cytogenetic study involving 179 Iranian women was X-chromosome mosaicism, which was present in 27.77% of cases (Kalantari 2013). It is said in the literature that karyotypes 45,X, with or without mosaicism, in numerical alterations of the X chromosome, can manifest themselves clinically with symptoms of primary or secondary amenorrhea (Turkyilmaz 2022). X-chromosome mosaicism is usually associated with sexual development and abnormal reproductive performance in women, resulting in infertility, recurrent miscarriages and cases of POF (Gersak and Veble 2011).

The results confirm previous observations and emphasize the critical role of alterations involving the X chromosome, with low frequency mosaicism, as one of the possible etiologies of POF (Ceylaner et al. 2010). Two intact X chromosomes are essential for the maintenance of ovarian function, since many genes that are likely involved in ovarian function escape X inactivation

and are necessary for normal ovarian function, development, and maintenance (Davison 1999; Zinn 2001). In addition, low-frequency mosaicism involving the X chromosome can influence the survival rate and accelerate the aging of ovarian cells through different mechanisms, including a decrease in the number of germ cells or acceleration of their postnatal destruction and early oocyte atresia (Neves et al. 2020; Issa and Elhady 2022).

Other numerical alterations of the monosomy type, involving autosomal chromosomes 15 and 21, were observed in our study. The alterations were found in two nulliparous patients (34-year-old monozygotic twin sisters), representing 13% of the cases. In both cases, a low-frequency mosaicism was observed. The literature describes that POF is related to familial occurrence in about 12% to 15% of cases (Van Kasteren et al. 1999; Ferrarini et al. 2013; Franić et al. 2016; Rudnicka et al. 2018). To date, in the literature, there have been no reports of patients with POF who presented the absence of autosomal chromosomes 15 or 21 in their karyotypes.

However, Hosseini et al. (2011), reported a case of a 27-year-old Iranian woman affected by POF who presented a balanced translocation between autosomal chromosomes 15 and 21. The literature describes the occurrence of partial deletion of 21q in a case of a woman affected by POF (Zeng 2019). Another case of POF was reported in a 36-year-old woman, in which cytogenetic analyses revealed the presence of a supernumerary marker, which was characterized by fluorescent *in situ* hybridization (FISH) and comparative genomic hybridization (array CGH). The marker was derived from chromosome 15 and contained only heterochromatic material (Bertini 2012). Another study identified a patient with POF who had an autosomal mosaicism involving trisomy 21 (Baronchelli et al. 2011).

Other autosomal chromosome-related changes have been identified in patients with POF; in a study conducted by Issa et al. (2022), reciprocal translocations between the X chromosome and chromosome 9 were found. In another study, conducted by Jiao et al. (2012), a Robertsonian translocation between chromosomes 13 and 14 was identified in women affected by POF.

Regarding the structural alterations identified in the present study, we found one patient (7%) who presented a terminal deletion in the long arm of an X chromosome in all the metaphases examined. Similar findings were observed in a cytogenetic study in women affected by POF in Egypt, which identified a terminal deletion in the long arm on one of the X chromosomes, in the absence of mosaicism in all the metaphases analyzed (Issa and Elhady 2022). The complete or partial absence of an X chromosome, as seen in Turner syndrome, leads to ovarian dysgenesis characterized by primary amenorrhea and phenotypic features such as short stature (Goswami and Conway 2005; Portnoi et al. 2006). However, terminal deletions of the chromosome Xq are among the most common cytogenetic alterations. Two critical regions associated with POF have been defined in previous studies on X chromosome rearrangements: Xq13-Xq21 and Xq23-Xq27; these regions have been characterized for ovarian development and function (Persani 2009; Beke et al. 2013; Barros 2020; Besson et al. 2023).

Previous studies have shown that deletion of both the short arm and the long arm of the X chromosome can result in primary or secondary amenorrhea (Sybert and McCauley 2004). These observations suggest that genes that are important for normal ovarian function are located on both arms of the X chromosome (Cordts 2010). The high frequency of chromosomal alterations found in the present study emphasizes the importance of routine cytogenetic (karyotyping) tests in the investigation of patients affected with POF, for diagnostic definition and adequate genetic counseling for patients and their families.

However, even in the face of normal karyotyping results, the possibility of genetic alterations cannot be ruled out, since possible mutations in different genes can cause POF. The most common single-gene cause that results in this condition is pre-mutation of the *FMR1* gene, located on the long arm of the X chromosome. This mutation is based on increased expansion of CGG trinucleotide repeats from 55 to 199 in the untranslated region. Patients with this pre-mutation have an increased risk of developing POF (Jin 2012; Rudnicka et al. 2018).

Therefore, a more detailed investigation is necessary for these patients and should involve tests using molecular techniques for diagnostic confirmation.

CONCLUSION

POF continues to be a serious medical problem and significantly affects the patient's life. In most cases, its etiopathology remains unexplained. The relationship between chromosomal alterations and some cases of POF is clearly demonstrated in the present study. The cytogenetic findings highlight the importance of chromosomal analysis via conventional cytogenetics in the investigation of this condition. In most cases, it was possible to identify both numerical (20%) and structural (7%) chromosomal alterations, mainly involving the X chromosome, including low frequency mosaicism, which is directly associated with this condition.

In addition, it was possible to detect numerical alterations of the monosomy type involving autosomal

chromosomes (13%) referring to pairs 15 and 21. This information is fundamental in clinical practice for the correct diagnosis, adequate prognosis and reproductive management through genetic counseling. Such results aim to contribute to medical decision-making during its diagnosis and help direct a multidisciplinary therapeutic approach by specialists.

Early diagnosis of POF is extremely important for maintaining the physical and mental health of these patients, as it can provide etiological explanation, help in the prevention of bone and cardiovascular health, and guide fertility options. Thus, the diagnosis represents a fundamental milestone in promoting the quality of life of these patients. These findings are essential to the understanding of POF and may have significant implications in the diagnosis and management of this condition.

ACKNOWLEDGMENTS

This work was supported by the Fundação de Amparo à Pesquisa do Estado do Amazonas (FAPEAM) and the Coordenacão de Aperfeiçoamento de Pessoal de Nível Superior (CAPES).

REFERENCES

Albright F, Smith PH, Fraser R. 1942. A syndrome characterized by primary ovarian insufficiency and decreased stature: Report of 11 cases with a digression on hormonal control of axillary and pubic hair. Am J Med Sci. 204(5):625–648. https://doi.org/10.1097/00000441-194211000-00001.

Ayed W, Amouri A, Hammami W, Kilani O, Turki Z, Harzallah F, Bouayed-Abdelmoula N, Chemkhi I, Zhioua F, Slama CB, et al. 2014. Cytogenetic abnormalities in Tunisian women with premature ovarian failure. C R Biol. 337(12):691–694. https://doi.org/10.1016/j.crvi.2014.09.003.

Baronchelli S, Conconi D, Panzeri E, Bentivegna A, Redaelli S, Lissoni S, Saccheri F, Villa N, Crosti F, Sala E, et al. 2011. Cytogenetics of premature ovarian failure: an investigation on 269 affected women. J Biomed Biotechnol. 2011(1):370195. https://doi.org/10.1155/2011/370195.

Barros F, Carvalho F, Barros A, Dória S, et al. 2020. Premature ovarian insufficiency: clinical orientations for genetic testing and genetic counseling. Porto Biomed J. 5(3):e62. https://doi.org/10.1097/j.pbj.0000000000000062.

Beke A, Piko H, Haltrich I, Csomor J, Matolcsy A, Fekete G, Rigo J, Karcagi V, et al. 2013. Molecular cytogenetic analysis of Xq critical regions in premature ovarian failure. Mol Cytogenet. 6(1):62. https://doi.org/10.1186/1755-8166-6-62.

Bertini V, Viola D, Vitti P, Simi P, Valetto A, et al. 2012. An idic(15) associated with POF (premature ovarian failure): Molecular cytogenetic definition of a case and review of the literature. Gene. 503(1):123–125. https://doi.org/10.1016/j.gene.2012.04.071.

Besson M da R, Taiarol M dos S, Fernandes EB, Ghiorzi IB, Nunes MR, Zen PRG, Rosa RFM, et al. 2023. Chromosomal abnormalities detected by karyotyping among patients with secondary amenorrhea: a retrospective study. Sao Paulo Med J. 141(5). https://doi.org/10.1590/1516-3180.2022.0426.r1.14012023.

Geckinli, Toksoy, Sayar, Soylemez, Yesil, Aydın, Karaman, Devranoglu, et al. 2014. Prevalence of X-aneuploidies, X-structural abnormalities and 46,XY sex reversal in Turkish women with primary amenorrhea or premature ovarian insufficiency. Eur J Obstet Gynecol Reprod Biol. 182:211–215. https://doi.org/10.1016/j.ejogrb.2014.09.033.

Ceylaner G, Altinkaya SO, Mollamahmutoglu L, Ceylaner S, et al. 2010. Genetic abnormalities in Turkish women with premature ovarian failure. Int J Gynecol Amp Obstet. 110(2):122–124. https://doi.org/10.1016/j.ijgo.2010.03.023.

Chen M, Jiang H, Zhang C. 2023. Selected Genetic Factors Associated with Primary Ovarian Insufficiency. Int J Mol Sci. 24(5):4423. https://doi.org/10.3390/ijms24054423.

Chon SJ, Umair Z, Yoon MS. 2021. Premature Ovarian Insufficiency: Past, Present, and Future. Front Cell Dev Biol. 9. https://doi.org/10.3389/fcell.2021.672890.

Cordts EB, Christofolini DM, dos Santos AA, Bianco B, Barbosa CP, et al. 2010. Genetic aspects of premature ovarian failure: a literature review. Arch Gynecol Obstet. 283(3):635–643. https://doi.org/10.1007/s00404-010-1815-4.

Davison RM, Davis CJ, Conway GS. 1999. The X chromosome and ovarian failure. Clin Endocrinol. 51(6):673–679. https://doi.org/10.1046/j.1365-2265.1999.00926.x.

Di-Battista A, Moysés-Oliveira M, Melaragno MI. 2020. Genetics of premature ovarian insufficiency and the association with X-autosome translocations. Reproduction. 160(4):R55—R64. https://doi.org/10.1530/rep-20-0338.

ESHRE. 2016. Guideline: management of women with premature ovarian insufficiency. Hum Reprod.

31(5):926–937. https://doi.org/10.1093/humrep/dew027.

Ferrarini E, Russo L, Fruzzetti F, Agretti P, De Marco G, Dimida A, Gianetti E, Simoncini T, Simi P, Baldinotti F, et al. 2013. Clinical characteristics and genetic analysis in women with premature ovarian insufficiency. Maturitas. 74(1):61–67. https://doi.org/10.1016/j.maturitas.2012.09.017.

Franić D. et al. 2016. Genetic Etiology of Primary Premature Ovarian Insufficiency. Acta Clin Croat. 629–635. https://doi.org/10.20471/acc.2016.55.04.14.

Gersak K, Veble A. 2011. Low-level X chromosome mosaicism in women with sporadic premature ovarian failure. Reprod Biomed Online. 22(4):399–403. https://doi.org/10.1016/j.rbmo.2011.01.002.

Goswami D, Conway GS. 2005. Premature ovarian failure. Hum Reprod Update. 11(4):391–410. https://doi.org/10.1093/humupd/dmi012.

Holland CM. 2001. 47,XXX in an Adolescent with Premature Ovarian Failure and Autoimmune Disease. J Pediatr Adolesc Gynecol. 14(2):77–80. https://doi.org/10.1016/s1083-3188(01)00075-4.

Hosseini S, Vahid Dastjerdi M, Asgari Z, Samiee H, et al. 2011. Premature ovarian failure in a woman with a balanced 15;21 translocation: a case report. J Med Case Rep. 5(1). https://doi.org/10.1186/1752-1947-5-250.

Ishizuka B. 2021. Current Understanding of the Etiology, Symptomatology, and Treatment Options in Premature Ovarian Insufficiency (POI). Front Endocrinol. 12. https://doi.org/10.3389/fendo.2021.626924.

Issa NM, Elhady GM. 2022. Cytogenetic abnormalities in a sample of females with premature ovarian failure. Middle East Fertil Soc J. 27(1). https://doi.org/10.1186/s43043-022-00098-3.

Jankowska K. 2017. Premature ovarian failure. Menopausal Rev. 2:51–56. https://doi.org/10.5114/pm.2017.68592.

Jiao X, Qin C, Li J, Qin Y, Gao X, Zhang B, Zhen X, Feng Y, Simpson JL, Chen Z-J, et al. 2012. Cytogenetic analysis of 531 Chinese women with premature ovarian failure. Hum Reprod. 27(7):2201–2207. https://doi.org/10.1093/humrep/des104.

Jin M, Yu Y, Huang H. 2012. An update on primary ovarian insufficiency. Sci China Life Sci. 55(8):677–686. https://doi.org/10.1007/s11427-012-4355-2.

Kalantari H, Madani T, Zari Moradi S, Mansouri Z, Almadani N, Gourabi H, Mohseni Meybodi A et al. 2013. Cytogenetic analysis of 179 Iranian women with premature ovarian failure. Gynecol Endocrinol. 29(6):588–591. https://doi.org/10.3109/09513590.2013.788625.

Lakhal B, Braham R, Berguigua R, Bouali N, Zaouali M, Chaieb M, Veitia RA, Saad A, Elghezal H, et al 2010. Cytogenetic analyses of premature ovarian failure using karyotyping and interphase fluorescence in situ hybridization (FISH) in a group of 1000 patients. Clin Genet. 78(2):181–185. https://doi.org/10.1111/j.1399-0004.2009.01359.x.

Luborsky JL, Meyer P, Sowers MF, Gold EB, Santoro N, et al. 2003. Premature menopause in a multi-ethnic population study of the menopause transition. Hum Reprod. 18(1):199–206. https://doi.org/10.1093/humrep/deg005.

Luo W, Ke H, Tang S, Jiao X, Li Z, Zhao S, Zhang F, Guo T, Qin Y, et al. 2023. Next-generation sequencing of 500 POI patients identified novel responsible monogenic and oligogenic variants. J Ovarian Res. 16(1). https://doi.org/10.1186/s13048-023-01104-6.

McGowan-Jordan J, Simons A, Schmid M, editors. 2016. ISCN 2016: An international system for human cytogenomic nomenclature (2016). S. Karger AG. https://doi.org/10.1159/isbn.978-3-318-06861-0.

Moorhead PS, Nowell PC, Mellman WJ, Battips DM, Hungerford DA, et al. 1960. Chromosome preparations of leukocytes cultured from human peripheral blood. Exp Cell Res. 20(3):613–616. https://doi.org/10.1016/0014-4827(60)90138-5.

Neves AR, Pais AS, Ferreira SI, Ramos V, Carvalho MJ, Estevinho A, Matoso E, Geraldes F, Marques Carreira I, Águas F, et al. 2021. Prevalence of cytogenetic abnormalities and FMR1 gene premutation in a Portuguese population with premature ovarian insufficiency. Acta Med Port. 34(9):580–585. https://doi.org/10.20344/amp.13490.

Persani L, Rossetti R, Cacciatore C, Bonomi M, et al. 2009. Primary ovarian insufficiency: X chromosome defects and autoimmunity. J Autoimmun. 33(1):35–41. https://doi.org/10.1016/j.jaut.2009.03.004.

Podfigurna-Stopa A, Czyzyk A, Grymowicz M, Smolarczyk R, Katulski K, Czajkowski K, Meczekalski B, et al. 2016. Premature ovarian insufficiency: the context of long-term effects. J Endocrinol Invest. 39(9):983–990. https://doi.org/10.1007/s40618-016-0467-z.

Portnoi MF, Aboura A, Tachdjian G, Bouchard P, Dewailly D, Bourcigaux N, Fridman R, Christin-Maitre S, et al. 2006. Molecular cytogenetic studies of Xq critical regions in premature ovarian failure patients. Hum Reprod. 21(9):2329–2334. https://doi.org/10.1093/humrep/del174.

Powell CM, Taggart RT, Drumheller TC, Wangsa D, Qian C, Nelson LM, White BJ, et al. 1994. Molecular and cytogenetic studies of an X;autosome translocation in a patient with premature ovarian failure and review of the literature. Am J Med Genet. 52(1):19–26. https://doi.org/10.1002/ajmg.1320520105.

Qin Y, Jiao X, Simpson JL, Chen ZJ, et al. 2015. Genetics of primary ovarian insufficiency: new developments and opportunities. Hum Reprod Update. 21(6):787–808. https://doi.org/10.1093/humupd/dmv036.

Rahman R, Panay N. 2021. Diagnosis and management of premature ovarian insufficiency. Best Pract Amp Res Clin Endocrinol Amp Metab. 35(6):101600. https://doi.org/10.1016/j.beem.2021.101600.

Rosa RFM, Dibi RP, Picetti J dos S, Rosa RCM, Zen PRG, Graziadio C, Paskulin GA, et al. 2008. Amenorréia e anormalidades do cromossomo X. Rev Bras Ginecol Obstet. 30(10). https://doi.org/10.1590/s0100-72032008001000006.

Rudnicka E, Kruszewska J, Klicka K, Kowalczyk J, Grymowicz M, Skórska J, Pięta W, Smolarczyk R, et al. 2018. Premature ovarian insufficiency – aetiopathology, epidemiology, and diagnostic evaluation. Prz Menopauzalny. 17(3):105–108. https://doi.org/10.5114/pm.2018.78550.

Sala C, Arrigo G, Torri G, Martinazzi F, Riva P, Larizza L, Philippe C, Jonveaux P, Sloan F, Labella T, et al. 1997. Eleven X chromosome breakpoints associated with premature ovarian failure (POF) map to a 15-Mb YAC contig spanning Xq21. Genomics. 40(1):123–131. https://doi.org/10.1006/geno.1996.4542.

Seabright M. 1973. High resolution studies on the pattern of induced exchanges in the human karyotype. Chromosoma. 40(4):333–346. https://doi.org/10.1007/bf00399426.

Sybert VP, McCauley E. 2004. Turner's Syndrome. New Engl J Med. 351(12):1227–1238. https://doi.org/10.1056/nejmra030360.

Turkyilmaz A, Alavanda C, Ates EA, Geckinli BB, Polat H, Gokcu M, Karakaya T, Cebi AH, Soylemez MA, Guney Aİ, et al. 2022. Whole-exome sequencing reveals new potential genes and variants in patients with premature ovarian insufficiency. J Assist Reprod Genet. 39(3):695–710. https://doi.org/10.1007/s10815-022-02408-0.

Van Kasteren YM, Hundscheid RDL, Smits APT, Cremers FPM, van Zonneveld P, Braat DDM, et al. 1999. Familial idiopathic premature ovarian failure: an overrated and underestimated genetic disease? Hum Reprod. 14(10):2455–2459. https://doi.org/10.1093/humrep/14.10.2455.

Wesevich V, Kellen AN, Pal L. 2020. Recent advances in understanding primary ovarian insufficiency. F1000Research. 9:1101. https://doi.org/10.12688/f1000research.26423.1.

Zeng J, Huang W, Huang M, Wang Z. 2019. The first report showing de novo partial 21q monosomy in an adult woman with occult primary ovarian insufficiency (POI). Clin Chem Lab Med (CCLM). 57(9):e230-e233. https://doi.org/10.1515/cclm-2018-1271.

Zinn AR. 2001. The X Chromosome and the Ovary. J Soc Gynecol Investig. 8(1_suppl):S34—S36. https://doi.org/10.1177/1071557601008001s11.

Caryologia
International Journal of Cytology, Cytosystematics and Cytogenetics

Firenze University Press
https://riviste.fupress.net/index.php/caryologia

OPEN ACCESS

Citation: Kumar, S. J., Amirtham, A., & Kank, A. B. S. (2025). Distribution pattern, ecology and cytology of a globally threatened South indian endemic fern *Elaphoglossum nilgiricum* Krajina ex Sledge (Lomariopsidaceae: Pteridophyta). *Caryologia* 78(1): 67-71. doi: 10.36253/caryologia-2954

Received: November 20, 2024

Accepted: June 9, 2025

Published: October 1, 2025

Data Availability Statement: All relevant data are within the paper and its Supporting Information files.

Competing Interests: The Author(s) declare(s) no conflict of interest.

Distribution pattern, ecology and cytology of a globally threatened South indian endemic fern *Elaphoglossum nilgiricum* Krajina ex Sledge (Lomariopsidaceae: Pteridophyta)

S. Jaya Kumar[1], A. Amirtham[2], A. Benniamin Sampada Kank[3,*]

[1] *Department of Botany, Nesamony Memorial Christian College, Marthandam, India-629165*
[2] *Department of Botany, St. Xavier's College (Autonomous), Palayamkottai, India-627002*
[3] *Western Regional Centre, Botanical Survey of India, 7, Koregaon Road, Pune, India-411001*
Corresponding author. E-mail: abenniamin@bsi.gov.in

Abstract. The Lomariopsidoid deer tongue fern genus *Elaphoglossum*, with about 600 epilithic species, is with either monomorphic or partially dimorphic simple fronds having acrostichoid sori. Due to the rare occurrence of fertile fronds, chromosome number reports are rarely available with the presence of maximum number of diploid species with n=41. Out of seven species of *Elaphoglossum* from India, five species are present on the Western Ghats of South India itself with three South Indian endemic species. The present study shows that the globally threatened endemic fern *Elaphoglossum nilgiricum* Krajina ex Sledge from the type locality Nilgiris, India is a tetraploid sexual with 2n=164 chromosomes. This is the first chromosome count for this globally threatened South Indian endemic fern *E. nilgiricum* Krajina ex Sledge.

Key words: Pteridophyte, *Elaphoglossum,* cytology.

INTRODUCTION

Pteridophytes, the primitive vascular plants, are the dominant group of terrestrial plants on the earth next to flowering plants. India, with varied habitats and climate, is with about 1200 species of pteridophytes (Fraser-Jenkins *et al.* 2017, 2018, 2021). The Lomariopsidoid deer tongue fern genus *Elaphoglossum*, with about 600 epilithic species, is with either monomorphic or partially dimorphic simple fronds having acrostichoid sori. There are only seven species of *Elaphoglossum* (*Elaphoglossum angulatum* (Blume) T. Moore, *E. beddomei* Sledge, *E. commutatum* (Mett. ex Kuhn) Alderw., *E. marginatum* T. Moore, *E. nilgiricum* Krajina ex Sledge, *E. stelligerum* (Wall. ex Baker) T. Moore ex Salom and *E. stigmatolepis* (Fee) T. Moore) in India (Fraser-Jenkins *et al.* 2021). Maximum number (six) of *Elaphoglossum* species are present in South India, where three

species {*E. beddomei* Sledge, *E. nilgiricum* Krajina ex Sledge, *E. stigmatolepis* (Fee) T. Moore} are endemic. All the above three South Indian endemic *Elaphoglossum* species are present in Nilgiris, Tamilnadu (India) itself (Manickam and Irudayaraj 2003). From India, chromosome number reports are available under four names of *Elaphoglossum* (*E. beddomei* Sledge – n=82 (4x), *E. conforme* Sw. n=41 (2x), n=82 (4x), *E. laurifolium* (Thours) Moore n =82 (4x), *E. stelligerum* (Wall. ex Bak.) Moore ex Alston & Bonner – n=82 (4x), n=164 (8x) (Bir and Verma 2010). Out of three South Indian endemic species of *Elaphoglossum*, only one species (*E. beddomei* Sledge n=82, 4x Irudayaraj and Manickam 1991) is cytologically known. The globally threatened endemic species *E. nilgiricum* Krajina ex Sledge is cytologically unknown. Next to morphology, cytology plays an important role in plant taxonomy as recently proved in *Sonchus* species from Punjab (Sidhu & Singh 2021). Usually diploid ferns are rare when compared to polyploid ferns (Benniamin *et al.* 2008) and thus, for conservation program cytological knowledge is also important. In the present study cytological study has been made on this endemic fern in order to know the chromosome number and ploidy level.

MATERIALS AND METHODS

For general ecological and taxonomical studies, herbarium specimens housed in St. Xavier's College Herbarium (XCH) Palayamkottai, India were observed. For cytological study materials were collected from the shola forest in Naduvattom, Nilgiris, India. The leaf tips from young 1-2cm length leaves were directly fixed in the fixative (Mixture of Ethyl Alcohol: Chloroform: Acetic Acid in 6:3:1 ratio) without any pretreatment. For the observation of mitotic chromosomes, simple acetocarmine squash technique was followed. Specimens were identified based on the book '*Pteridophyte Flora of the Western Ghats, South India*' by Manickam and Irudayaraj (1992) and confirmed with Dr. V. Irudayaraj.

RESULTS AND DISCUSSION

The globally threatened South Indian endemic deer tongue fern *Elaphoglossum nilgiricum* Krajina ex Sledge is restricted in distribution (Kerala, Tamilnadu - India) on the Globe. The observation on herbarium specimens preserved in St. Xavier's College Herbarium, Palayamkottai, India, shows the presence of only nine gather-

Table 1. Distribution and ecology of globally threatened deer tongue fern *Elaphoglossum nilgiricum* Krajina ex Sledge based on St. Xavier's College Herbarium (XCH-Palayamkottai) specimens.

S. No.	Voucher Number	Date of collection	Altitude	Collectors	Locality	Habitat ecology
1	RHT 33400	25.08.85	950M	VSM & KMM	Kerala, Pathanamthitta, Peermedu, Vandiperiyar Hills, Kakki dam.	Terrestrial; roadside; fully shaded. Fronds covered by imbricate shining scales; first record.
2	RHT 33678	03.09.85	1000M	VSM & KMM	Kerala, Pathanamthitta, Muzhiar-Kakki Hills, Muzhiar-Kakki road.	Moist mud slopes along the road.
3	XCH 284	13.10.91	2300M	VSM	tamilnadu, nilgiris, pykara stream.	Occasional epiphyte on partially exposed roadside.
4	XCH 588	28.10.91	2300M	VSM	Tamilnadu, Nilgiri, shola short cut from the T.R. Bazaar to Naduvattum.	Epiphyte, abundant on trees on the shola interior; sori are rare in frond.
5	XCH 1917	05.05.92	1700M	VSM	Tamilnadu Coimbatore, Valparai, Akkamalai forest.	Epiphyte in the interior of shola. Rare. Sterile. First record for the Anamalais.
6	XCH 2139	22.05.92	1700M	VSM	Tamilnadu, Coimbatore, Valparai, Akkamalai to grass Hill, path forest.	Epiphyte on stream banks in the evergreen forest. Rare. Sterile.
7	XCH 3180	04.05.93	850M	VSM	Kerala, Palghat, Silent valley forest.	Rare, on fully shaded in vallicolic open forest. Sterile. Lithophyte.
8	XCH 3447	27.05.93	1800M	VSM	Tamilnadu, Coimbatore, Valparai, Akkamalai forest stream.	Epiphyte, on fully shaded the evergreen forest; rare, sterile. Collected previously form the same stream.
9	XCH 3455	27.05.93	1800M	VSM	Tamilnadu, Coimbatore, Valparai, Akkamalai forest.	Epiphyte, on fully shaded in stream, the stream banks in evergreen shola; occasional, sterile.

XCH = St. Xavier's College Herbarium, Palayamkottai; VSM = V.S.Manickam; KMM=K.M.Matthew.

ings (Table 1) from South India (Six from Tamilnadu-Akkamalai Forest, Valparai, Naduvattom Forest, Nilgiris; three from Kerala-Around Kakki Hills and Silent Valley). Out of nine gatherings, six are epiphytes two are terrestrials and one is lithophyte. The present gathering from Naduvattom forest, Nilgiris (Fig. 1A,B) is also an epiphyte on large moist tree trunk along with another fern *Hymenophyllum gardneri* Bosch. Thus the endemic fern *E. nilgiricum* Krajina ex Sledge is restricted to southern Western Ghats (Kerala, Tamilnadu), India.

Elaphoglossum nilgiricum Krajina ex Sledge is a small epilithic or terrestrial fern with short creeping rhizome bearing simple fronds of about 15-25 cm. The distinguishing feature of this deer tongue fern is the absence of cartilaginous border of the lamina and the presence of shining, imbricate scales densely on the whole fronds (Fig. 1C-G). Fertile fronds are very rare and they are with slightly longer stipe. Sori on fertile fronds are acrostichoid.

The cytological study on the gathering from Naduvattom, Nilgiris shows the presence of ca. 164 chromosomes in the cells of leaf tip (Fig. 1H,I). Since the fertile fronds are very rare, meiotic chromosome count could not be made. This endemic fern *E. nilgiricum* Krajina ex Sledge is a tetraploid sexual (2n=ca.164) species like another South Indian common endemic fern *E. beddomei* Sledge (n=82) (Irudayaraj and Manickam 1991). Since, this fern is globally threatened one, before its extinction, it is important to know the chromosome number and ploidy level of this fern. The chromosome number of another endemic fern *E. stigmatolepis* (Fee) T. Moore is still unknown. It is important to find out the reason for the rare occurrence of the tetraploid endemic fern *E. nilgiricum* Krajina ex Sledge and the common occurrence of the tetraploid endemic fern *E. beddomei* Sledge in South India. Usually diploid epilithic ferns like Grammitidaceious species with erect rhizome and chlorophyllous spores are rare in contrast to terrestrial polyploid species with achlorophyllous spores (Benniamin *et al*. 2008). The above two deer tongue epilithic ferns are polyploid with short creeping rhizome and achlorophyllous spores (Manickam and Irudayaraj 1992). The size of the spores in the above tetraploid species are more or less similar without much of difference. i.e 45 x 30 µm in *E. nilgiricum* Krajina ex Sledge and 50 x 35 µm in *E. beddomei* Sledge (Manickam and Irudayaraj 1992).

The tetraploid *E. beddomei* is very common on southernmost part of the Western Ghats, Tirunelveli Hills in contrast to *E. nilgiricum* which is rarely distributed towards the northern part of the Southern Western Ghats (Anamalais, Nilgiris, Silent Valley) (Manickam and Irudayaraj 1992, 2003). Thus, although these two species are tetraploids with achlorophyllous spores, they require specific ecological niches with specific atmospheric temperature and moisture. Thus, the species *E. beddomei* with the requirement of more maritime moisture and less land moisture, is commonly present on Tirunelveli Hills, the extreme tip of the Western Ghats in the extreme southern part of Peninsular India with the sea surface on three sides (East, West and South). In contrast, *E. nilgiricum* Krajina ex Sledge occurs in northern part of the southern Western Ghats (Anamalais, Kakki Hills, Silent Valley) with more or less equal proportion of maritime and land moisture. Thus, each and every fern will require optimum temperature which is controlled by the proportion of maritime and land moisture depends upon the topography of the locality (Ramesh *et al*. 2020). In the meantime fronds of *E. beddomei* Sledge is sparsely covered by minute scales in contrast to densely scaly fronds of *E. nilgiricum* with the indication of high degree of drought tolerance in the later species (Manickam and Irudayaraj 1992). From the present study, it is clear that apart from morphology and cytology, ecology of specific niche plays an important role for the survival of the above two endemic deer tongue ferns. Both *in situ* and *ex situ* conservation measures should be adapted to conserve this globally threatened deer tongue fern *Elaphoglossum nilgiricum* Krajina ex Sledge.

ACKNOWLEDGEMENTS

The first author S. Jeya Kumar is thankful to Dr. K. Paulraj Principal, Nesamony Memorial College, Marthandam, India for his encouragements.

REFERENCES

Benniamin, A., Irudayaraj, V. and Manickam, V . S. 2008. How to identify rare and endangered ferns and fern allies. *Ethnobotanical Leaflets* 12: 108-117.

Bir, S. S and Verma, S. C. 2010. Chromosome Atlas of the Indian Pteridophytes (1951-2009). Bishen Singh Mahendra Pal Singh, Dehra Dun, India.

Fraser-Jenkins, C. R., Gandhi, K. N,, Kholia, B. S and Benniamin, A. 2017. An annotated checklist of Indian Pteridophytes. Part 1. (Lycopodiaceae to Thelypteridaceae). Bishen Singh Mahendra Pal Singh, Dehra Dun, India.

Fraser-Jenkins C R, Gandhi K N & Kholia B S. 2018. An annotated checklist of Indian Pteridophytes. Part 2. (Woodsiaceae to Dryopteridaceae).). Bishen Singh Mahendra Pal Singh, Dehra Dun, India.

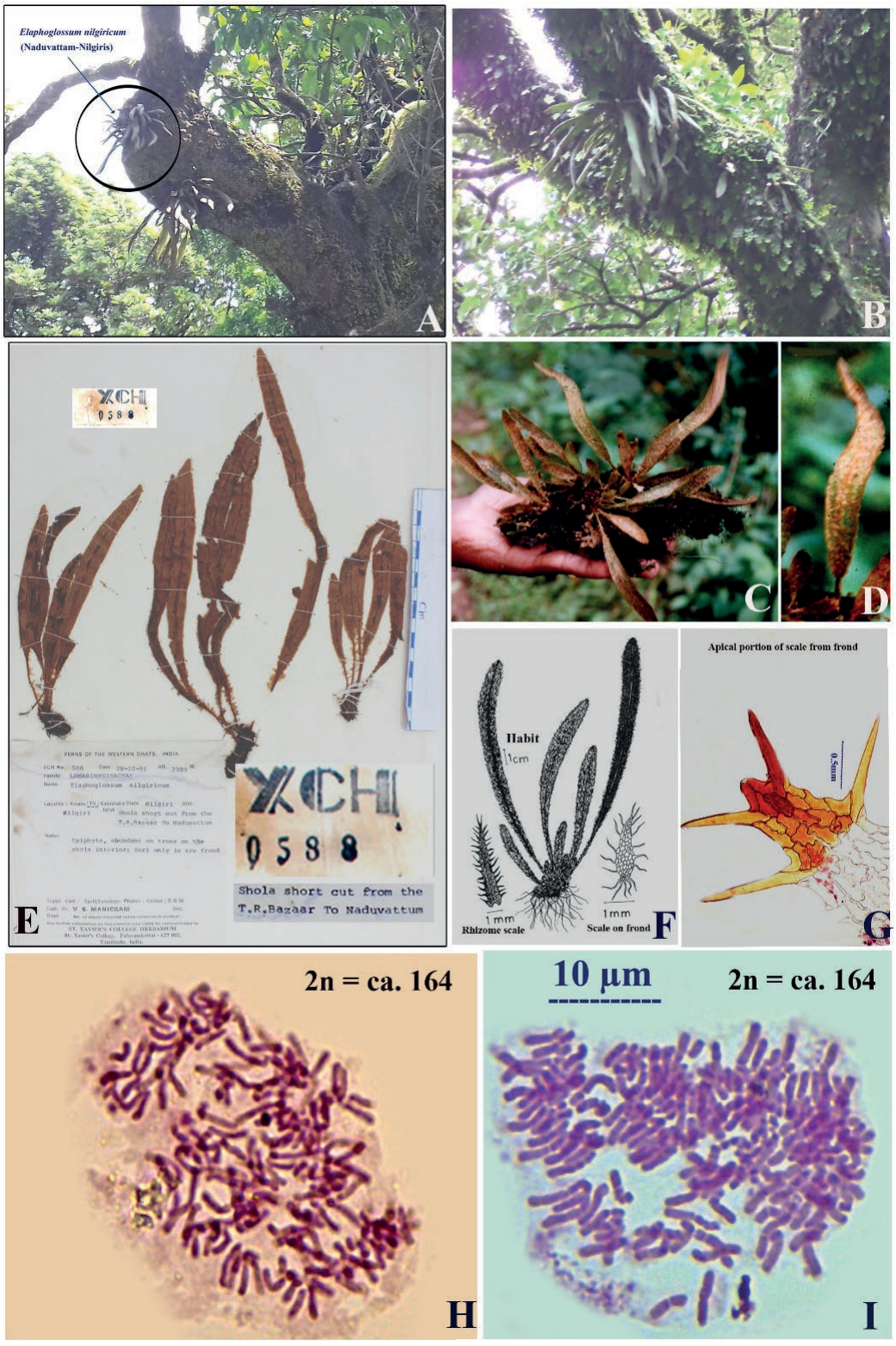

Figure 1. *Elaphoglossum nilgiricum* Krajina ex Sledge 1, 2. Epiphyte on a tree in a Shola forest in Naduvattom, Nilgiris, 3. Habit, 4. Simple frond clothed by soft scales, 5. Herbarium specimen (XCH 0588) from Nilgiris showing short creeping rhizome bearing simple fronds, 6. Illustration showing habit, scales from rhizome and frond, 7. Apical portion of scale from frond, 8, 9 - Mitotic chromosomes from leaf tip cells (2n = ca. 164).

Fraser-Jenkins C R, Gandhi K N, Kholia B S & Kandel D R. 2021. An annotated checklist of Indian Pteridophytes. Part 3. (Lomariopsidaceae to Salviniaceae). Bishen Singh Mahendra Pal Singh, Dehra Dun, India.

Irudayaraj, V. and Manickam, V, S. 1991. Cytology of an endemic fern- *Elaphoglossum beddomei* Sledge from South India. *Indian Fern J.* 8: 93-94.

Manickam, V. S. and Irudayaraj, V, 1992. Pteridophyte Flora of the Western Ghats, South India. BI Publications, Pvt Ltd. New Delhi.

Manickam, V. S. and Irudayaraj, V. 2003. Pteridophyte Flora of Nilgiris, South India. Bishen Singh Mahendra Pal Singh, Dehra Dun, India.

Ramesh, V., Vasudevan, N., Suresh, K., Amirtham, A. and Irudayaraj, V. (2020). Phytogeographical analysis on Lindsaeaoid ferns of India. *Indian Fern J.* 37(1&2): 321-333.

Sidhu, M. C. & R. Singh, R. (2021). A cytomorphological investigation of three species of the genus *Sonchus* L. (Asterales: Asteraceae) from Punjab, India. *Journal of Threatened Taxa* 13(11): 19640–19644.

OPEN ACCESS POLICY

Caryologia provides immediate open access to its content. Our publisher, Firenze University Press at the University of Florence, complies with the Budapest Open Access Initiative definition of Open Access: By "open access" , we mean the free availability on the public internet, the permission for all users to read, download, copy, distribute, print, search, or link to the full text of the articles, crawl them for indexing, pass them as data to software, or use them for any other lawful purpose, without financial, legal, or technical barriers other than those inseparable from gaining access to the internet itself. The only constraint on reproduction and distribution, and the only role for copyright in this domain is to guarantee the original authors with control over the integrity of their work and the right to be properly acknowledged and cited. We support a greater global exchange of knowledge by making the research published in our journal open to the public and reusable under the terms of a Creative Commons Attribution 4.0 International Public License (CC-BY-4.0). Furthermore, we encourage authors to post their pre-publication manuscript in institutional repositories or on their websites prior to and during the submission process and to post the Publisher's final formatted PDF version after publication without embargo. These practices benefit authors with productive exchanges as well as earlier and greater citation of published work.

PUBLICATION FREQUENCY

Papers will be published online as soon as they are accepted, and tagged with a DOI code. The final full bibliographic record for each article (initial-final page) will be released with the hard copies of *Caryologia*. Manuscripts are accepted at any time through the online submission system.

COPYRIGHT NOTICE

Authors who publish with *Caryologia* agree to the following terms:

- Authors retain the copyright and grant the journal right of first publication with the work simultaneously licensed under a Creative Commons Attribution 4.0 International Public License (CC-BY-4.0) that allows others to share the work with an acknowledgment of the work's authorship and initial publication in Caryologia.
- Authors are able to enter into separate, additional contractual arrangements for the non-exclusive distribution of the journal's published version of the work (e.g., post it to an institutional repository or publish it in a book), with an acknowledgment of its initial publication in this journal.
- Authors are permitted and encouraged to post their work online (e.g., in institutional repositories or on their website) prior to and during the submission process, as it can lead to productive exchanges, as well as earlier and greater citation of published work (See The Effect of Open Access).

PUBLICATION FEES

Open access publishing is not without costs. *Caryologia* therefore levies an article-processing charge of € 150.00 for each article accepted for publication, plus VAT or local taxes where applicable.

We routinely waive charges for authors from low-income countries. For other countries, article-processing charge waivers or discounts are granted on a case-by-case basis to authors with insufficient funds. Authors can request a waiver or discount during the submission process.

PUBLICATION ETHICS

Responsibilities of *Caryologia*'s editors, reviewers, and authors concerning publication ethics and publication malpractice are described in *Caryologia*'s Guidelines on Publication Ethics.

CORRECTIONS AND RETRACTIONS

In accordance with the generally accepted standards of scholarly publishing, *Caryologia* does not alter articles after publication: "Articles that have been published should remain extant, exact and unaltered to the maximum extent possible".

In cases of serious errors or (suspected) misconduct *Caryologia* publishes corrections and retractions (expressions of concern).

Corrections

In cases of serious errors that affect or significantly impair the reader's understanding or evaluation of the article, *Caryologia* publishes a correction note that is linked to the published article. The published article will be left unchanged.

Retractions

In accordance with the "Retraction Guidelines" by the Committee on Publication Ethics (COPE) *Caryologia* will retract a published article if:

- there is clear evidence that the findings are unreliable, either as a result of misconduct (e.g. data fabrication) or honest error (e.g. miscalculation)
- the findings have previously been published elsewhere without proper crossreferencing, permission or justification (i.e. cases of redundant publication)
- it turns out to be an act of plagiarism
- it reports unethical research.

An article is retracted by publishing a retraction notice that is linked to or replaces the retracted article. *Caryologia* will make any effort to clearly identify a retracted article as such.

If an investigation is underway that might result in the retraction of an article *Caryologia* may choose to alert readers by publishing an expression of concern.

COMPLYNG WITH ETHICS OF EXPERIMENTATION

Please ensure that all research reported in submitted papers has been conducted in an ethical and responsible manner, and is in full compliance with all relevant codes of experimentation and legislation. All papers which report in vivo experiments or clinical trials on humans or animals must include a written statement in the Methods section. This should explain that all work was conducted with the formal approval of the local human subject or animal care committees (institutional and national), and that clinical trials have been registered as legislation requires. Authors who do not have formal ethics review committees should include a statement that their study follows the principles of the Declaration of Helsinki

ARCHIVING

Caryologia and Firenze University Press are experimenting a National legal deposition and long-term digital preservation service.

ARTICLE PROCESSING CHARGES

All articles published in *Caryologia* are open access and freely available online, immediately upon publication. This is made possible by an article-processing charge (APC) that covers the range of publishing services we provide. This includes provision of online tools for editors and authors, article production and hosting, liaison with abstracting and indexing services, and customer services. The APC, payable when your manuscript is editorially accepted and before publication, is charged to either you, or your funder, institution or employer.

Open access publishing is not without costs. *Caryologia* therefore levies an article-processing charge of € 150.00 for each article accepted for publication, plus VAT or local taxes where applicable.

FREQUENTLY-ASKED QUESTIONS (FAQ)

Who is responsible for making or arranging the payment?

As the corresponding author of the manuscript you are responsible for making or arranging the payment (for instance, via your institution) upon editorial acceptance of the manuscript.

At which stage is the amount I will need to pay fixed?

The APC payable for an article is agreed as part of the manuscript submission process. The agreed charge will not change, regardless of any change to the journal's APC.

When and how do I pay?

Upon editorial acceptance of an article, the corresponding author (you) will be notified that payment is due.

We advise prompt payment as we are unable to publish accepted articles until payment has been received. Payment can be made by Invoice. Payment is due within 30 days of the manuscript receiving editorial acceptance. Receipts are available on request.

No taxes are included in this charge. If you are resident in any European Union country you have to add Value-Added Tax (VAT) at the rate applicable in the respective country. Institutions that are not based in the EU and are paying your fee on your behalf can have the VAT charge recorded under the EU reverse charge method, this means VAT does not need to be added to the invoice. Such institutions are required to supply us with their VAT registration number. If you are resident in Japan you have to add Japanese Consumption Tax (JCT) at the rate set by the Japanese government.

Can charges be waived if I lack funds?

We consider individual waiver requests for articles in Caryologia on a case-by-case basis and they may be granted in cases of lack of funds. To apply for a waiver please request one during the submission process. A decision on the waiver will normally be made within two working days. Requests made during the review process or after acceptance will not be considered.

I am from a low-income country, do I have to pay an APC?

We will provide a waiver or discount if you are based in a country which is classified by the World Bank as a low-income or a lower-middle-income economy with a gross domestic product (GDP) of less than $200bn. Please request this waiver of discount during submission.

What funding sources are available?

Many funding agencies allow the use of grants to cover APCs. An increasing number of funders and agencies strongly encourage open access publication. For more detailed information and to learn about our support service for authors.

APC waivers for substantial critiques of articles published in OA journals

Where authors are submitting a manuscript that represents a substantial critique of an article previously published in the same fully open access journal, they may apply for a waiver of the article processing charge (APC).

In order to apply for an APC waiver on these grounds, please contact the journal editorial team at the point of submission. Requests will not be considered until a manuscript has been submitted, and will be awarded at the discretion of the editor. Contact details for the journal editorial offices may be found on the journal website.

What is your APC refund policy?

Firenze University Press will refund an article processing charge (APC) if an error on our part has resulted in a failure to publish an article under the open access terms selected by the authors. This may include the failure to make an article openly available on the journal platform, or publication of an article under a different Creative Commons licence from that selected by the author(s). A refund will only be offered if these errors have not been corrected within 30 days of publication.

2025
Vol. 78 – n. 1

Caryologia

International Journal of Cytology, Cytosystematics and Cytogenetics

Table of contents